

Université Mohamed Khider – Biskra  
Faculté des Sciences et de la technologie  
Département : Génie Des Procédés  
Ref : .....



جامعة محمد خيضر بسكرة  
كلية العلوم و التكنولوجيا  
قسم:.....  
المرجع:.....

A thesis submitted for the fulfillment of the requirements of the Doctorate Degree in Process  
Engineering

# Characterization and Modeling of Electrode for Proton Exchange Membrane Fuel Cell System (PEMFCS)

Presented by:

**Chebbi Rachid**

Publicly supported it in 2016

Members of the jury :

<b>Dr. Barkat djamel</b>	<b>Professor</b>	<b>President</b>	<b>Biskra University</b>
<b>Dr. Beicha Abdellah</b>	<b>Professor</b>	<b>Supervisor</b>	<b>Jijel University</b>
<b>Dr. Omari mahmoud</b>	<b>Professor</b>	<b>Examiner</b>	<b>Biskra University</b>
<b>Dr. Boumerzoug Zakaria</b>	<b>Professor</b>	<b>Examiner</b>	<b>Biskra University</b>
<b>Dr. Brioua Mourad</b>	<b>Professor</b>	<b>Examiner</b>	<b>Batna University</b>
<b>Dr. Bounar Nedjmeddine</b>	<b>Assitant professor</b>	<b>Examiner</b>	<b>Jijel University</b>

## **PREFACE**

This thesis consist of four stages of the fuel cells researches, The first part is electrode preparation for proton exchange membrane fuel cells (PEMFCs), which consist of electrode formulation and fabrication using spray method , followed by characterizations. Second part is testing the electrode with different parameters such as pressure, temperatures, follow rates, humidifiers temperatures effects. Third part is the electrode degradation after operating and the last is modeling for proton exchange membrane fuel cell. This work mainly located in Fuel Cell Institute UKM Malaysia, which was performed In MEA lab.

## **ACKNOWLEDGEMENT**

My deep gratefulness goes first to Allah who helped me to fulfill this thesis.

I would like to start by acknowledging whose professors who were involved in developing my PhD research. First I would like to acknowledge and express my deep to Prof. Wan Ramli Wan Daud Director of fuel cell institute Bangi, Ukm Malaysia for the trust and placed me in the right way to my research. Also the advice, encouragement and his human quality that allowed me to succeed in this work

I express my thanks to Mr. Abdellah Beicha professor at the University of Jijel who guided my first steps in research.

Especially want to thank Mr. Djamel Barkat, Professor at the University of Biskra, which accept to be the honor of chairing the jury. I am very appreciative to the jury: Professors Omari Mahmoud, Zakaria Boumerzoug at the University of Biskra, professor Brioua Murad of the University of Batna, and also want to thank Mr. Bounar Nedjmeddine. Doctor at the University of jijel for accepting to review and evaluate the work.

Finally, I would like to acknowledge and thanks to Professor Mohamed Amber to the help In X-Ray Photoelectron of spectroscopy lab , faculty of material science UKM, Bangi Malaysia.

## **DEDICATION**

I dedicate this thesis to my lovely family, without their help, understanding and supported, would never achieved the goals.

Mainly mother and Father, wife, daughter Asma, brothers and sisters, extended my thanks to all friends.

In memory of my great father who passed away six month ago before my thesis submission

## ABBREVIATION & NOMENCLATURE

PEMFC Polymer electrolyte membrane fuel cell

PAFC Phosphoric acid fuel cell

AFC Alkaline Fuel Cell

MCFC Molten Carbonate Fuel Cell

SOFC Solid –Oxide Fuel Cell

MPL Micro-porous layer

GDL Gas Diffusion layer

CL Catalyst layer

PTFE polyterafluoethylene

PTFE/C diffusion layer

(Pt/C/PTFE) catalyst layer

MEA Membrane electrode assembly

HHV high heating value

LHV low heating value

EW (g/eq) equivalent weight

SEM Scanning Electron Microscopic

XRD. X - Ray Diffraction

XPS. X-Ray Photo-Electron Spectroscopy

TEM transmission Electron microscopic

$E$  fuel cell's reversible voltage, V

$F$  Faraday constant, C

$I$  current density,  $A\text{ cm}^{-2}$

$i_0$  exchange current density,  $A\text{ cm}^{-2}$

$i_{0c}$  cathode exchange current density,  $A\text{ cm}^{-2}$

$k_c$  factor related to reaction speed,  $A\text{ cm}^{-2}\text{ C}^{-1}$

$i_L$  limiting current density,  $A\text{ cm}^{-2}$

$l_d$  diffusion layer thickness, cm

$l_m$  membrane thickness, cm

$P_{cell}$  fuel cell's power density,  $W\text{ cm}^{-2}$

$P_{H_2}$  partial pressure of hydrogen, atm  
 $P_{O_2}$  partial pressure of hydrogen, atm  
 $R$  universal gas constant,  $8.314 \text{ J K}^{-1} \text{ mol}^{-1}$   
 $RH_a$  relative humidity of anode  
 $RH_c$  relative humidity of cathode  
 $r_{ion}$  ionic resistance,  $\Omega \text{ cm}^2$   
 $r_{el}$  electronic resistance,  $\Omega \text{ cm}^2$   
 $T$  temperature, K  
 $V$  voltage, V  
 $V_{activation}$  activation voltage drop, V  
 $V_{ohmic}$  ohmic voltage drop, V  
 $V_{concentration}$  concentration voltage drop, V

### **Greek letters**

$\psi$  electron transfer coefficient  
 $\Phi$  relative humidity, %  
 $\lambda$  water content  
 $\lambda_a$  water content  
 $\lambda_c$  water content  
 $\beta$  symmetry factor  
 $\rho_{dry}$  dry membrane density,  $\text{kg m}^{-3}$   
 $\sigma_d$  diffusion layer electronic conductivity,  $\text{A V}^{-1} \text{ cm}^{-1}$

## CONTENTS

General Introduction	1
<b>CHAPTER I</b>	<b>FUEL CELLS GENERALITY AND APPLICATIONS</b>
Introduction	3
I.1 What is fuel cell?	4
I.2 Main Categories of fuel cells.	5
2.a Phosphoric acid fuel cell (PAFC).	5
2.b Polymer electrolyte membrane fuel cell (PEMFC)	6
2.c Alkaline Fuel Cell (AFC).	8
2.d Molten Carbonate Fuel Cell (MCFC).	9
2.e Solid Oxide Fuel Cell (SOFC).	10
I.3 Proton exchange membrane fuel cells (PEMFCs).	12
I.4 Principle of proton exchange membrane fuel cells (PEMFCs).	13
I.5 Fuel source for proton exchange membrane fuel cells (PEMFCs).	14
I.6 Aspect thermodynamic for proton exchange membrane fuel cells (PEMFCs).	15
I.6.1 Variation of pressure and temperature for reversible voltage of fuel cell under non-standard state conditions.	17
I.6.1.a Reversible voltage variation with temperature.	17
I.6.1.b Reversible voltage variation with Pressure.	18
I.6.1.c Reversible voltage variation with concentration Nernst equation.	18
I.6.1 d Ideal reversible fuel cell efficiency.	19
I.6.1 e Real (Practical) reversible fuel cell efficiency.	19
I.7 Activation kinetics for fuel cell .Tafel Equation.	20
I.8 Cell Performance for proton exchange membrane fuel cells (PEMFCs).	21
I.9 Theory of Gas Diffusion Electrode.	23
I.9.1 Electrode Fabrication for proton exchange membrane fuel cells (PEMFCs).	24
• Gas Diffusion layer GDL for electrode Pt/C	
• Catalyst layer (CL) for electrode Pt/C.	

<b>I.9.2 Parameters affecting performance electrode for proton exchange membrane.</b>	<b>26</b>
<b>I.9.3 Membrane for proton exchange membrane fuel cells (PEMFCs)</b>	<b>29</b>
<b>I.9.4 Membrane electrode Assembly (MEA) for (PEMFCs)</b>	<b>31</b>
<b>I.10 Electrode components for (PEMFCs)</b>	<b>32</b>
<b>I.10.1 Electrocatalyst (Pt/C)</b>	<b>32</b>
<b>I.10.2 Carbon support catalyst for PEMFCs</b>	<b>32</b>
<b>I.10.3 Binder PTFE and protonic conduct Nafion® ionomers solution</b>	<b>34</b>
<b>I.11 PEM Simulation and Modeling</b>	<b>35</b>

**CHAPTER II      FABRICATION AND ANALYSIS BY SEM, XRD, TEM, AND XPS OF ELECTRODE**

<b>Introduction</b>	<b>37</b>
<b>II.1.1 Electrode Preparation</b>	<b>37</b>
<b>II.1.2 Membrane treatments.</b>	<b>40</b>
<b>II.1.3. Membrane Electrodes Assembly (MEA).</b>	<b>41</b>
<b>II.1.4. Single cells components for proton exchange membrane fuel cells (PEMFCs).</b>	<b>41</b>
<b>II.1.5 Design of operating system for proton exchange membrane fuel cell system (PEMFCs)</b>	<b>42</b>
<b>II.2 Analysis Methods</b>	<b>43</b>
<b>II.2.1 Scanning Electron Microscopic (SEM)</b>	<b>43</b>
<b>II.2.2 X - Ray Diffraction (XRD) Analysis</b>	<b>44</b>
<b>II.2.2.a Apparatus</b>	<b>44</b>
<b>II.2.2.b Sample preparations</b>	<b>44</b>
<b>II.2.3 TEM Analysis</b>	<b>44</b>
<b>II.2.4 Surface Analysis X-Ray Photo-Electron Spectroscopy (XPS)</b>	<b>46</b>

**CHAPTER III      DEGRADATION AND MODELING OF ELECTRODE FOR  
PROTON EXCHANGE MEMBRANE FUEL CELL SYSTEM (PEMFCs)**

<b>Introduction</b>	<b>48</b>
<b>III.1. Scanning Electron Microscopy (SEM)</b>	<b>48</b>
<b>III.2. XPS Technique</b>	<b>50</b>
<b>2.1 Carbon (C<sub>1s</sub>)</b>	<b>53</b>
<b>2.2 Oxygen (O<sub>1s</sub>)</b>	<b>56</b>
<b>2.3 Fluorine (F<sub>1s</sub>)</b>	<b>57</b>
<b>2.4 Silicon (Si<sub>2p</sub>)</b>	<b>59</b>
<b>2.5 Platinum (Pt<sub>4f</sub>)</b>	<b>59</b>
<b>III.3 Electrode Degradation</b>	<b>60</b>
<b>III.3.1 Operating cathode in a single cell 25 cm<sup>2</sup></b>	<b>60</b>
<b>III.3.2 SEM 20 wt% Pt/C</b>	<b>64</b>
<b>III.3.3 XPS Analysis for Cathode before test (E<sub>bT</sub>) and after test (E<sub>CaT</sub>)</b>	<b>65</b>
<b>III.3.4 XRD Analysis</b>	<b>73</b>
<b>III.3.5 Transmission electron microscopy (TEM)</b>	<b>74</b>
<b>III.4 PEM fuel cell modeling</b>	<b>76</b>
<b>III.4.1 Electrode preparation and single cell operation in fuel cell test apparatus.</b>	<b>76</b>
<b>III.4.2 Basic fuel cell operation</b>	<b>77</b>
<b>III.4.3 Model formulation</b>	<b>78</b>
<b>4.3.1 Electrochemical model</b>	<b>78</b>
<b>4.3.2 Cell reversible voltage</b>	<b>79</b>
<b>4.3.3 Activation voltage drop</b>	<b>79</b>
<b>4.3.4 Ohmic voltage drop</b>	<b>80</b>
<b>4.3.5 Concentration or mass transport voltage drop</b>	<b>81</b>



4. 4. 1. Determination of the activation loss parameters	82
4. 4 .2. Effect of the temperature on the performance of the PEM fuel cell	83
4. 4. 3. Effect of the partial pressures	84
<b>CONCLUSION</b>	88
<b>REFERENCES</b>	91
<b>Publications list</b>	100

<b>List of figures:</b>	<b>Titles</b>	<b>Pages</b>
Figure I.1	The principle of an electrolyze (a); of a fuel cell (b)	1
<b>Figure I.2</b>	NASA Space Shuttle Orbiter fuel cell.	2
<b>Figure I.3</b>	Schematic of H <sub>2</sub> /O <sub>2</sub> PAFC within Porous SiC Matrix, Porous Graphitic electrode Coated with a Pt catalyst.	6
<b>Figure I.4</b>	Shematic of H <sub>2</sub> /O <sub>2</sub> PEMFC within Porous Carbon electrodes (Carbon cloth or paper) Coated with a Pt catalyst.	7
<b>Figure I.5</b>	Schematics of H <sub>2</sub> /O <sub>2</sub> AFC within Porous Carbon or Nickel electrodes or Pt/C.	9
<b>Figure I.6</b>	Schematic the H <sub>2</sub> /O <sub>2</sub> .Molten Carbonate electrolyte immobilized in Ceramic matrix with Nickel based electrodes.	10
<b>Figure I.7</b>	Schematic the H <sub>2</sub> /O <sub>2</sub> SOFC.the ceramic electrolyte is solid state, a nickel-YSZ cermet and mixed conducting for cathode.	11
<b>Figure I.8</b>	Schematic of proton exchange membrane fuel cells (PEMFCs).	14
<b>Figure I.9</b>	Shematic of fuel cell (PEMFCs) curve within three losses regione.1-Cell Potential losses, 2- Linear Drop in the cell, 3- Mass transport.	22
<b>Figure I.10</b>	combined fuel cell I – V and power density curves for proton exchange membrane fuel cells (PEMFCs).	23
<b>Figure I.11.a.b</b>	Presented the substrate as Carbon Paper and treated with 15 wt % PTFE.	25
<b>Figure I.12</b>	Presented the morphology of catalyst layer using spraying method (a),(b),with MEA (d), and casting method for (c)	27
<b>Figure I.13</b>	Schematic of sulfonated polytetrafluoroethylene (PTFE) structure used as ion conducting electrolyte in PEMFCs.	29
<b>Figure I.14</b>	Membrane electrode assembly (MEA) and Cross Section MEA Fabricated in Sel Fuel Institute Ukm	32

<b>Figure I.15 a</b>	Presented carbon black type VulcanXC-72R (Cabot) USA VulcanXC72R (Cabot) USA	34
<b>Figure I.15 b</b>	Presented TEM of Platinum supported Carbon 20 wt% Pt/C.	34
<b>Figure II.1 a</b>	Backing Layer Substrate (Carbon Cloth with 15 wt% PTFE)	38
<b>Figure II.2</b>	Electrode Structure with diffusion layer (GDL).	39
<b>Figure II.3</b>	Membrane Electrode Assembly (MEA)	41
<b>Figure II.4</b>	Component of single cell for proton exchange membrane fuel cells(PEMFCs).	42
<b>Figure II.5</b>	Single cell test station for proton exchange membrane fuel cell system (PEMFCs).	43
<b>Figure II.6.a</b>	XRD Analysis machine with the sample holder	44
<b>Figure II.6.b</b>	XRD samples (Powder and $E_{CaT}$ ) for electrode preparation for proton exchange membrane fuel cells(PEMFCs)	45
<b>Figure II.7</b>	TEM Machine using a Philips CM 120 microscope Ukm.	45
<b>Figure III.1.a</b>	Scanning electron microscopic (SEM) for Diffusion layer (GDL) thesis 2001	49
<b>Figure III.1.b</b>	Scanning electron microscopic (SEM) for Catalyst layer (Pt/PTFE/C 10 wt% Pt/C magnificated 500 $\mu$ m without Nafion <sup>®</sup> Pt =0.38mgPt/cm	49
<b>Figure III.2.a.</b>	Scanning Electron Microscopy of E-TEK electrode 10 % Pt/C loading 0.4 mgPt/cm <sup>2</sup> .	49
<b>Figure III.2.b</b>	cross section of membrane electrode assembly (MEA) without diffusion layer (GDL),	49
<b>Figure III.3.a</b>	Scanning Electron Microscopy (SEM) for diffusion layer (GDL) magnificated 1 $\mu$ m.	50
<b>Figure III.3.b.</b>	Scanning Electron Microscopy (SEM) for Catalyst layer (Pt/PTFE/C 20 wt% Pt/C magnificated 1 $\mu$ m without	50

---

Nafion<sup>®</sup> Pt = 0.3mgPt/cm<sup>2</sup>.

<b>Figure III.4.a</b>	Scanning Electron Microscopy (SEM) for Catalyst layer (Pt/PTFE/C/ Nafion <sup>®</sup> ) using 20 wt% Pt/C magnificated 1 $\mu$ m.	50
<b>Figure III. 4.b</b>	SEM of membrane electrode assembly (MEA) and cross section of membrane (112) Fabricated in sel fuel Ukm	50
Figure III.5.a	XPS survey spectrum of a)-(PTFE/C) and b)- (Pt/C/PTFE) catalyst layer electrode	53
<b>Figure III.6.a</b>	Cure Fitting XPS-spectra for carbon (C <sub>1s</sub> ) a)-(PTFE/C) and b)- (Pt/C/PTFE) catalyst layer electrode	55
<b>Figure III.7</b>	Cure Fitting XPS-spectra for Oxygen (O <sub>1s</sub> ) a)-(PTFE/C) and b)- (Pt/C/PTFE) catalyst layer electrode	57
<b>Figure III.8</b>	Cure Fitting XPS-spectra for Fluorine (F <sub>1s</sub> ) a)-(PTFE/C) and b)- (Pt/C/PTFE) catalyst layer electrode	58
<b>Figure III.9</b>	Cure Fitting XPS-spectra for silicon (Si <sub>2p</sub> ) a)-(PTFE/C) and b)- (Pt/C/PTFE) catalyst layer electrode	59
<b>Figure III.10</b>	Cure Fitting XPS-spectra for platinum (Pt <sub>4f</sub> ) a)-(PTFE/C) and b)- (Pt/C/PTFE) catalyst layer electrode	60
<b>FigureIII.11.a.b</b>	Cell voltage and power density vs. current density plots of single cell (25 cm <sup>2</sup> ) with various air flow rates. (b) Cell voltage and power density vs. current density plots of single cell (25 cm <sup>2</sup> ) with various hydrogen flow rates.	61
<b>Figure III.12.a,b</b>	Cell voltage and power density vs. current density plots of single cell (25 cm <sup>2</sup> ) with various humidifier temperatures. b Cell voltage and power density vs. current density plots of single cell (25 cm <sup>2</sup> ) with various air/H <sub>2</sub> pressures ratio.	63

---

<b>FigureIII.13.a</b>	Scanning electron microscopic (SEM) for diffusion Layer (GDL) for magnificated 1 $\mu\text{m}$ ,	64
<b>FigureIII.13.b</b>	Scanning electron microscopic (SEM) for catalyst Layer (Pt/PTFE/C) without Nafion using 20 wt% Pt/C	64
<b>FigureIII.14.a</b>	Scanning electron microscopic (SEM) for catalyst Layer (Pt/PTFE/C) using 20 wt% Pt/C magnificated 1 $\mu\text{m}$	65
<b>FigureIII.14.b</b>	Scanning electron microscopic (SEM) for MEA and cross section using membrane 112 fabricated in sel fuel Ukm	65
<b>FigureIII.15.a.b</b>	XPS survey spectrum of catalyst layer before testing ( $E_{bT}$ ) and after testing ( $E_{CaT}$ ).	66
<b>FigureIII.16.a.b</b>	Cure Fitting XPS-spectra for carbon ( $C_{1s}$ ) of catalyst layer before testing ( $E_{bT}$ ) and ( $E_{CaT}$ ).	67
<b>Figure III.17</b>	a-Cathode mass concentrations for ( $E_{bT}$ ) and b- Cathode mass concentration degradation ( $E_{CaT}$ ) for electrode 20 wt% Pt/C loaded 0.3 $\text{mg}_{Pt}/\text{cm}^2$ .	68
<b>FigureIII.18</b>	a Cure fitting XPS-spectra for before testing ( $E_{bT}$ ) and b oxygen ( $O_{1s}$ ) of catalyst layer after testing ( $E_{CaT}$ ).	69
<b>FigureIII.19.a.b</b>	Cure fitting XPS-spectra for oxygen ( $F_{1s}$ ) before ( $E_{bT}$ ) and after testing for Electrode ( $E_{CaT}$ )	70
<b>Figure III.20.a.b</b>	Cure fitting XPS-spectra for oxygen ( $S_{2p}$ ) of catalyst layer before testing ( $E_{bT}$ ) and after test ( $E_{CaT}$ )	71
<b>Figure III.21.a.b</b>	Curve fitting XPS-spectra for platinum ( $Pt_{4f}$ ) of catalyst layder before and after testing ( $E_{bT}$ ) and ( $E_{CaT}$ ).	72
<b>Figure III.22</b>	XRD for 1.Catalyst 20 wt% Pt/C before operation and, 2. Catalyst (Cathode) after operation ( $E_{Cat}$ ) loaded 0.3 $\text{mg}_{Pt}/\text{cm}^2$	74
<b>Figure III.23</b>	TEM of electrode 20 wt% Pt/C –a before testing and –b after testing in single cell 25 $\text{cm}^2$ .	75
<b>Figure III.24</b>	Schematic of functioning principle of PEM fuel cell.	78

<b>Figure III.25</b>	Fuel cell's voltage as a function of cell's current density at $T = 298\text{K}$ , data: $\blacktriangle$ Pt loading = $0.18 \text{ mg cm}^{-2}$ , $\blacksquare$ Pt loading = $0.38 \text{ mg cm}^{-2}$ and $\bullet$ E-TECK electrode with Pt loading = $0.4 \text{ mg cm}^{-2}$ model: (dashed line) Pt loading = $0.18 \text{ mg cm}^{-2}$ , (solid line) Pt loading = $0.38 \text{ mg cm}^{-2}$ and (dotted line) E-TECK electrode with Pt loading = $0.4 \text{ mg cm}^{-2}$ .	82
<b>Figure III.26</b>	Fuel cell's voltage as a function of cell's current density for different temperatures at Pt loading = $0.38 \text{ mg cm}^{-2}$ ; model: (dotted line) 298K, (solid line) 313K and (dashed line) 353K	84
<b>Figure III.27</b>	Fuel cell's power density as a function of cell's current density for different temperatures at Pt loading = $0.38 \text{ mg cm}^{-2}$ ; model: (solid line) 298K and (dashed line) 353K.	85
<b>Figure III.28</b>	Fuel cell's voltage as a function of cell's current density for different fuel cell's reactants partial pressure at $T = 298\text{K}$ and Pt loading = $0.38 \text{ mg cm}^{-2}$ ; model: (dashed line) $P_{\text{H}_2} = 0.995 \times 10^5 \text{ Pa}$ and $P_{\text{O}_2} = 0.606 \times 10^5 \text{ Pa}$ , (solid line) $P_{\text{H}_2} = 1.01 \times 10^5 \text{ Pa}$ and $P_{\text{O}_2} = 1.01 \times 10^5 \text{ Pa}$ .	86

<b>List of Tables:</b>	<b>Titles</b>	<b>Pages</b>
<b>Table I. 1</b>	Comparison Summary of the five Major Fuel Cell Types	12
<b>Table I.2</b>	Comparison between PEMFCs and DMFCs	15
<b>Table I.3</b>	Water Uptake,Weight Percent,and swelling for Nafion Membranes.	31
<b>Table II.3</b>	XPS measurement parameters	46
<b>Table III.1</b>	Semi-quantitative analysis of (PTFE/C) diffusion layer using XPS technique	52
<b>Table III.2</b>	Semi-quantitative analysis of (Pt/C/PTFE) catalyst layer of using XPS technique	52
<b>Table III.3</b>	Semi-quantitative analysis of (E-TEK) electrode using XPS technique	52
<b>Table III.4.a</b>	XPS parameters for carbon ( $C_{1s}$ ) curve fitting for the diffusion layer (PTFE /C)	55
<b>Table III.4.b</b>	XPS parameters for carbon ( $C_{1s}$ ) curve fitting for the Pt/C/PTFE catalyst layer	55
<b>Table III.5.a</b>	XPS parameters for oxygen ( $O_{1s}$ ) curve fitting for the PTFE/C diffusion	56
<b>Table III.5.b</b>	XPS parameters for oxygen ( $O_{1s}$ ) curve fitting for the (Pt/C/PTFE) catalyst layer	57
<b>Table III.6.a</b>	XPS parameters for fluorine ( $F_{1s}$ ) curve fitting for the PTFE/C diffusion	58
<b>Table III.6.b</b>	XPS parameters for fluorine ( $F_{1s}$ ) curve fitting for the Pt/PTFE/C catalyst layer	58
<b>Table III.7.a</b>	XPS parameters for silicon ( $Si_{2p}$ ) curve fitting for the PTFE/C diffusion layer	59
<b>Table III.7.b</b>	XPS parameters for silicon ( $Si_{2p}$ ) curve fitting for the Pt/PTFE/C catalyst layer	59
<b>Table III.8</b>	XPS Parameters for platinum ( $Pt_{4f}$ ) curve fitting for the	60

---

Pt/PTFE/C catalyst layer

**Table III.9** Characteristic of electrode with Different Flow rate of Air/H<sub>2</sub>. 62

**Table III.10** Characteristic of electrode with Different Pressures and Humidifiers Temperatures of Air/H<sub>2</sub>. 63

**Table III. 11** Cathode microscopic evolution (aging) for (E<sub>bT</sub>) and (E<sub>CaT</sub>). 68  
for electrode 20 wt% Pt/C loaded 0.3 mgPt/cm<sup>2</sup>

**Table III.12** Experimental and calculated parameters used in the simulation 77

**Table III.13** Variation of the parameters  $\psi$  and  $i_0$  with platinum loading at T = 298K 83

---



## GENERAL INTRODUCTION

The beginning of this universe, energy leads the human being activities, and consider as a key for survive and development. Coal is the first source of energy use at that time with growing of population, the demand of energy increase, which necessity other sources to satisfy the demand. Petroleum and gas come later to support the coal and reduce the tension. These fossil fuels energies reduce the demand but increase the concentration of  $\text{CO}_2$  in atmosphere by combustion of these fossil fuels. The rising using this energy gives birth a new phenomenon called greenhouse effect, which due to the increasing in the carbon dioxide ( $\text{CO}_2$ ) in the atmosphere. The  $\text{CO}_2$  result from combustion combined with humidity ( $\text{H}_2\text{O}$ ) to form carbonic acid,  $\text{NO}_x$ , and  $\text{SO}_x$  with humidity in the atmosphere give born to nitric acid ( $\text{HNO}_3$ ) and sulfuric acid ( $\text{H}_2\text{SO}_4$ ) respectively. All these changes in compounds structures harm the environment. For this reason researchers increases their interest in replacing this energy by another energy that can be clean and friendly. therefore to solve these problems should change these fossil energies by new energies that have less pollution and got may be the same efficiency. Researchers found these energies they call it renewable energy, which can replace the old (fossil) energy by new energy. That have less pollution (zero carbon dioxide) and renewable.

Proton exchange membrane fuel cells (PEMFCs) is the one of these promising clean energies that required for high efficiency, low pollution (Zero Pollution) and friendly use. This type of renewable energy is typically operated on pure hydrogen ( $\text{H}_2$ ) as fuel and oxygen ( $\text{O}_2$ ) as oxidant. The PEM fuel cell combines the hydrogen fuel with the oxygen ( $\text{O}_2$ ) from the atmosphere to produce Water, heat and electricity. Only Hydrogen as fuel and oxygen as oxidant with platinum as catalyst to convert chemical energy to electrical energy. Forever the struggle is to reduce the cost of proton exchange membrane fuel cell by studying the different components and parameters effect like catalyst loading, monomers, binder, operating conditions (pressure, temperature, humidifiers temperature....), and also electrode and MEA degradation. The objective for this work is: first electrode fabrication based on Pt as catalyst supported by carbon black 10 wt% Pt/C and 20 wt% Pt/C. Second is to characterize the electrodes by Scanning Electron Microscopic (SEM), X-Ray photo spectroscopic (XPS), for the first structure , and the Scanning Electron Microscopic (SEM), X-Ray photo spectroscopic (XPS), X-Ray Diffraction (XRD) and Transition Electron Macroscopic (TEM). Then followed by the physicals parameters effect such as: Humidifiers temperature, Pressures and Flowrate Air/ $\text{H}_2$  on the electrode

performance, also the electrode microscopic degradation especially on cathode loaded 20wt% Pt/C after 100 hours of testing in single cell 25 cm<sup>2</sup> surface area, by using the XPS, XRD and TEM. The last part is to simulate the effects of these parameters by using a model explaining these physical parameters effect. The structure of this thesis is as follows on:

### **Chapter I**

Consist of history and development of fuel cell especially for proton exchange membrane fuel cell (PEMFCs), which inclusion the principle and aspect thermodynamic, theory of gas diffusion electrode, electrode fabrication and components, parameters affecting performance.

### **Chapter II**

The chapter describes the experimental part. First is the electrode fabrication for two types of electrodes using platinum supported carbon 10 wt % and 20 wt %. The 10 wt % Pt/C used to study the diffusion layer and catalyst layer in the electrode, and 20 wt % Pt/C % used for the physical parameters effects and electrode (Cathode) degradation. The loading for three electrodes  $E_{GDL} = 0.38 \text{ mgPt/cm}^2$  platinum loading with diffusion layer using 10 wt % Pt/C, and  $E_{TeK} = 0.4 \text{ mgPt/cm}^2$  E-TEK electrode (Commercial) respectively. The second Structure of electrode 20 wt % ( Pt/C) named E =  $0.3 \text{ mgPt/cm}^2$ , which also contain the treatments of membranes (Nafion ®117) ,(Nafion ®112) for 10 and 20 wt % Pt/C %. Finally the testing of electrodes for the structures 20 wt % Pt/C % in single cell connected to the test station.

### **Chapter III**

Consist of the analysis techniques for different structures 10 wt% Pt/C and 20 wt% Pt/C, which analyzed by SEM, XPS, for the 10 wt% Pt/C structure for diffusion layer and catalyst layer. Second is the operating of electrode in single cell for 20 wt% Pt/C more than 100 hours with different parameters (pressures, flow rate, humidifiers temperatures), than analysis the electrode (cathode) 20 wt% Pt/C by using SEM, XPS, XRD, TEM techniques after aggressive operating condition as pressures effect, humidifier temperature, flow rate of reactants and on/ off the system more than 100 hours in single cell 25 cm<sup>2</sup>. Last part of this chapter is focused on the simulation and modeling for PEM fuel cell. The obtained model used to analyze the impact of individual fuel cell's operating parameters on cell's performance; it is also possible to determine the activation loss parameters of the PEM fuel cell.

***CHAPTER I***  
***FUEL CELLS GENERALITY AND***  
***APPLICATION***

**Introduction**

In 1839, the first fuel cell was conceived by sir William Robert Grove (1811-1896). He mixed hydrogen and oxygen in the presence of catalyst and electrolyte to make electricity and water. The principles was discovered by accident during an electrolysis experiment using a battery, then disconnect the battery from the electrolyze connected the two electrodes together, he observed a current flowing in the opposite direction, consuming the gases of hydrogen and oxygen Fig I.1. The invention come later to be known as "fuel cell" in 1889, the term "fuel cell" was first coined by Ludwig Mond and Charles Langer Who attempted to build a working fuel cell using air from industrial coal gas. Another source states that is was William white Jaques who first coined the term fuel cell, Jaques also the first researcher to use phosphoric acid in electrolyte bath in 1920, fuel cell research in Germany paved the way to the development of the carbonate cycle in solid oxide fuel cells of today.

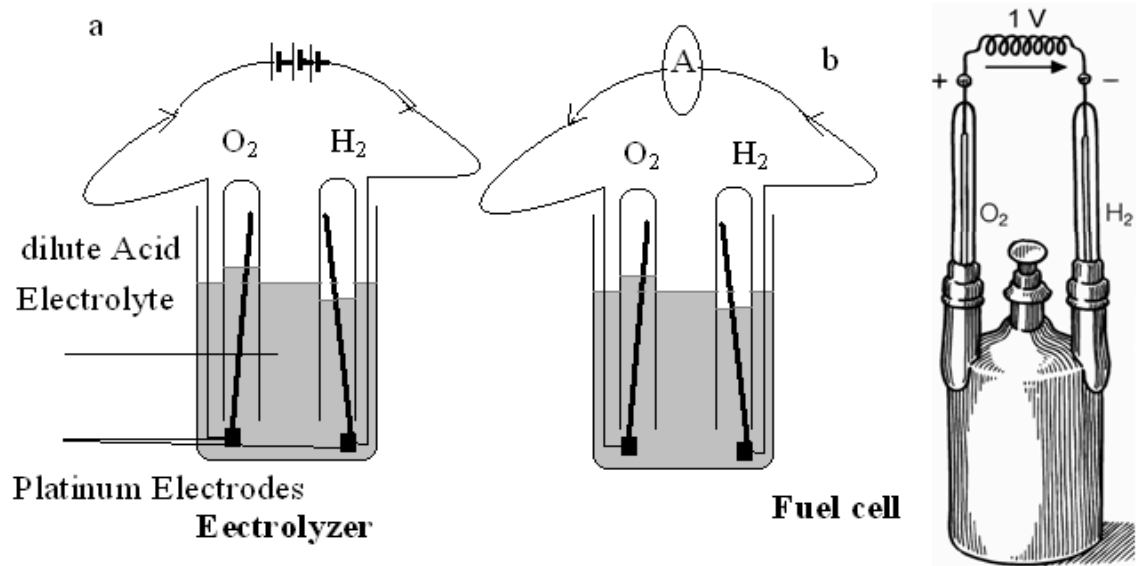


Figure I.1. The principle of an electrolyzer (a); of a fuel cell (b) [1]

In 1932, engineer Francis T Bacon began his vital research into fuels cells used porous platinum electrodes and sulphuric acid as electrolyte bath. Later he changed Platinum by inexpensive metal by nickel electrodes and used an alkaline electrolyte that less corrosive. It took bacon until 1959 to perfect his design and demonstrate a five –kilowatt fuel cell that could power a welding machine, and named by his famous fuel cell design ‘Bacon Cell’ [2]. In the early 1960s, attention turned again to the platinum-catalysed acid electrolyte cell in different forms.

One used a polymer acid electrolyte, which made it simple and reliable. Its combined electrode-electrolyte structure made it automatically water-rejecting, and at its original modest power levels ( $37\text{mA}/\text{cm}^2$ ) [3] it required no wet proofing. its original electrolyte material restricted its operating temperature and thus its performance, but it was developed by general electric for modest power requirements (1Kw in 29 kg unit) of the Gemini mission, where its ability to produce portable water for astronauts was a great advantage in the lightweight capsule. The successes in the space program by Gemini and Apollo spacecraft in design and production of fuel cells, but encountered technical barriers and high investment costs for commercialisation potential of fuel cells and is the One of three fuel cells aboard the Space Shuttle. These fuel cells provide all of the electricity as well as drinking water when Space Shuttle is in flight. It produces 12 kilowatts electricity, and occupies 154 liters as presented in Fig I.2 (Photo courtesy of NASA).

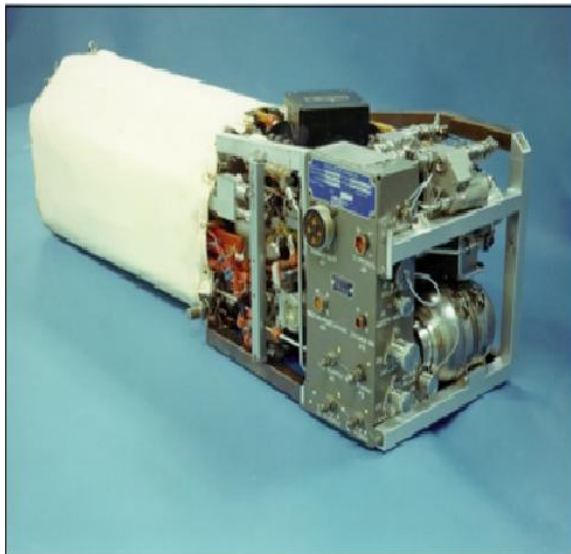


Figure 1.2 NASA Space Shuttle fuel cell

Since then, fuel cells have been used in many other applications. Fuel cells are used for primary and backup power for commercial, industrial and residential buildings and in remote or inaccessible areas. They are used to power fuel cell vehicles, including automobiles, buses, forklifts, airplanes, boats, motorcycles and submarines.

### **I.1 What is fuel cell?**

A fuel cell is a device that converts the chemical energy of a fuel into direct electrical energy in a constant temperature process. This device so great about pollution, changing the climate or running with out of oil, natural gas and coal. Fuel cells operate on a wide range of fuels,

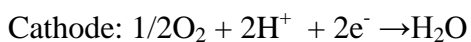
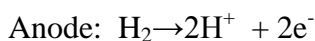
including hydrogen, and are seen as a clean, high efficiency than the existing fuel burning engines and high power source.

## **I.2 Main Categories of fuel cells.**

A number of fuel cell varieties have been developed to differing, and the most basic nomenclature to describe them according to the electrolyte material utilized. They are made up of three segments which are sandwiched together: the anode, the electrolyte, and the cathode. Two chemical reactions occur at the interfaces of the three different segments. The net result of the two reactions is that fuel is consumed, water or carbon dioxide is created, and an electric current is created, which can be used to power electrical devices, normally referred to as the load. At the anode a catalyst oxidizes the fuel, usually hydrogen, turning the fuel into a positively charged ion and a negatively charged electron. The electrolyte is a substance specifically designed, which the ions can pass through it, but the electrons cannot. The freed electrons travel through a wire creating the electric current. The ions travel through the electrolyte to the cathode. Once reaching the cathode, the ions are reunited with the electrons and the two react with a third chemical, usually oxygen to create water or carbon dioxide. Five major types of fuel cells, differentiated from one another on the basis of their electrolyte:

### **I.2.a Phosphoric acid fuel cell (PAFC).**

In the phosphoric acid, liquid  $\text{H}_3\text{PO}_4$  electrolyte (ether pure or highly concentrate) is contained in a thin SiC matrix between two porous graphite electrodes coated with a platinum catalyst. Hydrogen is used as the fuel and air or oxygen may be used as the oxidant as presented in the Fig I.3 and the reactions occurred at the surface of electrodes as following:



PAFC use platinum catalysts, which susceptible to carbon monoxide can be important when running on reformed or impure feed stocks at high temperature carbon monoxide tolerance at the anode can be as high as 0.5-1.5%, and sulfur tolerance present as  $\text{H}_2\text{S}$  is around 50 ppm (Parts per Million) [4]. the operating temperature from 180 -210°C with the electrical efficiencies are 40% and combined heat and power achieving 70%.the main advantage for PAFC are:

excellent reliability /long-term performance, electrolyte is relatively low-cost, and Mature technology. Other hand the disadvantages are: expensive platinum catalyst, susceptible to CO, and corrosive electrolyte.

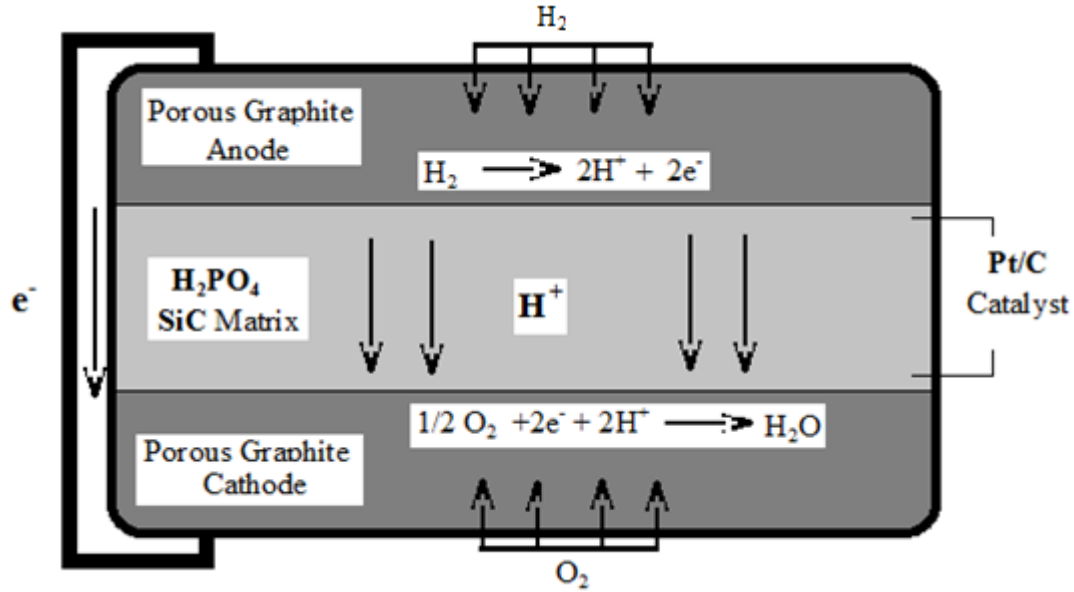
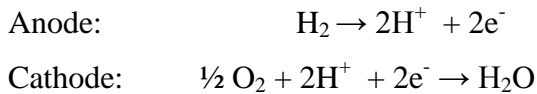


Figure I. 3 Schema present the H<sub>2</sub>/O<sub>2</sub> PAFC within Porous SiC Matrix, Porous Graphitic electrode Coated with a Pt catalyst

**I.2.b Polymer electrolyte membrane fuel cell (PEMFC)**

The PEMFC is constructed from a proton-conducting polymer electrolyte membrane, usually a perfluorinated sulfonic acid polymer. Anode and cathode reaction in the PEMFC is similar like PAFC are:



The anode and cathode component are presented in Fig. I.4. The polymer membrane in PEMFC use in hydrated state with thickness between (20-200µm), flexible, and transparent. The operating temperature for Proton exchange membrane fuel cell is limited to 90°C or lower. While the H<sub>2</sub> is the fuel of choice, liquid fuels can use as methanol (DMFC), formic acid. The main advantages that make PEMFC leads all these fuel cells are: High power density (300-1000 mW/cm<sup>2</sup>), Good start-stop capabilities, low temperature and possibility portable application.

Beside the disadvantages are: Expensive platinum catalyst and polymer membrane, water management Problem.

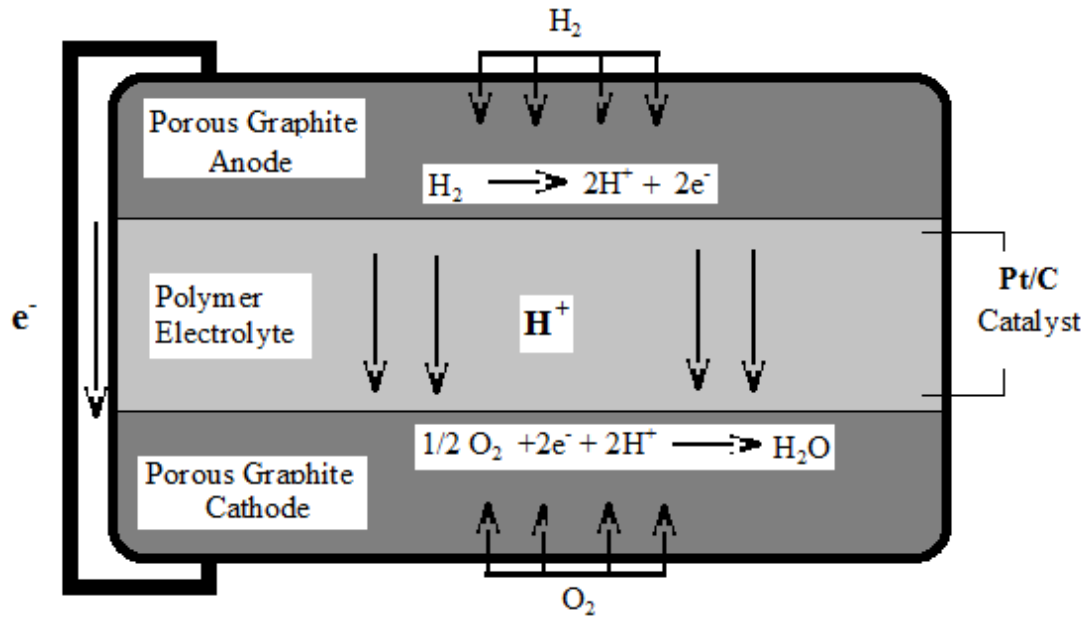


Figure I. 4 Schema present the H<sub>2</sub>/O<sub>2</sub> PEMFC within Porous Carbon electrodes (Carbon cloth or paper) Coated with a Pt catalyst

And the other type of similar for proton exchange membrane fuel cell is DMFC, which use the same components exception the fuel.

In DMFC methanol is fed directly as the fuel, the methanol systems have several advantages over fuel cell system based on hydrogen and compressed a natural gas[4,6].The liquid nature of methanol under room temperature and atmospheric pressure simplify the methanol transport and application. Methanol has the highest hydrogen-to-carbon ratio among alcohol, which means the the highest energy could be generated and less carbon dioxide emitted

In DMFCs the methanol is introduced to the anode, where it is split into protons and free electrons and gives out carbon dioxide, the hydrogen ions flow through the polymer electrolyte membrane to the electrode, where the air or oxygen introduced..

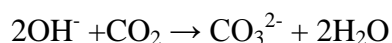
At the cathode, the hydrogen ions are bonded with the oxygen to form water and the movement of the electrons from anode to cathode creates current that can be used to power an electrical device.



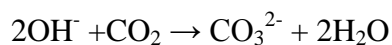
In DMFC the catalyst is similar to PRMFCs ,which use the Pt/Rh (Platinum and Ruthinium) that considered to be the best anode catalyst and Pt catalyst is the best for cathode[7].

### **I.1.c Alkaline Fuel Cell (AFC).**

The first alkaline electrolyte used in fuel cell was KOH in the 19<sup>th</sup> century. The fuel was solid carbon and oxygen. This was followed by the work of Francis Bacon, whose goal was to develop a 5 kW system using pure hydrogen and oxygen as the reactants [8]. The AFC employs an aqueous potassium hydroxide electrolyte, in contrast to acidic fuel cells where H<sup>+</sup> is transmitted from the anode to cathode, in an alkaline fuel cell OH<sup>-</sup> is conducted from the cathode to the anode, and the reaction occurs as following.



Thus water consumed at the cathode of an AFC while it is produced (twice as fast) at the anode, if the excess water not moving from the system, the performance it will degrade. AFC use nickel as catalyst rather than Platinum but can use it at cathode, which required pure Hydrogen (H<sub>2</sub>) and pure oxygen (O<sub>2</sub>) as fuel and oxidant thus presented in the Fig I.5 depending upon the concentration of KOH in the electrolyte, In presence of CO<sub>2</sub> in an AFC degrade the KOH (electrolyte) as follows:



Over time, the concentration of OH<sup>-</sup> in the electrolyte declines and the K<sub>2</sub>CO<sub>3</sub> can begins to precipitate out of the electrolyte. The AFC can operate at temperature between 60-250°C , as advantage for this type of fuel cell are: low cost for catalyst and electrolyte and disadvantage is operating Pure H<sub>2</sub>/O<sub>2</sub>.

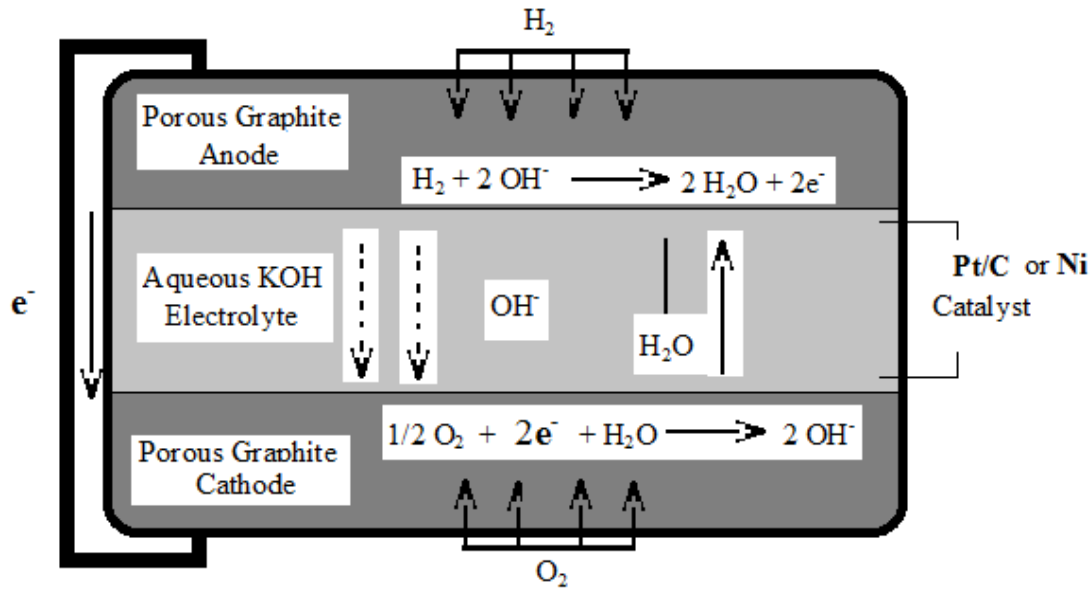


Figure I. 5 Schematic the  $\text{H}_2/\text{O}_2$  AFC within Porous Carbon or Nickel electrodes or Pt/C.

#### I.2.d Molten Carbonate Fuel Cell (MCFC).

Molten Carbonate Fuel Cell (MCFC) are approaching the stage of commercialization, after having been under study and development for more than 50 years [2], the electrolyte in the MCFC is a molten mixture of alkaline carbonates,  $\text{Li}_2\text{CO}_3$  and  $\text{K}_2\text{CO}_3$ , immobilized in a  $\text{LiOAlO}_2$  matrix. The carbonate ion,  $\text{CO}_3^{2-}$  act as the mobile charge carrier in the MCFC. the electrodes a nickel based; the anode usually consist of a Nickel/Chrome alloy while the cathode consist of a lithiated Nickel oxide as presented in the Fig I.6.

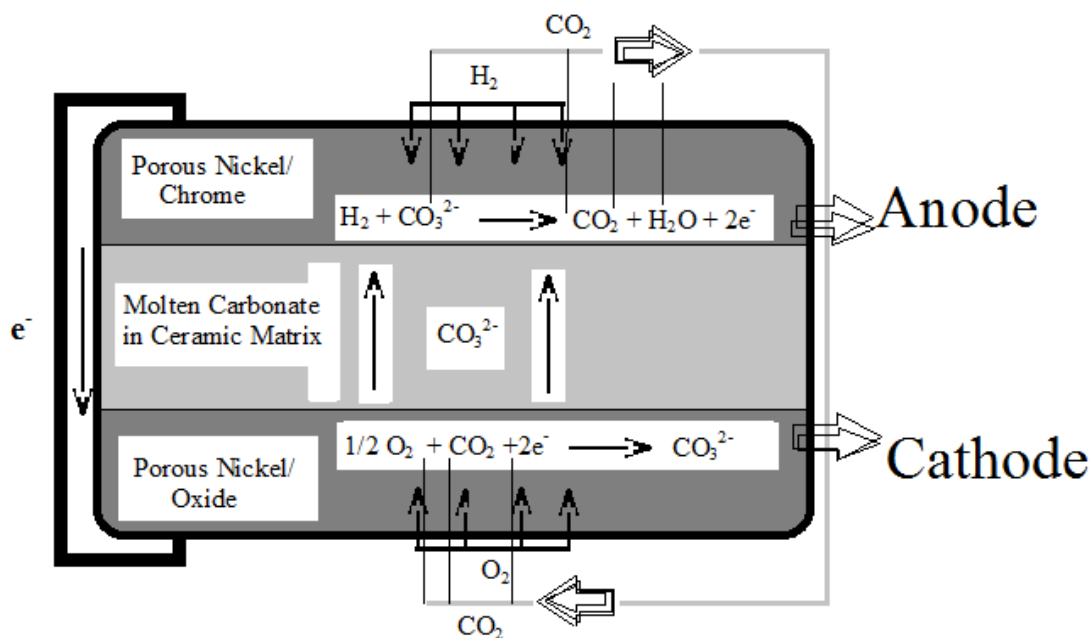
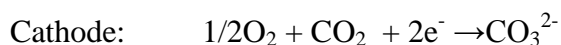
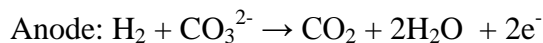


Figure I.6 Schematic the H<sub>2</sub>/O<sub>2</sub>. Molten Carbonate electrolyte immobilized in Ceramic matrix with Nickel based electrodes.

The anode and cathode reactions are therefore:

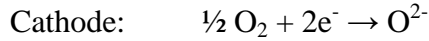
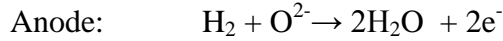


In the MCFC the CO<sub>2</sub> is produce at the anode and consumed in the cathode, therefore MCFC systems must exact the CO<sub>2</sub> from the anode and recirculate it to the cathode. The relatively high operating temperature is 650°C. MCFC can run on Hydrogen (H<sub>2</sub>), simple hydrocarbons (CH<sub>4</sub>), and simple alcohols. Carbon Monoxide tolerance is not an issue for MCFC; rather than as a poison, CO act as a fuel. Heat and power can reach 90%. The most advantages for MCFC are: Fuel Flexibility, inexpensive catalyst and high –quality waste heat for co-generation applications and the disadvantages are: Must implement CO<sub>2</sub> recycling, Electrolyte corrosive, degradation lifetime issues, and relatively expensive materials.

### **I.2.e Solid Oxide Fuel Cell (SOFC)**

Solid Oxide Fuel Cells (SOFC) began with Nernst's 1899 demonstration of the ionic conductivity of solid state Yattia-stabilized Zirconia (YSZ) [9]. Modern SOFC developed has been revived worldwide in Europe , Unite state ,and Asia are competing to bring small and large SOFC to the

market. The SOFC uses a solid ceramic electrolyte consist of Yattia-stabilized Zirconia (YSZ), which in an oxygen ion (oxygen vacancy) conductor. Since  $O^{2-}$  is the mobile conductor in this case, the anode and cathode reactions are:



The most common material for the anode electrode in SOFC is a nickel-YSZ cermet (a cermet is a mixture of ceramic and metal).the cathode electrode usually a mixt ion-conducting and electronically conducting ceramic material as presented in Fig I.7.

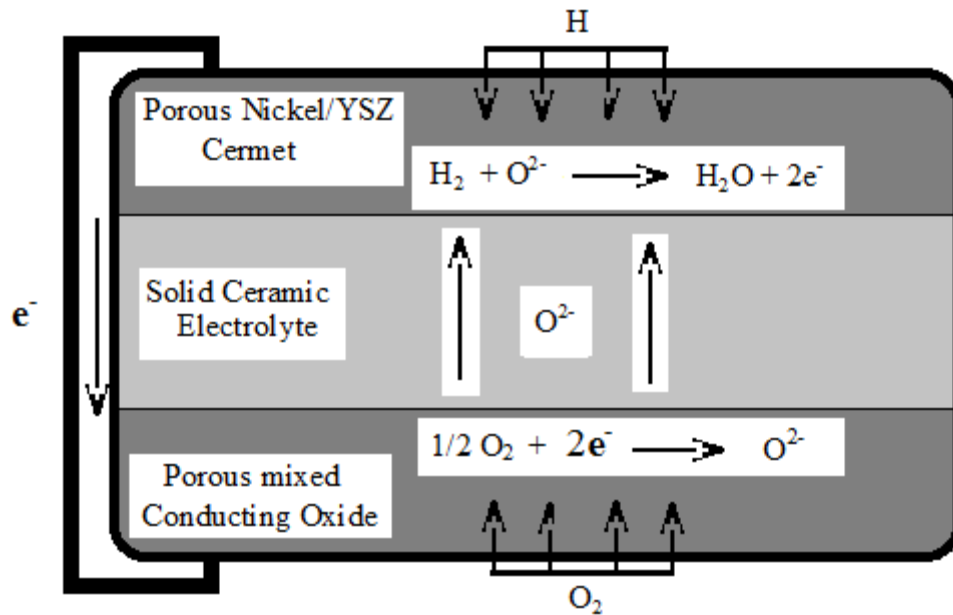


Figure I. 7 Schematic the  $H_2/O_2$  SOFC.the ceramic electrolyte is solid state,a nickel-YSZ cermet and mixed conducting for cathode

The current operating temperature of most of SOFC system is around 800-1000°C, although new technology has demonstrated 600°C operation. The advantage of this fuel cell are: fuel flexibility, non-precious metal catalyst, solid electrolyte and relatively high power density. Other hand disadvantage sealing issues and high temperature. the differences between these fuel cells types are in the electrolytes, which gives differences in reaction chemistry, operating

temperature, cell materials, cell design. The fuel cell performance and efficiencies follow these changes as presented in the Tab I.1.

Tables I. 1.Comparaison Summary of the five Major Fuel Cell Types

Fuel Cell Type	Electrical Efficiency %	Power Density (mW/cm <sup>2</sup> )	(kW Power Rang	Internal Reforming	CO Tolerance
PAFC	40	150-300	50-1000	No	poison<1%
PEMFC	40-50	300-1000	0.001-1000	No	poison<50ppm
AFC	50	150-400	1-100	No	poison<50ppm
MCFC	45-55	100-300	100-1000.000	Yes	Fuel
SOFC	50-60	250-350	10-1000.000	Yes	Fuel

All these fuel cell types use the H<sub>2</sub> as best fuel, the high-temperature fuel cell can also run on simple hydrocarbon fuels or CO via direct electro-oxidation or internal reforming. Today, the PEMFC and SOFC appear poised to best meet potential application. PEMFCs are especially suitable for portable and small stationary applications while SOFCs appear suitable for distributed-power and utility-scale power applications. This is the reason we concentrate to study proton exchange membrane fuel cells (PEMFCs) because their specific characteristics like zero pollution, high power density, low operating temperature, solid electrolyte.

**I.3 Proton exchange membrane fuel cells (PEMFCs).**

Proton exchange membrane (PEM) fuel cells is the one of the most promising types of fuel cells precedents because of their no mobile solid polymer electrolyte, relatively lower operating temperatures (<80 °C), lightweight, high power density and friendly (Zero emission). However, survivability, durability, operation, and rapid startup of fuel cell vehicles under sub-freezing temperatures, also the barriers to the technology that should be addressed before mass-market penetration of hydrogen powered PEMFC vehicles [10]. The PEM fuel cells still allows better

vehicular fuel economy and meets more stringent emission standards than internal combustion engines, also PEM fuel cells system running on hydrohen are seen as a future alternative to convrntional combustion engines for automotive application [11].

#### **I.4 Principe of proton exchange membrane fuel cells (PEMFCs)**

Proton exchange membrane fuel cells consist to deliver the energy from chemical fuels as hydrogen or other fuels direct to electrical energy. The PEM fuel cells systems composed of three components to convert the chemicals to electrical energy. Anode as a negative pole to split hydrogen molecules to atoms and electrons using Pt or other metals as catalyst, cathode as a positive pole to collect the electrons and protons coming from anode through the membrane to form water and heat. PEM fuel cell system functions as presented in Fig I. 8. Fuel hydrogen and oxidant oxygen or air are fueled to anode and cathode respectively, hydrogen fed to the anode in contact to Pt catalyst with the proper flow rate and pressure to oxidize to  $H^+$  and electrons ( $e^-$ )  $H_2 \rightarrow H^+ + e^-$ . The hydrogen proton move toward to the membrane and cross to the cathode to react with the oxygen and electrons  $O_2 + 4H^+ + 4e^- \rightarrow H_2O$  to form water and heat, the reaction mechanism are given as:

$O_{2(g)} \rightarrow O_{2ads}$  adsorption process in presence of catalyst

$O_{2ads} + 2e^- \rightarrow [O_{2ads}]^{2-}$  electron transfer

(1)  $[O_{2ads}]^{2-} + H^+ \rightarrow [HO_{2ads}]^-$ , (2)  $[HO_{2ads}]^- + H^+ + e^- \rightarrow [H_2O_{2ads}]^-$

(3)  $H_2O_2^- + 2H^+ + e^- \rightarrow 2H_2O$ , Final Reaction: (4)  $O_{2(g)} + 4H^+ + 4e^- \rightarrow 2H_2O$ . [12-13]

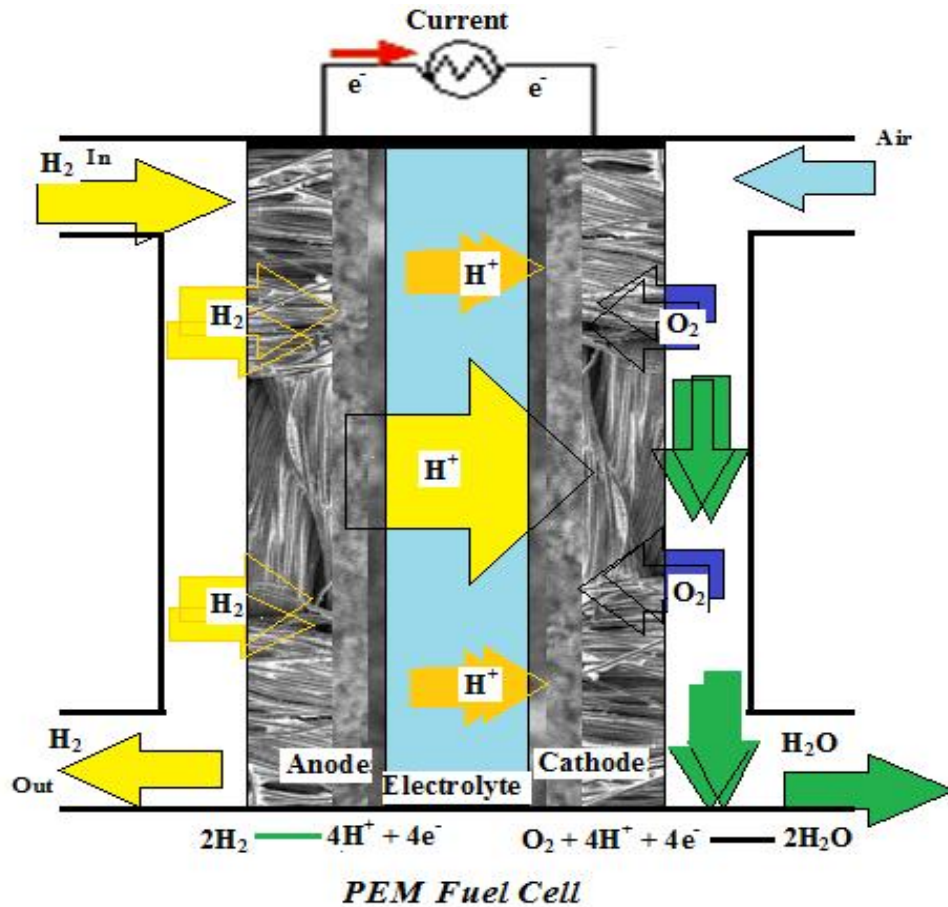


Figure I.8 Schematic of proton exchange membrane fuel cells (PEMFCs)

Two kinds of proton exchange membrane fuel cell in current use one use hydrogen (PEMFCs) as fuel other use methanol (DMFCs), these two fuel cell using same membrane as solid materials, but different in construction of electrode and fuel, the characteristics for both fuel cells enclosed in the Tab I.2. Each cell produces approximately 1.1 volts, so to reach the required voltage the cells are combined to produce stacks. Each cell is divided with bipolar plates which separating them to provide a hydrogen fuel distribution channel, as well as a method of extracting the current.

**I.5 Fuel source for proton exchange membrane fuel cells (PEMFCs)**

Hydrogen is the best or ideal fuel for PEMFCs as it yield the highest levels of fuel cells performance, but it is a secondary fuel which has to be produced from primary fuels (Naturel Gas, Petroleum, or coal), biomass or by electrolysis of water . The near term of hydrogen production and delivery as byproduct from chemical reactions, and supply through the pipes as

natural gas [15]. Hydrogen can be stored as a compressed gas, as a cryogenically cooled liquid or as metal hydride.

Table I.2 Comparison between PEMFCs and DMFCs. **Cédric G.** 2009(5) [14]

	Proton exchange membrane fuel cells (PEMFCs) Hydrogen ( H <sub>2</sub> )	Direct methanol fuel cells (DMFCs) Methanol (CH <sub>3</sub> OH)
catalyseur (Pt mg/cm <sup>2</sup> )	1 - 0,5	2 – 5
Tension d'utilisation (V)	0.75	0.5
Température d'utilisation (°C)	60-80	60
Cross over	/	4.10 <sup>-7</sup>
Sous-produits	H <sub>2</sub> O	CO <sub>2</sub>
Densité de puissance (mW/cm <sup>2</sup> )	300	80

**I.6. Aspect thermodynamic for proton exchange membrane fuel cells (PEMFCs)**

Thermodynamics is the study the transformation energetic for different forms. Since fuel cells are energy conversion devices, which convert the chemical energy (Fuels) into electrical energy. Thermodynamics is the key to understand the transformation or conversion the free energy of an electrochemical reaction into electrical energy (electrical work) [16-17] - this conversion can be based on thermodynamics laws.

There are two ways to transferred between a close system and its surrounding: via Heat (Q) or work (W).this allowed to us to write first law as:

$$dU = dQ - dW \tag{I.1}$$

This expression states that the change in the internal energy of a closed system (dU) must be equal to the heat transferred to the system (dQ) minis the work dones by the system (dW). (dW) consider as mechanical work  $W_{mech}$  so we can write as following .

$$dW_{mech} = pdV \tag{I.2}$$



Where  $p$  is the pressure and  $dV$  is the volume change; this case of thermodynamic for any system. In fuel cell later we will use the electrical work  $(dW)_{elec}$ .

$$dU = dQ - pdV \quad I.3$$

for a reversible system transfer of heat at constant pressure, the entropy  $S$  of the system will change followed the second law of thermodynamic as:

$$dS = dQ_{rev} / T \quad I.4$$

For fuel cell we are interested in electrical work and the maximum amount of electrical work that we can extract from a fuel cell reaction. The free energy is related to intern energy and entropy  $S$ . From the equation from intern energy a constant temperature and pressure we can write:

$$dU = T dS - pdV \quad I.5$$

Since we know that  $(dU/dS)_V = T$ , and  $(dU/dV)_S = -p$  we obtain

$$G = U - TS + PV \quad I.6$$

$$G = H - TS \quad I.7$$

$$dG = dH - TdS - SdT \quad I.8$$

for isotherm process and writing this relationship in term molar quantities gives

$$\Delta G_r = \Delta H_r - S\Delta_r T \quad I.9$$

This function is called the Gibbs free energy and depends on the temperature and pressure.

$$dG = dU - TdS - SdT + pdV + Vdp \quad I.10$$

For a reversible system and first Law car write as following:

$$dU = T dS - dW$$

$$dU = T dS - (pdV + dW_{elec}) \quad I.11$$

From the Equation I.10 and I.11 on obtain:

$$dG = - SdT + Vdp - dW_{elec} \quad I.12$$

For a constant temperature, and constant pressure ( $dT, dp = 0$ ) this reduce to

$$dG = - dW_{elec} \quad I.13$$

the relation between the electrical work  $W_{elec}$  and gibbs free energy is give equation (I.11) by using molar quantities, this equation can be written as:

$$W_{elec} = \Delta G_r \quad I.14$$

The potential of a system to perform electrical work is measured by voltage (also called electrical potential). The electrical work done by moving a charge  $Q$  measured in coulombs through an electrical potential difference  $E$  between anode and cathode ( $V_{rev,c} - V_{rev,a}$ ) in volts is:

$$W_{elec} = E Q \quad I.15$$

If the charge is assumed to be carried by electrons:

$$Q = n F \quad I.16$$

Where  $n$  is number of mole of electrons transferred and  $F$  is Faraday's constant combining Equations I.14, I.15, I.16 yields

$$\Delta G_r = - n F E \quad I.17$$

Thus, the Gibbs free energy sets the magnitude of the reversible voltage for an electro-chemical reaction, for PEMFCs with the Hydrogen and Oxygen as fuel and oxidant the reaction (I.15) has a Gibbs free energy change of  $-237$  KJ/mol under standard-state conditions for liquid water product.



the reversible voltage is .

$$\begin{aligned} E^{\circ} &= - \Delta G_r^{\circ} / nF \\ &= - (-237.000 \text{ J/mol}) / (2 \text{ mol } e^- / \text{mol reactant}) (96.400 \text{ C/mol}) \\ &= 1.23 \text{ V.} \end{aligned}$$

### **I.6.1 Variation of pressure and temperature for reversible voltage of fuel cell under non-standard state conditions**

Standard state reversible fuel cell voltage ( $E^{\circ}$  value) are only useful under standard state conditions (Room Temperature, atmosphere pressure, unit activities of all species), but for other condition the temperature and pressure influence on the reversible fuel cell voltage, the thermodynamics Equation can predict the reversible voltage of a fuel cell under any arbitrary set of conditions.

#### **I.6.1.a Reversible voltage variation with temperature**

The reversible voltage varies with the temperature must go back to Gibbs free energy, From Equation I.5 and I.6 we can write;

$$dG = -TdS + Vdp \quad \text{I.19}$$

$$(dG/dT)_p = -S \quad \text{I.20}$$

Use a molar reaction quantities, this become:

$$(\Delta G_r /dT)_p = -\Delta S_r \quad \text{I.21}$$

From the equation I.17 allow us to express how the reversible cell voltage varies as a function of temperature:

$$(\Delta E /dT)_p = \Delta S_r/nF \quad \text{I.22}$$

The reversible voltage at an arbitrary temperature T, at constant pressure,  $E_T$  can be calculated by:

$$E_T = E^o + \Delta S_r/nF (T - T_o) \quad \text{I.23}$$

Generally,  $\Delta S_r$  assumed to be independent to the temperature and for more accurate for  $E_T$  can calculate  $\Delta S_r$  by integrated the heat capacity related to the temperature.

For proton exchange membrane fuel cell  $\Delta S_r = - 44.43 \text{ J}/(\text{mol.K})$  for  $\text{H}_2\text{O}_{(g)}$  as product the voltage of cell voltage with the temperature is approximate as

$$E_T = E^o + -44.43 \text{ J}/(\text{mol.K}) /2.96400 (T - T_o) \quad \text{I.24}$$

### **I.6.1.b Reversible voltage variation with Pressure**

Same method of calculation based on equation I.19 can get the relation between pressure and reversible voltage as:

$$(\Delta E /dp)_T = \Delta n_g RT/nFp \quad \text{I.25}$$

Where  $\Delta n_g$  represent the change in the total number of moles of gas upon reaction. If  $n_p$  (Products) and  $n_r$  (reactants), then  $\Delta n_g = n_p - n_r$ . usually the increasing in reversible voltage by only 15mV for fuel cell using  $\text{H}_2$ -  $\text{O}_2$  [17]

### **I.6.1.c Reversible voltage variation with concentration Nernst equation**

The Nernst equation account for the same pressure affects that as previous in equation I.25.the general Nernst equation defined as:

$$E = E^o + RT/nF \ln (\prod a^{v_i}_{\text{Products}} / \prod a^{v_i}_{\text{Reactants}}) \quad \text{I.26}$$

Although temperature enters into the Nernst equations a variable, the Nernst equations does not account for how the reversible voltage varied with temperature.at the arbitrary temperature  $T \neq T_o$  the Nernst equation must modified as:

$$E = E_T + RT/nF \ln (\prod a^{v_i}_{\text{Products}} / \prod a^{v_i}_{\text{Reactants}}) \quad \text{I.27}$$

Where  $E_T$  is given from equation (I.23) as:

$$E_T = E^{\circ} + \Delta S_r/nF (T - T_0) \quad \text{I.28}$$

#### **I.6.1.d Ideal reversible fuel cell efficiency**

Fuel cell efficiency ( $\epsilon$ ) of a conversion process as the amount of useful energy that can be extracted from the process relative to the total energy involve by that process:

$$\epsilon = \text{useful energy}/\text{total energy} \quad \text{I.29}$$

If we wish to extract work from a chemical reaction, the efficiency is

$$\epsilon = \text{work}/\Delta H_r \quad \text{I.30}$$

for fuel cell the maximum amount of energy available to do work is given by the Gibbs free energy. Thus, the reversible efficiency of a fuel cell can be written as

$$\epsilon_{\text{thermo,fc}} = \Delta G_r / \Delta H_r \quad \text{I.31}$$

For the room temperature and pressure, the  $\text{H}_2\text{-O}_2$  fuel cell has  $\Delta G_r^{\circ} = - 273.3\text{kJ/mol}$  and  $\Delta H_r^{\circ} = - 286\text{kJ/mol}$

Where, HHV and LHV are the higher heating value, and the lower - heating value respectively, is the heat required to vaporize the water.

$$\epsilon_{\text{thermo,fc}} = - 273.3\text{kJ/mol} / - 286\text{kJ/mol} = 0.83 \quad \text{I.32}$$

#### **I.6.1.e Real (Practical) reversible fuel cell efficiency**

The real or practical reversible for fuel cell must always be less than the reversible thermodynamic efficiency, because the reasons as follows:

First voltage losses and second is Fuel utilization losses. Then the real efficiency of a fuel cell  $\epsilon_{\text{real}}$  can be written as:

$$\epsilon_{\text{real}} = (\epsilon_{\text{thermo,fc}}) \times (\epsilon_{\text{voltage}}) \times (\epsilon_{\text{fuel}}) \quad \text{I.33}$$

Where,  $(\epsilon_{\text{thermo,fc}})$  Equation I.31,  $\epsilon_{\text{voltage}}$  is the voltage efficiency of fuel cell, and  $\epsilon_{\text{fuel}}$  is the fuel utilization efficiency. The two terms efficiency are describes as follows

$$\epsilon_{\text{voltage}} = V/E \quad \text{I.34}$$

This efficiency is the ratio between the operating voltages of the fuel cell (V) to the thermodynamically reversible voltage of a fuel cell (E).

Second term of equation I.33 is

$$\varepsilon_{\text{fuel}} = (i/nF) / v_{\text{fuel}}(\text{mol/sec}) \quad \text{I.35}$$

The supplying fuel is adjustable follow the current needs, so for that the maximum fuels depend on the current, which can adjust the fuel by stoichiometry factor, then can write the fuel utilization efficiency as

$$\varepsilon_{\text{fuel}} = 1/\lambda \quad \text{I.36}$$

Combining effects Equation (I.33) of thermodynamics, reversible kinetic losses, and fuel utilization losses, the practical efficiency for a real fuel cell can be figured at following equation:

$$\varepsilon_{\text{real}} = (\Delta G_r / \Delta H_{r\text{HHV}}) \times (V/E) \times (i/nF) / v_{\text{fuel}} \quad \text{I.37}$$

### **I.7 Activation kinetics for fuel cell .Tafel Equation**

Fuel cell depends on many parameters to obtain good performance, thermodynamics and also kinetics. At equilibrium, the current densities for forward and reverse reactions are both given from equilibrium with the account the change in the forward and reverse activation barriers:

$$i_1 = i_o e^{(anF\eta/RT)} \quad \text{I.38}$$

$$i_2 = i_o e^{((1-\alpha)nF\eta/RT)} \quad \text{I.39}$$

The net current ( $j_1-j_2$ ) is then

$$i = i_o ( e^{(anF\eta/RT)} - e^{((1-\alpha)nF\eta/RT)} ) \quad \text{Equation Bulter-Volmer} \quad \text{I.40}$$

Activation kinetic is depend to  $j_o$  current exchange currency ,and  $i_o$  represent the rate of exchange between the reactant and product state at equilibrium,  $j_o$  can defined from the forward or reverse reaction direction at equilibrium. From the Bulter-Volmer Equation (I.40), the activation can present by two useful approximations. When the activation overvoltage ( $\eta_{\text{act}}$ ) in the Bulter-Volmer Equation is either small or very large:

1-activation overvoltage ( $\eta_{\text{act}}$ ) is very small: less about 15 mV the activation overvoltage can write as

$$i = i_o nF \eta_{\text{act}} / RT \quad \text{I.41}$$

2-activation overvoltage ( $\eta_{\text{act}}$ ) is very large; greater than 50-100mV at room temperature, the second exponential term in the Bulter-Volmer Equation become negligible, only the forward – reaction direction dominates: the Bulter-Volmer Equation simplifies to:

$$i = i_o e^{(anF\eta/RT)} \quad \text{I.42}$$

Solving this equation for  $\eta_{act}$  yields

$$\eta_{act} = -RT/\alpha nF \ln i_0 + RT/\alpha nF \ln i \quad I.43$$

A plot of  $\eta_{act}$  versus  $\ln i$  should be straight line. Determination of  $j_0$  and  $\alpha$  is possible by fitting the line of  $\eta_{act}$  versus  $\ln i$  or  $\log i$ , the equation (I.43) is generalized in the form

$$\eta_{act} = a + b \ln i \quad I.44$$

This equation known as the Tafel Equation and  $b$  is called the Tafel slope

in fuel cell (PEMFCs) we interested in a large amount of net current are produced, and the Tafel Equation shown the behavior of electrochemical process and kinetics parameters as exchange current and current, activation overvoltage.

Activation overvoltage losses are minimized  $i_0$ . there are for major ways to increase  $i_0$ : 1- increase reactant concentration, 2-increase reaction temperature, 3- decrease the barrier (By employing the catalyst), and 4- increase the number of reaction sites.

### **I.8 Cell Performance for proton exchange membrane fuel cells (PEMFCs)**

The performance for fuel cell (PEMFCs) device can be summarized with a graph of its current-voltage characteristics. The Fig I .9 shows the voltage output of the fuel cell for given current output, this curve called current – voltage (I – V) curve.

There are three major regions of fuel cell losses, which give a fuel cell I – V as presented in the Fig I.9.

-First activation losses ( $\eta_{act}$ ) which results from the activation energy barriers of the electrode (losses due to the electrochemical reaction), low activation overvoltage can be achieved by utilization of electro-catalyst with high exchange current density, and by maximizing of electrochemical active surface area.

-Second, Ohmic losses ( $\eta_{Ohmic}$ ): The most common form the resistance overvoltage arises from the passage of electric current through an electrolyte solution surrounding the electrode [18-19]. the Fig I. 9 show losses mainly due to the ionic and electronic resistance of fuel cell, for proton exchange membrane fuel cell the total resistance ca be written:

$$R_T = R_m + R_c + R_{ec} \quad I.45$$

Where,  $R_m$  is the ionic resistance of the membrane,  $R_c$  the ionic contact resistance between the membrane and three-dimensional electrodes and the electronic resistance of electrode, and  $R_{ec}$  the electronic contact and material resistance of the component in the cell between electrode and graphite plates. To improve  $R$ , membrane with lower resistance can be used the thinner one, for example 112 is thinner than 117 [20] ,also to reduce the Ohmic losses and increase the performance of the cell, many parameters that can be explored include preparation of electrode (Pt particles, support as carbon or carbon nanotube, binder, protonic conductor), in addition to external parameters as, flowrates and Pressures ( $H_2$ /Air/ $O_2$ ),

-Third is a concentration losses (concentration overvoltage) ( $\eta_{conc}$ ), which consist of poor mass transport of the reactant at high current density , This is small, but has important effect (particularly for some electro-analytical technique).

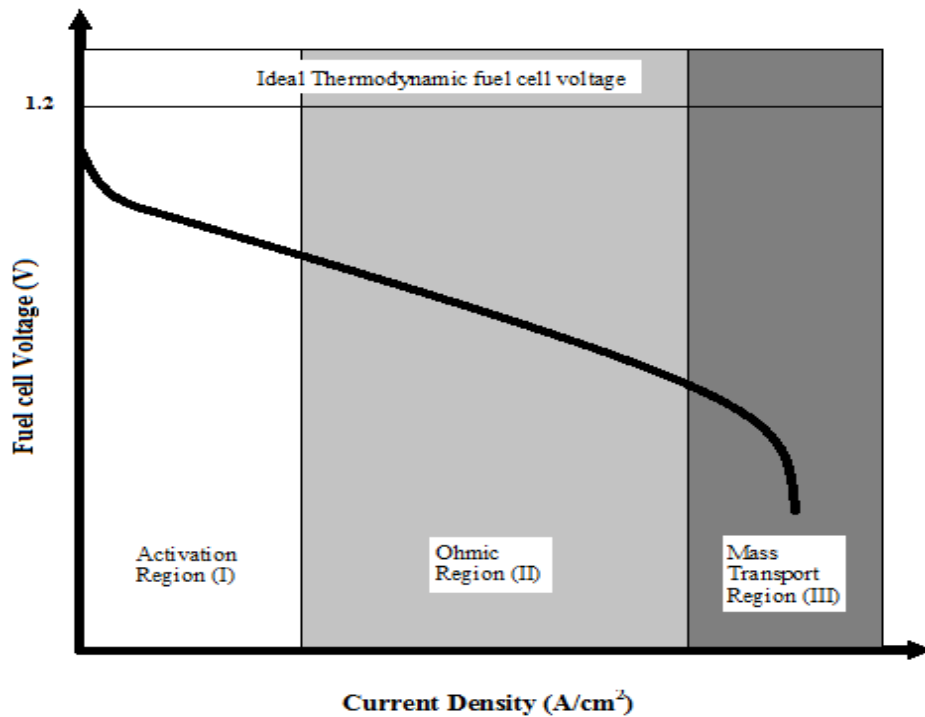


Figure I.9. Schematic of fuel cell (PEMFCs) curve within three losses regione. 1-Cell Potential losses, 2- Linear Drop in the cell, 3- Mass transport.

An ideal fuel cell would supply any amount of current (as long as it is supplied with sufficient fuel) while maintaining a constant voltage output of real fuel cell is less than the ideal

thermodynamically predicted voltage. The power density curve Fig I. 10, shown the power density delivered by a fuel cell as a function of the current density:

$$P = I V$$

I.46

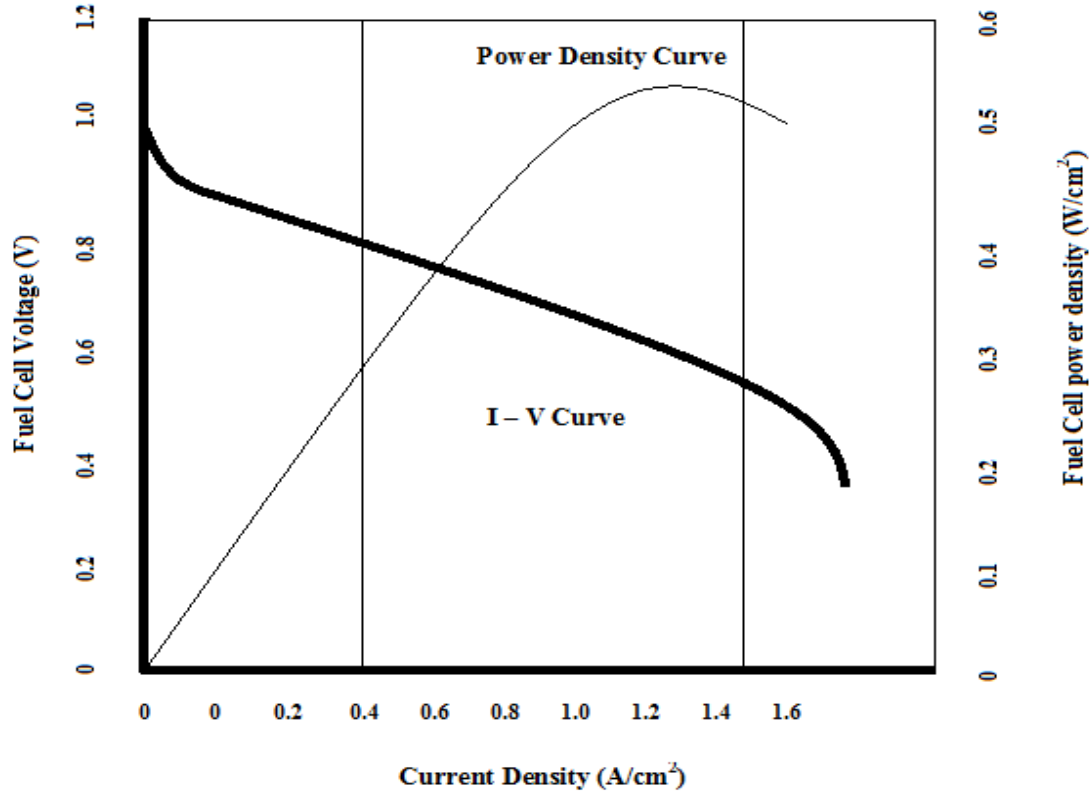


Figure I.10. combined fuel cell I – V and power density curves for proton exchange membrane fuel cells (PEMFCs)

### I.9 Theory of Gas Diffusion Electrode

Electrode for proton exchange membrane fuel cells (PEMFCs) is the site of energy conversion reactions, so the previous studies are all related to the electrode kinetics, and how the electrode fabricated to be useful for oxidation and reduction reactions. The principle function of a porous gas diffusion electrode is to provide a large reaction zone area with a minimum mass transport hindrance, for the access of reactant and removal of products. In porous gas diffusion electrode three zones (Gas diffusion layer , Catalyst Layer, Electrolyte), which, can be present in contact with metal and electrolyte. the metal use in porous gas diffusion electrode must have a very high surface area (100m<sup>2</sup>/g) with a carbon specific area 1000m<sup>2</sup>/g).



Porous gas diffusion electrode can have a high surface area and high porosity by introducing a reforming agent to enlargement the pores size during the electrode manufacturing, and removed after fabrication by calcinations process. [21] reported that PEM fuel cell at higher temperatures has been improved by modifying a Pt black cathode catalyst layer structure with the optimal amounts of the “pore-former” ( $\text{NH}_3\text{HCO}_3$ ), Introduction of the ammonium carbonate into the Pt black catalyst layer of the high temperature membrane electrodes enhanced the total porosity of the catalyst and the performance increase. Beside this the basic structure (carbon or metal) with addition of binder and/or impregnation materials used during their fabrication, in which the electrode has hydrophobic (Carbon) or hydrophilic (Metal powder surface). Hydrophobic gas diffusion electrodes are made of the fine carbon powder or carbon nanotube bonded with a polymer as polyterafluoethylene usually is on suspension phase (PEFE), the carbon is light and has a large surface area, which is suitable for the deposition of very active catalysts. Polyterafluoethylene bonded carbon electrode are easy to manufacture on a large scale. The conductivity of carbon is not sufficient for high current ( $200 \text{ mA/cm}^2$ ) and only a carbon bipolar plate is acceptable for high current. Gas diffusion electrode at last two porous diffusion layer should be presented in the fabrication of electrode, one is gas diffusion layer (GDL) and the second is electrocatalyst layer (CL), which the electrochemical reactions take places with electrolyte (Nafion® ) in solid form.

### **I.9.1 Electrode Fabrication for proton exchange membrane fuel cells (PEMFCs)**

In PEMFCs) Pt and Pt alloy considered as the best electro-catalyst, to date for both hydrogen oxidation and oxygen reduction reactions. Which the cathode potential always bigger than anode hydrogen oxidation from 200 mV to 400 mV for oxygen potential [22]. Le development et la fabrication de electrode (Anode and Cathode) related how to construct the electrode from substrate until final layer named catalyst layer. Generally three layers exists in electrode for proton exchange membrane fuel cell.

1-Substrate: Consist of carbon paper or carbon cloth Fig I.11 (a,b) treated by hydrophobic solution as PTFE and pass to the heat treatment. The substrate use to to support the Gas Diffusion Layer (GDL) and permitted to the gas to diffuse through the electrode.

- **Gas Diffusion layer GDL for electrode Pt/C**

The porous gas diffusion layer (GDL) consider as a second main layer in electrode for PEMFCs ,because the existence of this layer ensure the diffusivity of reactants toward the catalyst layer and can conduct the electron from baking layer to the catalyst layer. GDL consider as wet-proofing (hydrophobic) that ensured and keep pore of the gas diffusion layer not ripped by water. The GDL composed by Carbon back and PTFE mixed together. Changes in compositions of GDL like Carbon Black, PTFE, Micro-porous layer MPL, effects on electrode performance. Thickness of the gas diffusion layer can be from 100-300  $\mu\text{m}$  equal to the loading 1-3  $\text{mg}/\text{cm}^2$  depend on the carbon loading in GDL

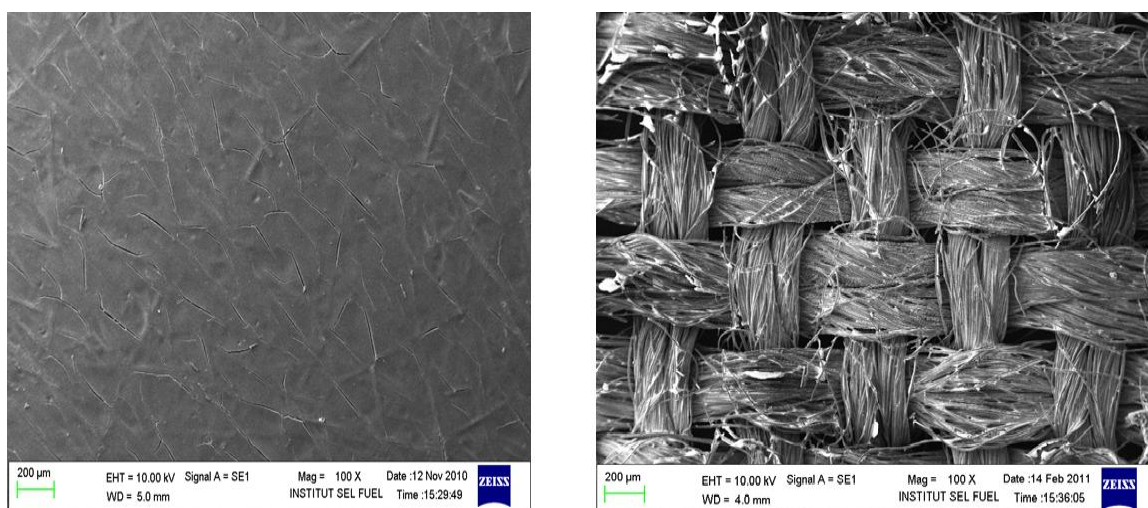


Figure I.11 presented the substrate as (a) Carbon Paper and (b) carbon cloth treated with 15 wt % PTFE

- **Catalyst layer (CL) for electrode Pt/C**

Catalyst layer can be classified as major part of the electrode as compared to the other two layers, baking layer and diffusion layer GDL, and contact with diffusion layer and membrane .the catalyst can apply directly to the membrane and also on Gas diffusion layer GDL, which can achieved the best activity of the catalyst. Catalyst is the most expensive part for the catalyst layer, furthermore, the catalyst layer can be classified into three groups based on the active component:

- a\*Pt based catalyst (platinum supported carbon as previous work [23])
- b\*Pt catalyst that modified by alloys as ,PtVFe and Pt-Co/C [24-26].
- c\*Non-Pt-based catalyst such as non-noble metals, and also organo-metallic complex.

Catalyst fabrication consists of catalyst Pt/C or Pt/M/C. The catalyst and 5wt.% Nafion® ionomer solution were mixed in isopropyl alcohol to form homogeneous catalyst ink for the anode and cathode/or catalyst ink was composed of 20 wt.% Pt/C, Nafion® ionomer, and PTFE. The Nafion® contents [27; 28].

### **I.9.2 Parameters affecting performance electrode for proton exchange membrane fuel cells**

Electrode fabrication is a vital part in proton exchange membrane fuel cells, which all chemical reactions and conversion to energy occurs in the electrode interface. For this important, the structure design for electrode should be recognized that the electrode is a field where multi-components and multi-phases are taking places [23]. The electrode structure consist of three layers, namely catalyst (CL), gas diffusion layer (GDL), and backing layer, in which the components are presented. The most components presented in the electrode for PEMFCs are: catalyst, support of catalyst usually is activated carbon, substrate, Teflon (PTFE), Nafion® ionomers, forming agent as  $\text{Li}_2\text{CO}_3$ ,  $\text{NH}_3\text{HCO}_3$ . Increasing and decreasing in each component effect on the electrode performance. These parameters effects have studies by different researchers trying to achieve the best and the optimum values for each component for the ideal electrode structure. The backing layer contains carbon paper or carbon cloth and Teflon (PTFE), the second layer, gas diffusion Layer (GDL), third is catalyst layer (CL) [19; 29] the last one contain Teflon, Nafion®. Teflon solution used as water proofing and binder with Nafion® as protonic conductor and binder. Varieties of electrodes were prepared using different methods and components loading of, Pt, PTFE, Nafion, forming agent in the catalyst layer and also in the diffusion layer. Fabrication parameters improve the performance as: Catalyst loading, increasing the loading of catalyst increase the performance [30], Thickness of GDL, Carbon substrate, carbon powder types, catalyst and catalyst alloys. [31-32] prepared the Electrode by using Pt combined with other non-noble metals such as iron (Fe) and vanadium (V) to form PtVFe, which improved the better performance and The deposition methods of electrode preparation effect on the performance as spraying, the plasma sputtering system method, chemical vapor deposition, casting, The fabrication method and ink preparation effect presented in Fig 2.5.the SEM of catalyst layer for electrode  $0.38 \text{ mg/cm}^2$  and cross section of membrane electrode assembly are presented in Fig 2.5.a,d, which show the catalyst surface with the catalyst located in front of the surface of electrode. Moreover, give the good performance compared to E-TEK as

reported in previous work [19; 29] the preparation methods as casting process using carbon paper as substrate. Fig 2.5.b,c show the surface of the catalyst layer using a rolling machine (casting) with the cracks and the platinum agglomerate with PTFE/These cracks and Pt agglomeration can give advantage to loss some performance of electrode. Which allow to water to stagger and block the diffusion of electrons and reactants through this crack area of electrode. Moreover in the MEA can observe the contact electrode with the membrane have some crinkles these crinkles fill by water formed in cathode and stop gas to diffuse award to the catalyst.

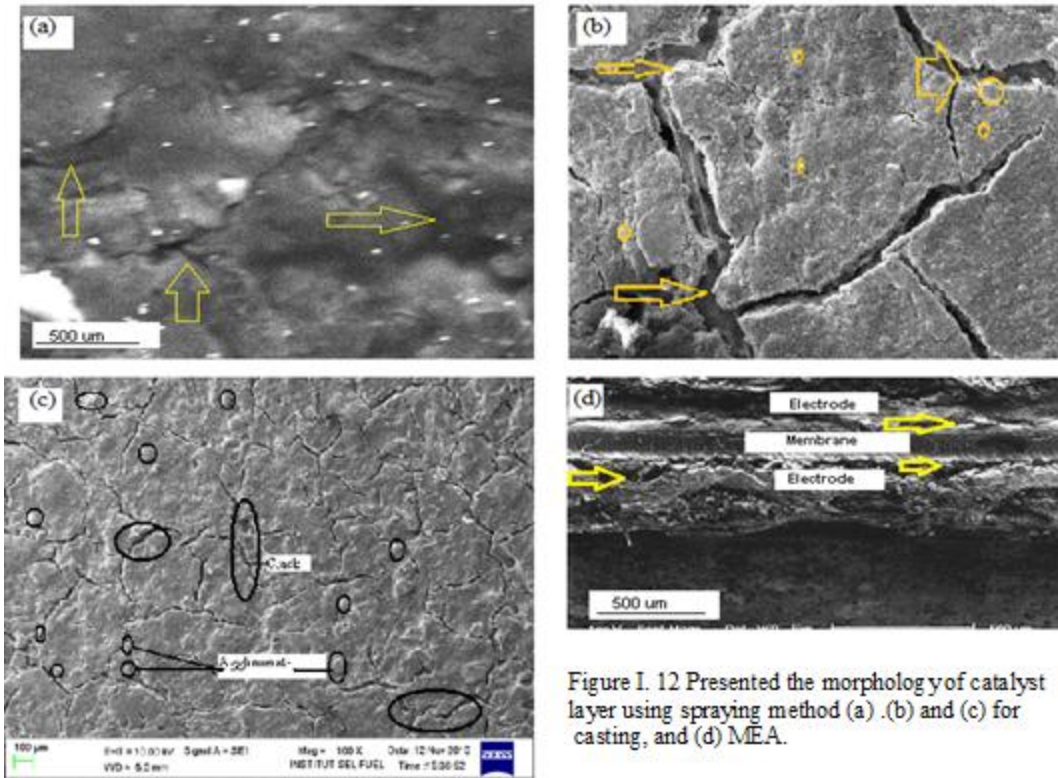


Figure I. 12 Presented the morphology of catalyst layer using spraying method (a) .(b) and (c) for casting, and (d) MEA.

Operating parameters: operating electrode in fuel cell system have many parameters effect on the performance, for example increasing the pressure of gases ( $H_2$ ,  $O_2$ , and Air) increase in the performance, concentration of gases (oxidant and reactants) flow-rate of gases must have proper ration  $O_2/H_2$  , and the operating Temperature of the single cell or stacks. All these parameters can reduce the electrode performance and also aggression of physical parameters effect like pressures and temperature water flooded, on and off the system during the operation cause an aging in the electrode (Anode and cathode). Moreover the electrode microstructures changer during the operation for long time, which the components of electrode (anode and cathode) degrade from the original state.[32] demonstrates the impact of a potential cycling treatment on a

platinum catalyst carbon-supported, and propose a new corrosion mechanism for fuel cell catalyst degradation. Under the applied harsh conditions, whole Pt particles detach from the support and dissolve into the electrolyte without re-deposition [33]. Therefore, the so-called accelerated degradation test (ADT) is developed. These ADT methods include: (i) thermal degradation under hot air conditions, (ii) aging in hot aqueous acid solution, (iii) open-circuit cell studying the durability issues are reviewed. The degradation of Pt-based PEMFC catalysts can be categorized into two aspects: the corrosion of carbon Support and the degradation of catalytic metals. [34; 35] reported that the main degradation processes in MEAs include Pt sintering, agglomeration and redistribution, corrosion of the carbon support in the electrodes, chemical and structural degradation of the membrane, and poisonous effects aroused by contaminants from external components. Also, agglomeration and particle growth of nanostructure, Pt is the most dominant mechanism for catalyst degradation in PEM fuel cells. degradation of catalysts related to oxidation of carbon or carbonization, which accelerate Pt sintering and make it more catalyst durable, furthermore carbon in presence of water according to the reactions:  $C+H_2O \rightarrow CO_2 +4H^+ +4e^-$  ---  $E > 0.207 V$  and  $C+H_2O \rightarrow H_2 +CO$  The reaction product CO might poison the catalyst Pt [31-32]; [34]. The electrochemical corrosion of the carbon surface leads to changes in the surface chemistry of the carbon and an increase in hydrophobicity for the catalyst layer and gas diffusion layer, which result in a decrease in the gas permeability. [32-36] believe that two other mechanisms are predominately responsible for coarsening: Pt particles detaching from the support and dissolving into the electrolyte without redispersion, and/or a combination of Pt particle coalescence and Pt solution/precipitation within the solid ionomer. Whatever mechanism the particle growth follows, dissolution of Pt is an important step during the catalyst degradation process. The dissolution/ detachment of Pt and/or other alloyed catalytic metals into the electrolyte ( $Pt \rightarrow Pt^{2+} + 2 e^-$ ),  $PtO + H^{2+} \rightarrow Pt^{2+} + H_2O$ . The diffusion from cathode to anode by reduction of platinum  $Pt^{2+} + 2 e^- \rightarrow Pt$  explain two processes responsible for platinum coarsening, namely Ostwald ripening on the nanometer-scale and diffusion of oxidized platinum species on the micrometers-scale with precipitation of platinum particles in the ionomer [37]. But research still going on to improve the dissolution or detachment catalyst from the support. In term of effect of the structure of electrode. [38] reported that after the operation of electrode in single cell using carbon fiber paper for 48 h, the crystalline degree of the Nafion® electrolyte as well as the carbon support and platinum catalyst decreased,

which depends strongly on the operation conditions, e.g., humidification temperature, also [39] cited the Aging under experimental conditions make a slight evolution of the electrode microstructure. The changes showed the increasing in carbon concentration, concentration of CO the carbon catalyst-support increases, the platinum decreases by using XPS.

**I.9.3 Membrane for proton exchange membrane fuel cells (PEMFCs)**

Last decade the electrolyte use for electrolysis and fuel cell it was a liquid form, which may cause hazard problem transportation. The developments of solid electrolyte give advantage for technologies and reliable applications. Most modern solid polymer electrolytes are perfluorinated ionomers with the fix side chain of sulfuric acid bonded covalently to the inert, but chemically stable. The membranes consist of two very different sub-structures:

- 1- hydrophilic and ionic conductive phase related to the bond sulfuric acid group.
- 2- a hydrophobic and relatively inert polymer that is not ionic conductive but provides chemical stability as presented in Fig 1.13 [9]

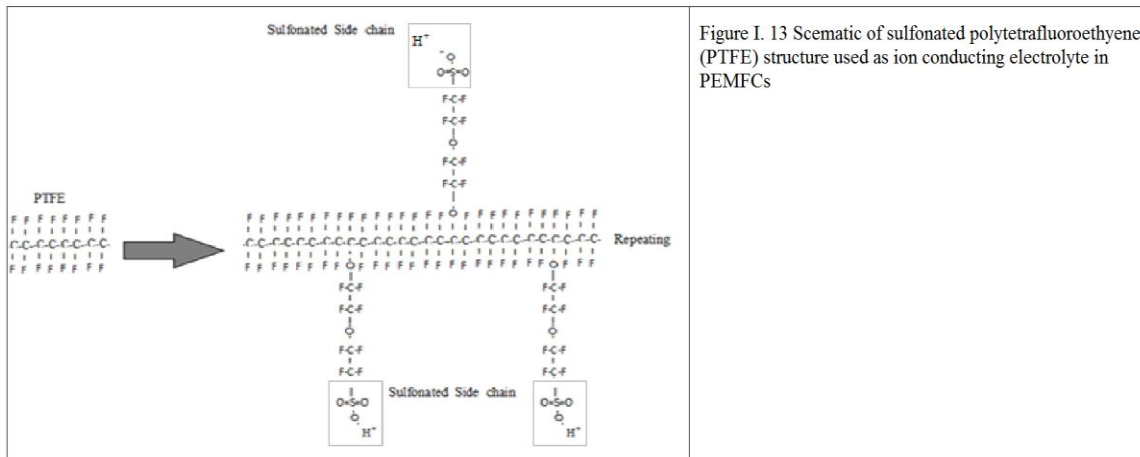


Figure I. 13 Schematic of sulfonated polytetrafluoroethylene (PTFE) structure used as ion conducting electrolyte in PEMFCs

The most solid membrane used in fuel cell specially for PEMFCs and DMFCs is Nafion® like other perfluorinated ionomers is created by sulphonation ( $\text{SO}_3^-$ ) of the basic PTFE structure as shown in presedent Fig. I.13. the membrane work only in hydrate state, which allowed to  $\text{H}^+$  ino for motion in  $\text{H}_3\text{O}^+ -\text{SO}_3^-$  groups, dry perfluorinatedionomerss are almost or completely non-conductive.two mode of transport existit:

1-Under low water content : in this case the ionically conductive of the membranes behave a nearly Isolated clusters, and proton transport is dominated by vehicular mechanism or diffusion and the mode of transport is purely physical.

2-With the high hydration in the electrolyte: in this case high effective proton conductive and the proton  $H_3O^+$  moving along a connected pathway in the ionomer structure .this mode call

The ionic conductivity of the electrolyte that related to the clustering of the sulfonic acide side groups. hydration level give the structural relationship between the non-conductive polymer backbone and the conductive side chains, which is the critical factor in the electrolyte water uptake,conductivity,and swelling behavior. this structural relationship can be mesure by the equivalent weight (EW) of the ionomeric membrane.

$$EW \text{ (g/eq)} = 100 \times k \times 446 \quad \text{I.46}$$

Where: k is the number of tetraflouroethylene groupe per polymer chain.the higher the EW,the higher the amount of inert backbone relative to conducting side chains.the EW for fuel cell electrolytes is typical from 800-1200, and the most commonly use is Nafion®, for exemple nafion 112 represent 51um thick dry membrane with 1100 EW.for the water uptake in the membrane (electrolyte) is given by;

$$\lambda = H_2O/SO_3H \quad \text{I.47}$$

$\lambda$ ,is commonly referenced in terms of water molecules per sulfonic acid site. Water –soaked values range from~30 for an EW of 900, to~ 20 for an EW 1100 by weight percent (wt%), beside these some additional data commontly used for nafion given in the Tab I. 3 .for the membraness in a low humidity environment, the water uptake is much lower. For water Uptake of

Nafion®1100 EW at 30°C Correlated as:

$$\lambda = 0.043 + 17.18 a - 39.85 a^2 + 36.0 a^3 \text{ for } 0 < a < 1 \quad \text{I.48}$$

where a is water vapor activity,which is relative humidity RH:

$$a = RH = y_v P/P_{\text{sat}}(T) \quad \text{I.49}$$

in the equation I.48 has a maximum value a fully humidified conditions of  $\lambda = 14$  at 30°C, since the wate uptake  $\lambda$  decrease with increasing the temperature , the value around  $\lambda = 10$  at 80°C

Table I. 3 Water Uptake,Weight Percent,and swelling for Nafion Membranes [37].

Nafion Designation	Water Uptake $\lambda$ ( H <sub>2</sub> O/SO <sub>3</sub> H )	Water percentage(%)	Weight Thickness	Strain from Water Uptake , $t_{wet}/ t_{dry}$
112	21 – 22	21 – 26	14 – 21	
115	21 – 22	21 – 26	14 – 18	
117	21 – 22	21 – 26	13 – 15	
105	21 – 28	32 – 33	26– 30	

3-Nafion ionic conductivity, the conductivity of membrane is related to the water uptake in the membrane water increase,the ionic concentration increase, which increase the the conductivity. Also the temperature has effect of the ionic conductivity as given by:

$$\sigma_i \text{ (S/cm)} = \exp [ 1268(1/303 - 1/T) (0.005193 \lambda - 0.00326) ] \quad \text{I.50}$$

these relation to give idea the ionic conductivity in the membrane as fonction of water uptake, temperature. Also Nafion® loading in the electrode affect of on electrode performance as showed by [40].

**I.9.4 Membrane electrode Assembly (MEA) for (PEMFCs)**

Membrane electrode Assembly (MEA) is the heart for PEMFCs because all process of energy conversion happens in this sandwich as we call it, MEA consist of two electrodes anode and cathode and membrane electrolyte commonly Nafion® , these two electrodes incorporate in MEA by hot pressing, with the prepares pressures and temperature, these physical parameters effect also on the electrode performance, High pressures and low pressures must take on consideration, high temperatures in hot pressing damage the membrane Nafion® , Which can stand until 140°C. after this temperature start the degradation of membrane (Tg). in previous work we realize MEA at temperature 120°C - 130°C and pressure 1000 psi for 90 seconds Rachid [19,29] ,the ,MEA Fabricated as Cross section and MEA under this conditions presented in Fig I. 14



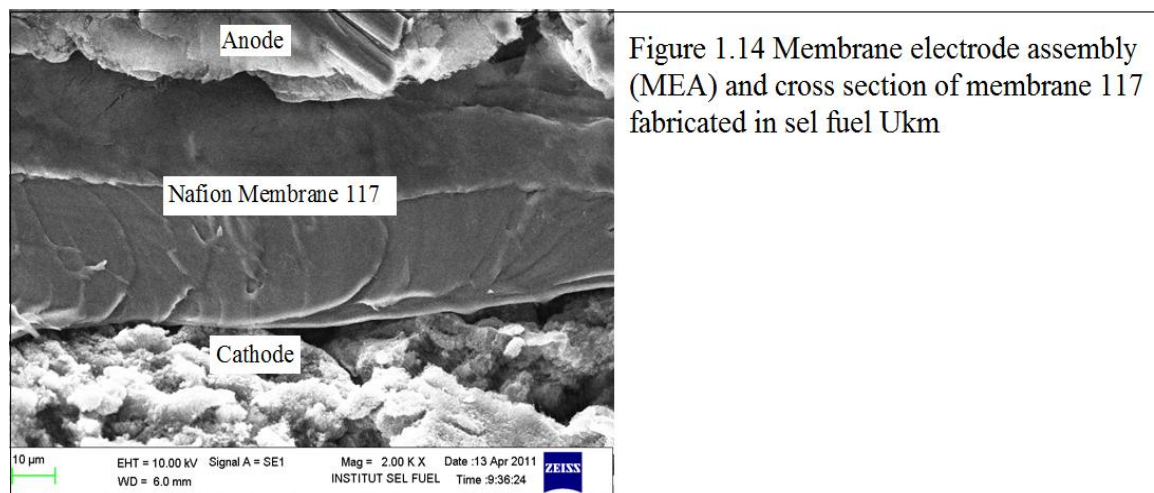
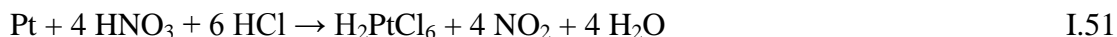


Figure 1.14 Membrane electrode assembly (MEA) and cross section of membrane 117 fabricated in sel fuel Ukm

## **I.10 Electrode components for (PEMFCs)**

### **I.10.1 Electrocatalyst (Pt/C)**

Noble metal, used for many applications in electrochemistry . However, this material is known to be rare (about 200 tonnes milled at year), and therefore difficult to refine, expensive (€ 30.500. kg-1).Platinum is an extremely rare metal occurring at a concentration only 0.005 ppm in the Earth's crust [41].this Nobel material is the most important factor in any chemical engineering reactions and fuel cells technology, in PEMFCs the catalyst Pt consider as the reference for the conversion, because their chemicals and physicals characteristics as non-reactive, resistance to corrosion, even at high temperatures. Proton exchange membrane fuel cells use Platinum with support like Carbon (Pt/C) by preparing Pt/C from hexachloroplatinic acid  $H_2PtCl_6$  using different preparation method, or as commercial Pt/C as powder. For Pt/C preparation many methods use to prepare catalyst support even in other applications. For PEMFCs , Pt metal can dissolves in hot aqua regia to give soluble hexachloroplatinic acid ("H<sub>2</sub>PtCl<sub>6</sub>", formally (H<sub>3</sub>O)<sub>2</sub>PtCl<sub>6</sub>·nH<sub>2</sub>O ) using the following reaction:



### **I.10.2 Carbon support catalyst for PEMFCs**

#### **2. Carbon Black and structure**

Carbon is distinct among chemical elements since it is found in dramatically different forms and with varying micro-textures. The diverse morphologies of carbon make it an attractive material that is widely used in a large range of electrochemical applications. Carbon exists in various

allotropic forms due to its valency [42], with the most well known being carbon black, diamond, fullerenes, graphene, and carbon nanotubes

Carbon black is usually produced by the “furnace black” process, namely the partial combustion of petrochemical or coal tar oils [43]. Due to the nature of the source materials, heat treatment is used (250-500° C) to remove impurities from the formed carbon [44-46]. Carbon black consists of spherical particles (diameter less than 50 nm) that may aggregate and form agglomerates (~ 250 nm diameter), which The carbon particles have para-crystallite structures [47] consisting of parallel graphitic layers with 0.35-0.38 nm interplanar spacing. The crystalline graphitic portion of carbon black has sp<sup>2</sup> hybridization involving a triangle in-plane formation of sp<sup>2</sup> orbitals while the fourth 4 p<sub>z</sub> orbital lies normal to this plane forming weaker delocalized π bonds with other neighboring carbon atoms [48-50]. chemical (ZnCl<sub>2</sub>/ H<sub>3</sub>PO<sub>4</sub> addition to carbon precursor) or gas (steam CO<sub>2</sub>) treatment of carbon black at high temperatures (800-1100°C) and high pressure leads to the formation of activated carbon black; this form of carbon is characterized by larger and more crystalline graphitized carbon particles (~ 20-30 μm) with distinct micro-porosity and varying BET surface area (200-1200 m<sup>2</sup>g<sup>-1</sup>) [47].

To make carbon black more efficacy must be activated the carbon black, two methods to activated.

**1- Physical activated** :The physical activation is between 650 °C and 900 °C, in an oxidizing atmosphere (carbon dioxide steam , water or a mixture of two) [51]. According to [52] The porous structure of the charcoal obtained may different function of the oxidizing gas used by [53] disagree that to use of carbon dioxide as oxidizing agent promotes development microporosity while steam of water promotes porosity dimensions greater. Thus a mixture of water and carbon dioxide is often used [54].

**2-Chemical activation:** Chemical activation is contrary to the physical activation, That the chemical activation is carried out in gas inert but at temperatures relatively low (between 400 °C and 600 °C) after impregnating the precursor by an agent activating, which may be a Lewis acid (ZnCl<sub>2</sub>, AlCl<sub>3</sub>) and phosphoric acid, or same alkali metal carbonates[55]. It also uses agents basic such as sodium hydroxide (NaOH) and potassium hydroxide (KOH) [56 -

58]. According to a study conducted by [59] on the viscose rayon (or regenerated cellulose) the impregnation with chemicals causes several reactions from offset pyrolysis, and avoid mass loss that observed during the physical activation.

The performance of the noble metal catalysts in the form of nanoparticle supported on high surface area carbon will depend strongly on the support material characteristics like: , type of carbon (Carbon Black, Acetylene, Carbon Nanotube,...), chemical/electrochemical stability, good electrical conductance, carbon treatment ( heat Treatment), high surface area, suitable pore-size area distribution and low impurity or surface group contents, these parameters has extra effect on the electrode performance. The most used carbon support for catalysts preparation is the commercial material Vulcan XC-72 and VulcanXC-72R (Cabot) USA Fig I.15 a and b.The only difference between the two materials is that the XC-72 is in the form of pellets, whereas XC-72R is in powder form, but even this morphological difference might influence considerably the fuel cell performance [60]. Excellent proprieties and parameters may give good electrode performance as demonstrate by many researches for fuel cell systems.

### **I.10.3 Binder PTFE and protonic conduct Nafion® ionomers solution**

In the beginning of fuel cell system Teflon was present as a binder for catalyst and catalyst supported because the chemical and physical proprieties (Inert, resist at high temperature...)

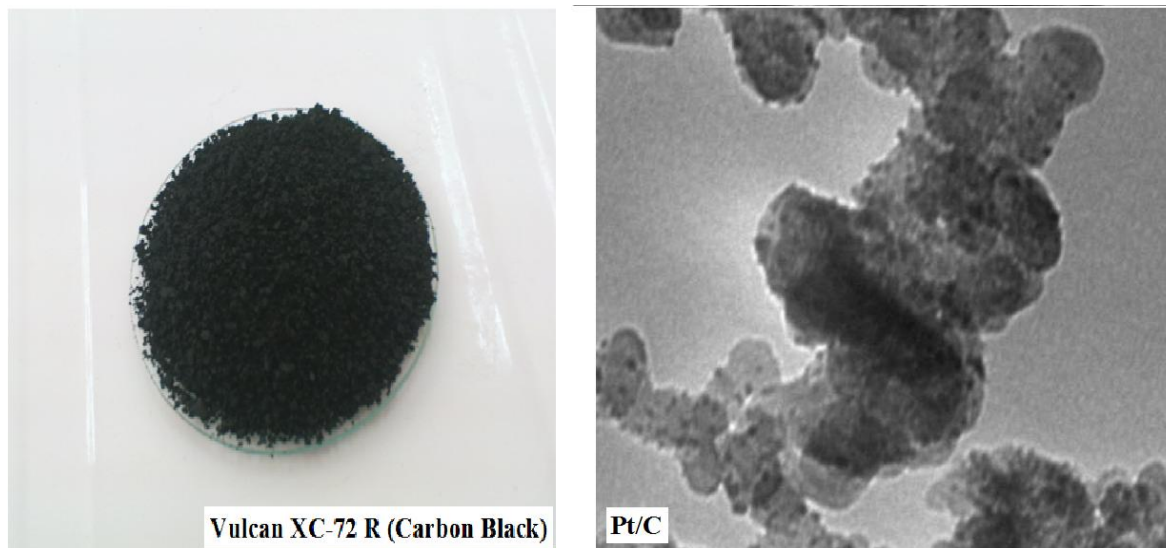


Figure I. 15 -a Presented carbon black type VulcanXC-72R (Cabot) USA and b- Presented TEM of Platinum supported Carbon 20 wt% Pt/C

also contain more electrons (for an equal length) than a corresponding polyethylene chain. Taken together (the good packing and the extra electrons) that means that the van der Waals dispersion forces will be stronger than in even high density polyethylene.

### **I.11 PEM Simulation and Modeling**

PEM fuel cell systems have been showing up as a promising alternative due their high efficiency and low impact to the environment. Theoretical approach with mathematical simulation is very effective for designing and analyzing the performance of the PEM fuel cell.

Some work has been reported in the literature on steady-state fuel-cell modeling (e.g., [61-64], as well as dynamic modeling [65-67]). These studies are mostly based on empirical equations and/or the electrochemical reactions inside the fuel cell. Several researches regarding influences of certain operating parameters on fuel cell characteristics. There are many other models have been developed and reported in literature, but they didn't focus on impact of individual operating parameters on fuel cell output characteristics.

**CHAPTER II**  
**FABRICATION AND ANALYSIS BY**  
**SEM, XRD, TEM, AND XPS OF**  
**ELECTRODE**

## **Introduction**

This chapter describes the experimental work. The first part is the Electrode Fabrication for two type of platinum supported carbon 10% and 20 wt % .the 10 wt % Pt/C use to study the effect of the diffusion layer on the electrode performance, and 20 wt % Pt/C % use for the electrode degradation. The loading for three electrodes  $E_{GDL} = 0.38 \text{ mg}_{Pt}/\text{cm}^2$  platinum loading with diffusion layer,  $E_{Out GDL} = 0.4 \text{ mg}_{Pt}/\text{cm}^2$  without diffusion layer, and  $E_{Tek} = 0.4 \text{ mg}_{Pt}/\text{cm}^2$  E-TEK electrode, respectively. The second Structure of electrode 20 wt % ( Pt/C) named E = 0.3  $\text{mg}_{Pt}/\text{cm}^2$ , which included The treatments of membranes (Nafion ®117) ,(Nafion®112) for 10 and 20 wt % Pt/C % respectively. Finally the testing of electrodes Performance in single cell connected to the test station.

The second part of experimental work is the technique analysis for both structure of electrodes by using scanning electron microscopic (SEM), X-ray photo-electron spectroscopy (XPS) for 10 wt% Pt/C and SEM, X - ray diffraction (XRD) analysis, Transmission electron microscopy (TEM), XPS for 20wt% Pt/C.

### **II.1.1 Electrode Preparation**

As mentioned in chapter I, gas diffusion electrodes are porous structures, which consist of electrocatalyst dispersed on high surface area carbon black that has been combined with polytetrafluoroethylene (PTFE) and Nafion ionomer. The PTFE plays an important role, not only as a binder, but also provides a gas permeable pathway, by functioning as a wet proofing agent [68]. The catalyst in low platinum loading electrode must be present at the surface of the layer (catalyst layer), where the site for electrochemical reactions.

Carbon cloth supplied from (E-TEK, Inc) as substrate, platinum supported carbon 10 wt% Pt/C (Fluka, chemie AG), activated carbon black (Ajax Chemicals, Sydney Australia), 20 wt% Pt/C Teflon (PTFE) 60wt% (Aldrich Chemical, Inc) have been used.

1- Two different structures have been used in preparation of the electrodes, one is with diffusion layer (PTFE/C) at  $E_{GDL} = 0.38 \text{ mg}_{Pt}/\text{cm}^2$ , and the other one is without diffusion layer (PTFE/C) at  $0.4 \text{ mg}_{Pt}/\text{cm}^2$ . The composition of catalyst layer is 70wt% Pt/C and 30 wt% Teflon (PTFE) [69].

Electrode generally consists of three layers [70], namely, backing layer (carbon cloth or carbon paper & Teflon), diffusion layer (carbon black/Teflon), and catalyst layer (Pt/C/Teflon). The simple process to fabricate electrode for fuel cells with different structures.

1. A backing layer was prepared by teflonizing carbon cloth with Teflon emulsion. The carbon cloth was first made hydrophobic by impregnation in a 15 wt% Teflon (PTFE) using 60wt% Teflon solution for 3-4 min as shown in the Fig II.1.a.

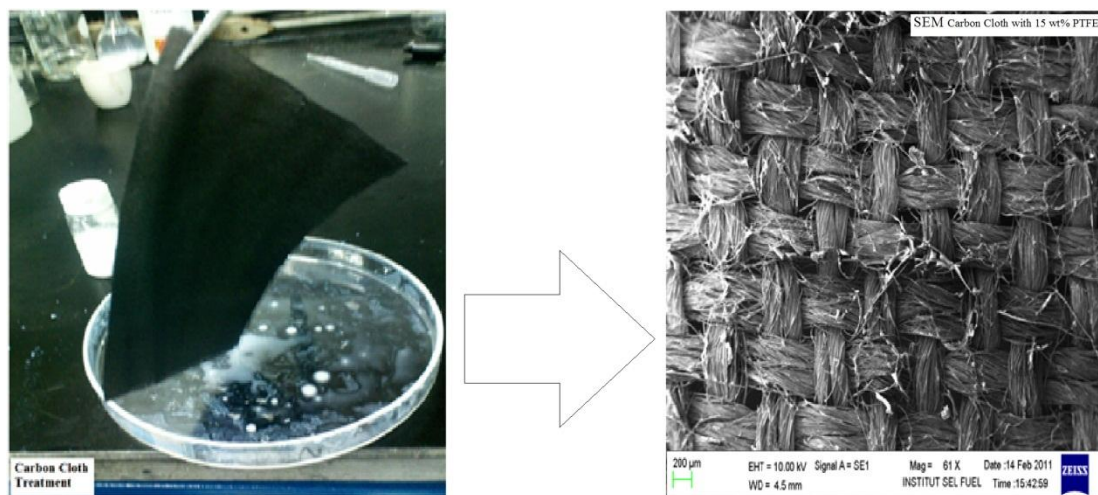


Figure II.1.a Backing Layer Substrate (Carbon Cloth with 15 wt% PTFE)

It was then dried in an oven at 80°C to remove the solvent (water). This backing layer is in contact with the diffusion layer as shown in Fig II.2 these layers are typically 350 μm. The thickness of this layer was measured after impregnating carbon cloth with 15 wt % Teflon solution usually this thickness depends on the thickness of carbon cloth or carbon paper. In our experiment the carbon cloth was 350 μm. According to [71] the thickness of the backing layer, the diffusion layer was varied between 300-400 μm, and the catalyst layer are dependent on the loading of each layer as demonstrated in Fig II.2.

2. The diffusion layer is prepared from carbon black with 30wt%Teflon (using PTFE 60 wt %) which were mixed with water and alcohol as solvent, using a magnetic stirrer for a few hours. The prepared ink was applied on the backing layer using the spraying method as shown in Fig II.1.b. This layer was dried at 80°C for one hour (1h) to remove the residual water and alcohol.

The diffusion layer is in contact with the catalyst layer, and the loading of diffusion layer is 3-4 mg/cm<sup>2</sup>, which corresponds to the thickness of about 400 μm as shown in the Fig II.2.

3. The catalyst layer is very important in proton exchange membrane fuel cell. This layer was prepared from platinum supported carbon black 10% Pt/C and 30wt% Teflon. Firstly a homogenous suspension was prepared by mixing and stirring in the beaker containing platinum-supported carbon black 10 wt% and 30 wt% Teflon with Isopropyl alcohol as solvent. This mixture takes a few hours, until a homogenous solution is obtained. The ink was applied onto the diffusion layer (PTFE/C) using spraying method and slurry casting, then dried at 80°C for one hour to remove the solvents (water and alcohol). Finally the electrode was baked at 200°C for 20 min in an oven to remove the residual surfactant in the catalyst layer, and then sintered at 280°C for 20 min. The thickness of the catalyst layer depends on the loading of platinum supported carbon in the layer.

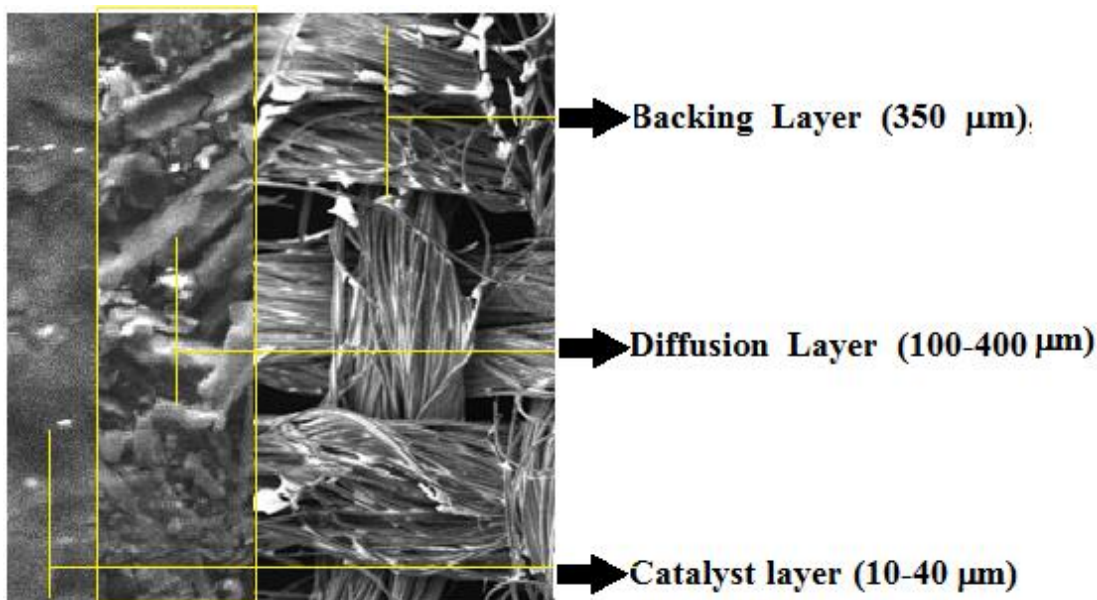


Figure II. 2. Electrode Structure with diffusion layer (GDL).

Typical Electrode Dimension

Carbon Cloth Support	350μm
Diffusion Layer	300-400 μm
Catalyst Layer	(10-40μm)

Nafion117 in dry state 175 um and swollen state 210 um Calculated.



The catalyst layer can be described as a Pt/C/Ionomer composite, where each of the three components is uniformly distributed within the layer. Structure at  $E_{GDL} = 0.38 \text{ mg}_{Pt}/\text{cm}^2$ , and the other one is without diffusion layer (PTFE/C) at  $0.4 \text{ mg}_{Pt}/\text{cm}^2$ , which is loading deposit on backing layer, were all dried at  $80^\circ\text{C}$  (to remove water and isopropyl alcohol). This is followed by thermal treatment at  $200^\circ\text{C}$  to remove the dispersion agent contained in PTFE. Then sintered at  $280^\circ\text{C}$  for 20 minutes. This layer typically varies between 10-40  $\mu\text{m}$ . For the second electrode  $0.3 \text{ mg}/\text{cm}^2$  with 20 wt% the heat treatments was the same as previously only the sintered processes at  $350^\circ\text{C}$ .

**\*Catalyst layer.** Catalyst layer prepared from platinum supported carbon black 20 wt% Pt/C and 30wt% Teflon. Firstly a homogenous suspension was prepared by mixing and ultrasonic in the beaker containing platinum-supported carbon black 20 wt% and 30 wt% Teflon with isopropyl alcohol and water as solvent with appropriate ration. This mixing takes 30 min at room temperature, in ultrasonic machine model; until a homogenous solution is obtained with The speed of ultrasonic was 15 %. The ink was applied onto the diffusion layer (PTFE/C) into two or three micro-layers using spraying method and casting, and then dried at  $100^\circ\text{C}$  for one hour to remove the solvents (water and alcohol). Finally the electrode was baked at  $260^\circ\text{C}$  for 1h in an oven to remove the residual surfactant in the catalyst layer, and then sintered at  $350^\circ\text{C}$  for 1h. Finally the loading for anode and cathode  $0.3 \text{ mg}_{Pt}/\text{cm}^2$ . The second layer for catalyst layer is electrolyte layer (Nafion<sup>®</sup>), this layer was coated using manual brush method and the weight of Nafion<sup>®</sup> was  $0.8\text{-}0.9 \text{ mg}/\text{cm}^2$ .

### **II.1.2 Membrane treatments**

Treatment of Nafion<sup>®</sup> membrane sheet of Nafion<sup>®</sup> (112 and 117) membrane ( $25 \text{ cm}^2$ ) as previous work [19]. First cleaned with distilled water using backer and heater at  $80\text{-}90^\circ\text{C}$ , followed by heating in 5% of  $\text{H}_2\text{O}_2$  Baker.Inc for one hour at  $70\text{-}80^\circ\text{C}$  (to remove organic impurities). It was then heated in 0.5M  $\text{H}_2\text{SO}_4$  Baker for one-hour at  $70\text{-}80^\circ\text{C}$ . The  $\text{H}_2\text{SO}_4$  was removed by repeated washing treatment in boiling water. The membrane was then stored in dark for overnight in distilled water before assembled with the electrodes.

### **II.1.3 Membrane Electrodes Assembly (MEA)**

The electrodes with  $E = 0.3 \text{ mg}_{\text{Pt}}/\text{cm}^2$  and membrane were incorporated in to a single cell assembly by the hot pressing procedure, using Press (Scientific Press-Motorized Hydraulic 20 tons), at temperature  $120^\circ\text{C}$  and pressure 1000 psi for 2-3 min. Then the membrane electrode assembly was cooled at room temperature for 30 minutes, than MEA Fig II.3 fixed in  $25 \text{ cm}^2$  single cell supply from ElectroChem equipped by two graphite plates, and the ribbed channels for the distribution of reactant gases behind the porous gas diffusion electrodes, a gasket containing the gas inlet and outlet, a copper plate used as the current collector from the fuel cell is positioned behind each of the graphite plates. (MEA) incorporates in electroChem.Inc single cell with the surface area  $25 \text{ cm}^2$ .the single cells connected to GasHub.Ltd test station equipped by two humidifier for oxygen and hydrogen that can operated with different humidifiers temperature. Two flow controllers for hydrogen and oxygen, this test station connect to the digital voltlab computer to get single cell output voltage, versus current density, and also power density.

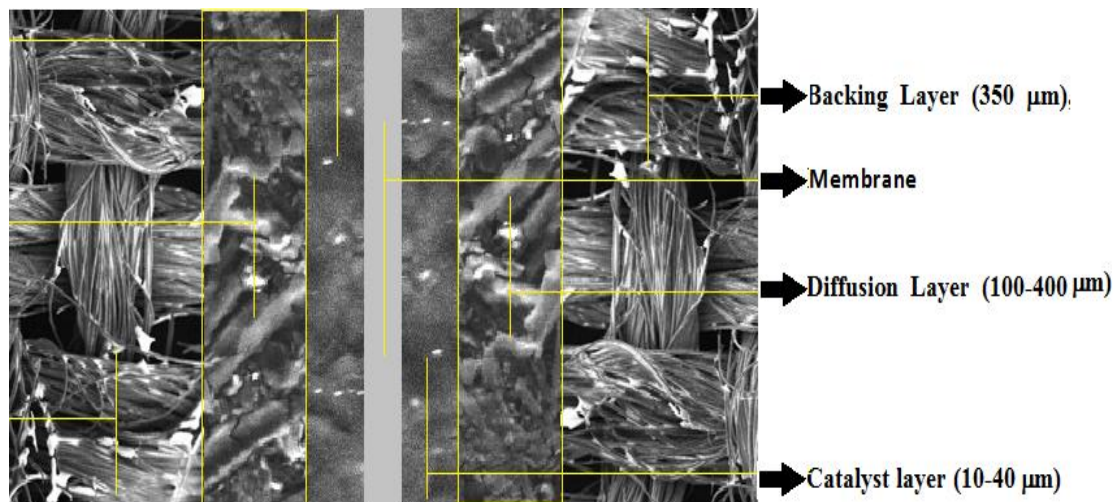


Figure II.3 Membrane Electrode Assembly (MEA)

### **II.1.4 Single cells components for proton exchange membrane fuel cells (PEMFCs)**

Proton exchange membrane incorporate in single to generate the power needed. The single cell (PEMFCs) contains generally:

\*MEA as the main component (Anode cathode separately by membrane) and placed between two graphite plates with Teflon gasket as appear in Fig II.4.a-b.

\*Graphite plate with gas channel to facilities flowing the gases (the Air and Hydrogen) to the anode and cathode, usually this graphite should be a high electric conductivity, and use to collect the amount of the current from the electrode.

\*Copper plates; copper consider as the high conductivity for this reason most of fuel cell system use Copper or Aluminum (light), which .the copper plates use to conduct current produced by the system , usually use the copper because is a good conducted for current.

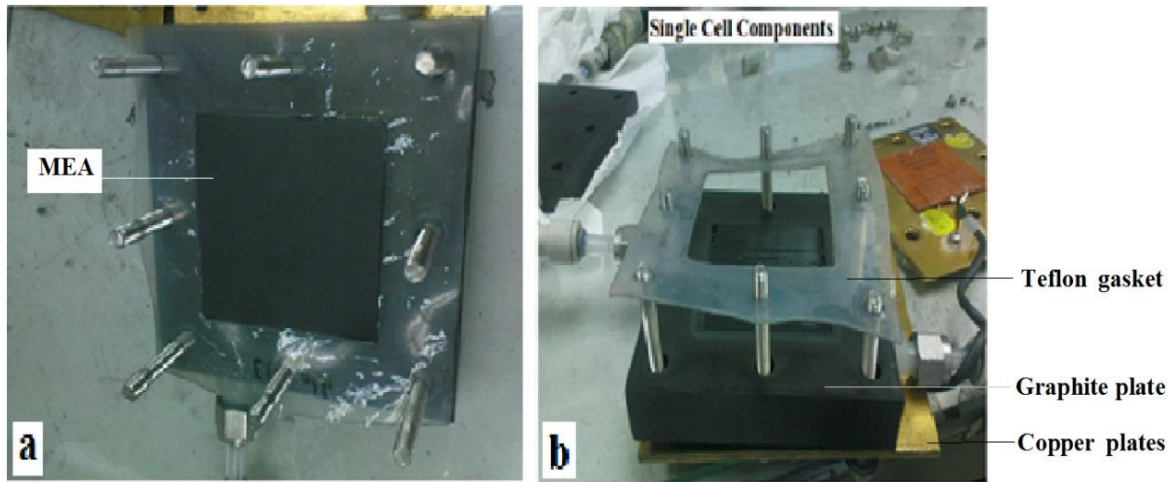


Figure II.4.a-b Component of single cell for proton exchange membrane fuel cells(PEMFCs)

### **II-1.5. Design of operating system for proton exchange membrane fuel cell system (PEMFCs)**

The major components for proton exchange membrane fuel cell are presented in Figure II.5 that designed and operation in previous work [19]; the operating of single cell in this work we and use the Gas Hub test station (Singapore) in fuel cells Lab Ukm. The main components for this test station used for proton exchange membrane fuel cells are: two cylinders of gas ( $H_2$ , Air), two humidifiers, Two mass flowrate controller, two gauge pressures to control gas pressures for Air and hydrogen and the last the test station is related the computer system to measure the current, voltage and also the power.

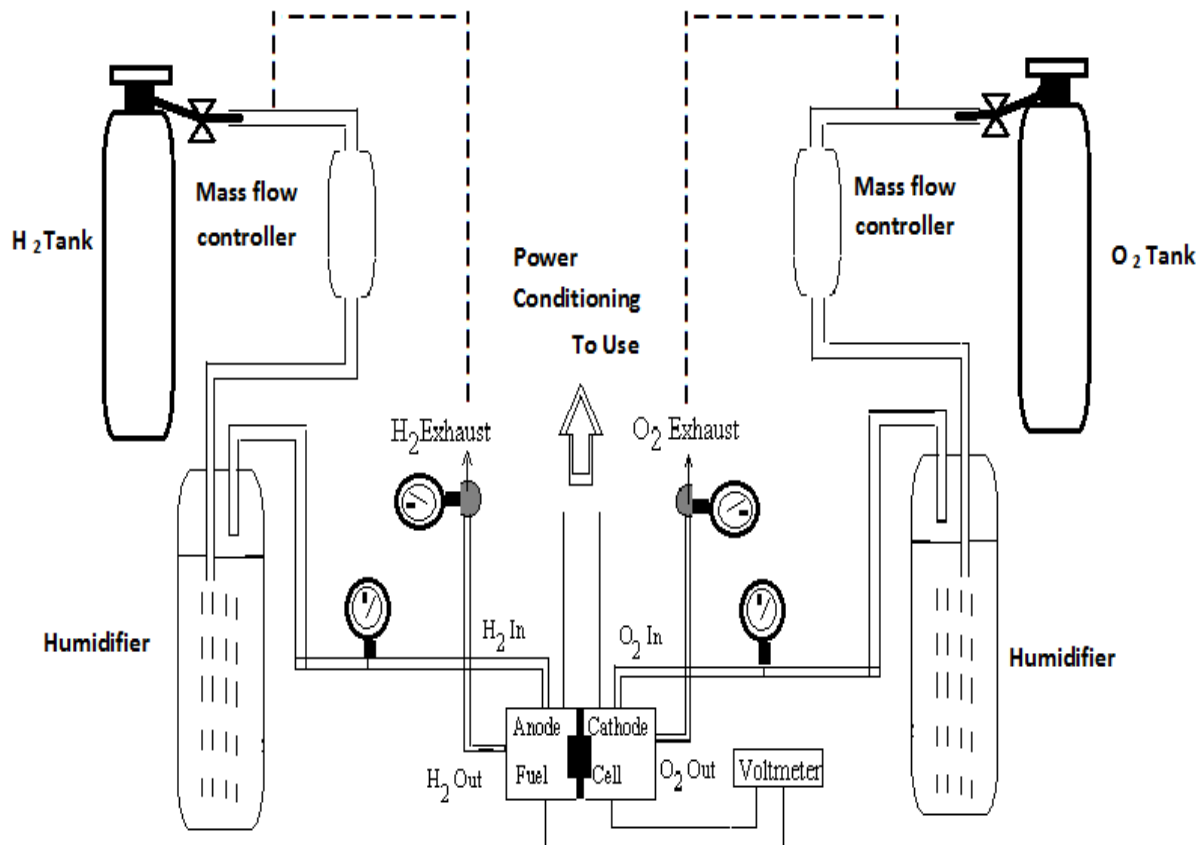


Figure II.5 Single cell test station for proton exchange membrane fuel cell system (PEMFCs)

## II.2 Analysis Methods

### II.2.1 Scanning Electron Microscopic (SEM)

Scanning Electron Microscopic (SEM) used to identify the surface of sample and catalyst distribution and also the phases presented in the surface.

Eight samples were prepared for conducting this experiment. The size of each sample is about one centimeter square (1 cm<sup>2</sup>). The samples consist of catalyst layers for electrode prepared 10wt% Pt/C loaded 0.38 mgPt/cm<sup>2</sup>, the prepared diffusion layer, the cross section of the membrane electrode assembly without diffusion layer loaded 0.38mgPt/cm<sup>2</sup>, the commercial electrode (E-TEK) 10 wt% Pt/C loaded 0.4 mgPt/cm<sup>2</sup>. Second the catalyst layer for electrode loaded 0.3mgPt/cm<sup>2</sup> using 20wt% Pt/C, the catalyst layer for electrode loaded E = 0.3mgPt/cm<sup>2</sup> using 20wt% Pt/C using Nafion® solution, and the cross section of the membrane electrode assembly using Nafion® 112.

### **II.2.2 X - Ray Diffraction (XRD) Analysis**

The goal of catalyst characterization by XRD is to have information on the crystal structure of the metal nanoparticles. Information on platinum crystallite size and crystallinity of the nanoparticles allow correlation with the activity.

#### **II.2.2.a Apparatus**

The apparatus used for the analysis of X-ray diffraction is a Bruker D8 Advance Bragg-Brentano equipped with a copper anticathode powered 40kV and 40 mA. The copper anticathode generates radiation of length wave,  $Cu\alpha_1 = 1.54060 \text{ \AA}$  and  $= 1.54443 \text{ \AA}$   $Cu\alpha_2$ . The resolution function instrumental is obtained by the refinement of a diffractogram of the solid. the machine related to computer with Free software Fitik is used to deconvolute the peaks diffraction.

#### **II.2.2.b Sample preparations**

four samples passed to the XRD analysis, Raw Material (Powder 20 wt%),  $E_{bT}$  (Electrode before Test),  $E_{CaT}$ (Electrode –Cathode-After Test), sample was prepared each sperately using hold powder as shown in the Fig II.6.a-b. Figure 6.a shown the XRD machine and sample holder, the catalyst powder was putin the holder cuerfully with smouth distribution of Pt 20 wt% prticules using a glass to avid the toughness, it's the same for the rest of samples. The sample holder with the sample placed in the XRD support for analysis.

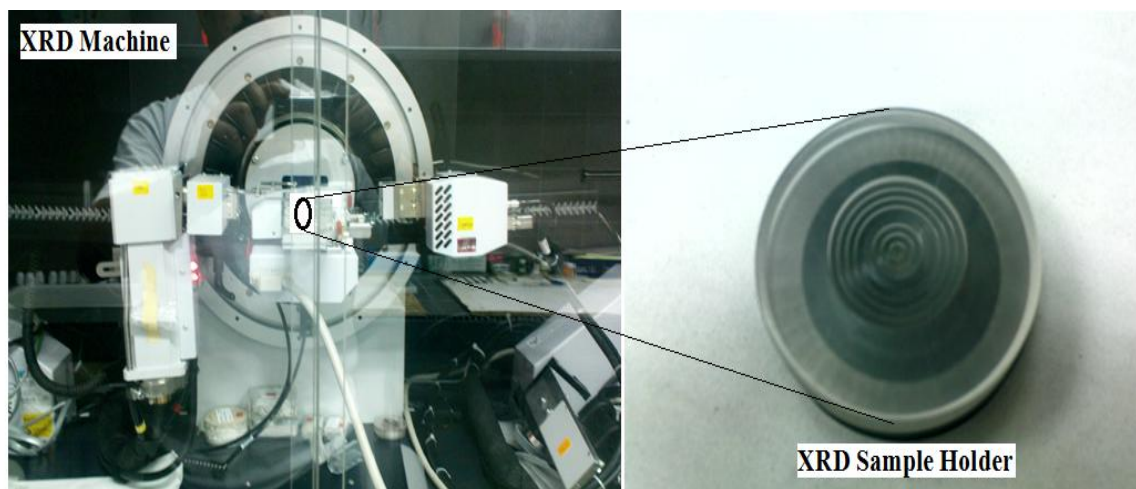


Figure II.6. a XRD Analysis machine with the sample holder

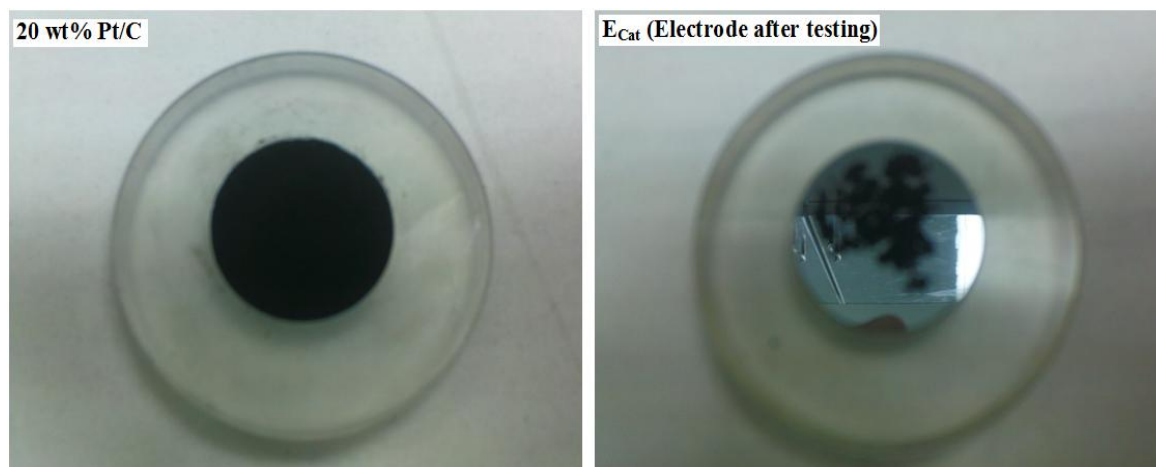


Figure II.6.b XRD samples (Powder and  $E_{Cat}$ ) for electrode preparation for proton exchange membrane fuel cells (PEMFCs)

XRD (X-ray diffraction) is for the samples using the scan type  $2\theta/T$  start from 5- 80 end, with the step size 0.025  $^{\circ}$ . The Timing for one step is 0.1s. The XRD machine operating with Generator 40 Kv, 40mA, UKM Applied Physic Dept Malaysia.

**II.2.3 TEM analysis:** The catalyst supported carbon 20 wt% was characterized by TEM analysis using a Philips CM 120 microscope as shown in the Fig II.7. The two samples dissolved in alcohol (isopropyl 1-2). To prepare the sample, a small Drop of the solution was put on an Au grid and the solvent was evaporated.

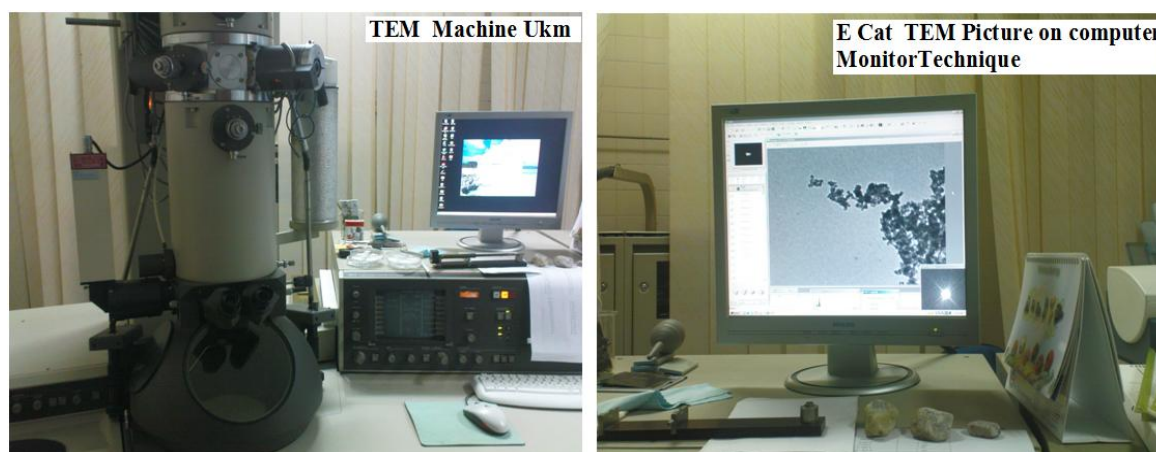


Figure II.7 TEM Machine using a Philips CM 120 microscope Ukm.

**II.2.4 Surface Analysis X-Ray Photo-Electron Spectroscopy (XPS)**

Electrode samples with a thickness of 400  $\mu\text{m}$  in average and surface area of  $1\text{cm}^2$  was initially prepared. The electrode sample surfaces were cleaned to avoid any contamination by wrapping it with clean aluminum foil. Solid sample was directly analyzed without any further treatment.

Electrode samples were analyzed by X-ray Photoelectron Spectroscopy (XPS) using XSAM-HS spectrometer from KRATOS equipped with Magnesium as an X-ray source ( $\text{MgK}\alpha$ ). XPS measurement was made in ultra-high vacuum to allow the photoelectrons to reach the detector without striking a gas atom and avoid the contamination of the clean surface. The gate valve was opened slowly and the sample was inserted using special arm. The sample was left in chamber valve (SAC) and before the gate valve was again closed. The vacuum was left for a few hours until the pressure reached about  $10^{-6}$  Torr, before analysis was carried out. The XPS measurement parameters used are listed in the Tab II.1.

Table II.1 XPS measurement parameters

<b>Technique</b>	<b>XPS</b>
<b>Scan Type</b>	Spectrum
<b>X-ray anode</b>	Magnesium ( $\text{MgK}\alpha$ )
<b>Exciting energy</b>	1253.6 Ev
<b>Gun Current</b>	10Ma
<b>Gun Voltage</b>	12 Kv
<b>Analyzer mode</b>	FAT
<b>Magnification</b>	ELECSTAT
<b>Pass energy</b>	20 eV for narrow scan and 160 eV for wide scan
<b>Maximum Sweep</b>	1
<b>Fat Code</b>	3

**CHAPTER III**  
**DEGRADATION AND MODELING OF**  
**ELECTRODE FOR PROTON**  
**EXCHANGE MEMBRANE FUEL CELL**  
**SYSTEM (PEMFCs)**



## **Introduction**

This chapter consists: first of the analysis techniques for different structures 10 wt% Pt/C and 20 wt% Pt/C, which analyzed by SEM, XPS, for the 10 wt% Pt/C structure for diffusion layer and catalyst layer. Second is the operating of electrode in single cell for 20 wt% Pt/C more than 100 hours .third SEM, XPS, XRD, TEM for electrode (cathode) 20 wt% Pt/C Analysis after aggressive operating condition as pressures effect, humidifier temperature, flow rate of reactants and the last is making a model explain the effect of these parameters as pressure, cell temperature and catalyst for electrode loaded  $0.38 \text{ mg}_{\text{Pt}}/\text{cm}^2$  using 10 wt% Pt/C.

### **III.1. Scanning Electron Microscopy (SEM)**

The samples were analyzed to identify the surface and catalyst distribution. The first structure for electrode 10wt% Pt/C loaded  $0.38 \text{ mg}/\text{cm}^2$ , Fig III.1.a shown the surface for diffusion Layer (GDL) contain carbon black and Teflon binder (PTFE/C) no catalyst was observed, for the Fig III.1.b represent the Scanning Electron Microscopy of catalyst layer (Pt/C/PTFE) 10 % Pt/C loading  $0.3 \text{ mgPt}/\text{cm}^2$  that showed the catalyst as slight particles with the good distribution on the surface of electrode and the Fig III.2.a shown the Scanning Electron Microscopy of E-TEK electrode 10 % Pt/C loading  $0.4 \text{ mgPt}/\text{cm}$ . the electrode prepared with the diffusion layer (GDL) has a good catalyst distribution compared to the commercial electrode (E-TEK). Fig III.2.b shown the cross section of membrane electrode assembly (MEA) without diffusion layer (GDL), which can observe the catalyst layer contact direct to the baking layer (carbon cloth).this contact reduce the efficiency of gas diffusion electrode.

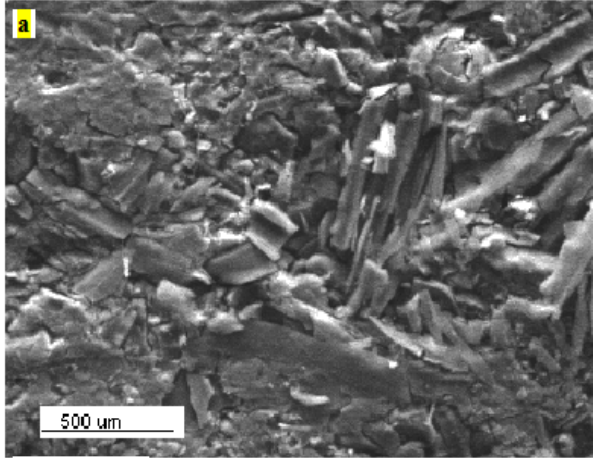


Figure III. 1.a Scanning electron microscopic for diffusion layer (GDL) Thesis 2001

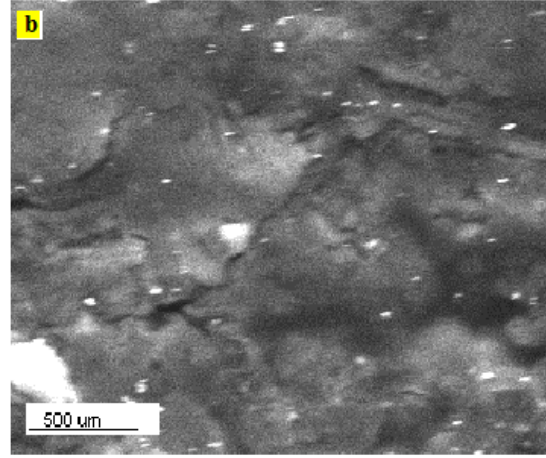


Figure III. 1.b Scanning electron microscopic (SEM) for catalyst layer (PT/PTFE/C) 10 % Pt/C magnified 500 μm without Nafion<sup>®</sup> loaded Pt=0.38 mg/cm<sup>2</sup>

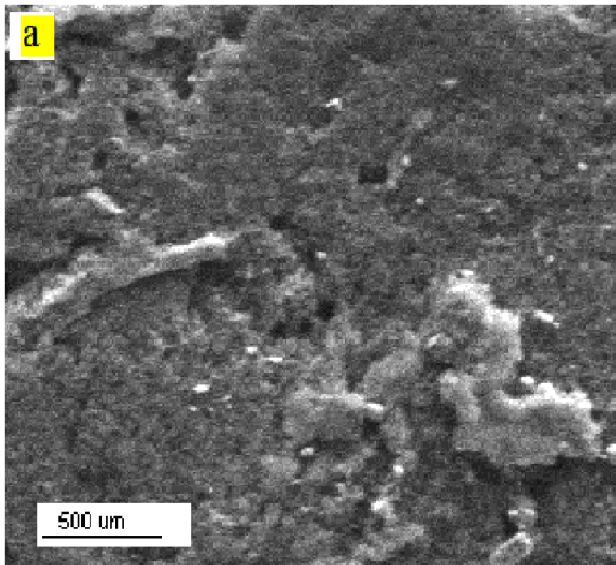


Figure III. 2.a Scanning electron microscopic (SEM) of E-Tek electrode 10 % Pt/C loaded 0.4mgPt/cm<sup>2</sup> Chebbi.R 2001

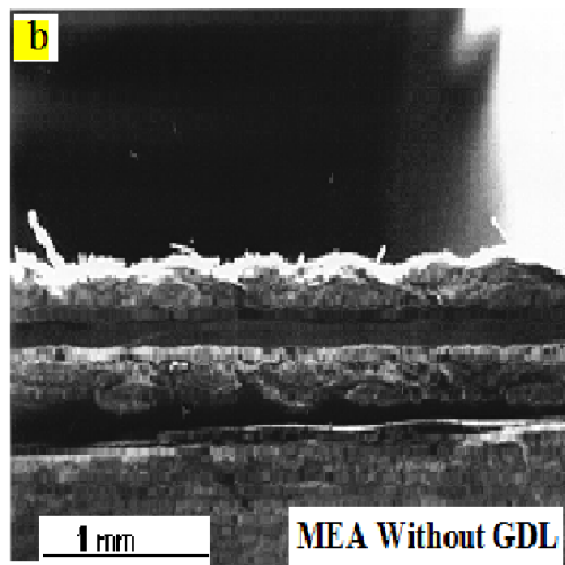


Figure III. 2.b Scanning electron microscopic (SEM) of Cross section of membrane electrode assembly without diffusion layer (GDL)

For the second electrode structure with the loading 0.3mg/cm<sup>2</sup> using 20wt% Pt/C, this structure analyzed by SEM to identify the distribution of the catalyst layer and also diffusion layer (GDL).

Fig III.3.a Shown the diffusion layer almost the same as before in the first structure , that can observe the distribution of teflon (PTFE) all over the layer, and Fig III.3.b shown the surface

## CHAPTER III DEGRADATION AND MODELING OF ELECTRODE FOR (PEMFCs)

of electrode without Nafion<sup>®</sup> solution, Which shown the catalyst distribution with some agglomeration mentioned by yellow circles. Figure III.4.a shown the same electrode but with Nafion<sup>®</sup> solution using brush method and the Figure III.4.b shown the SEM of electrode assembly using membrane Nafion<sup>®</sup> 112.

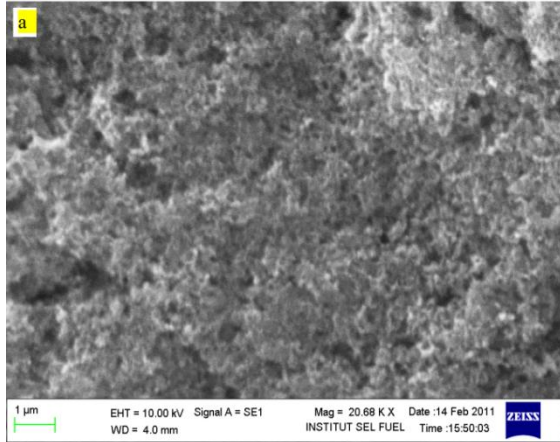


Figure III.3.a Scanning electron microscopic (SEM) for diffusion layer (GDL) magnificated 1 um

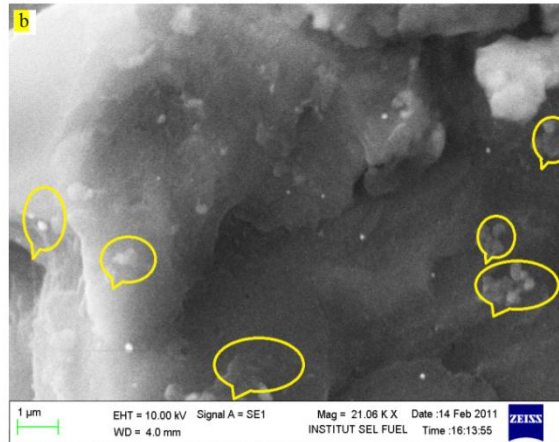
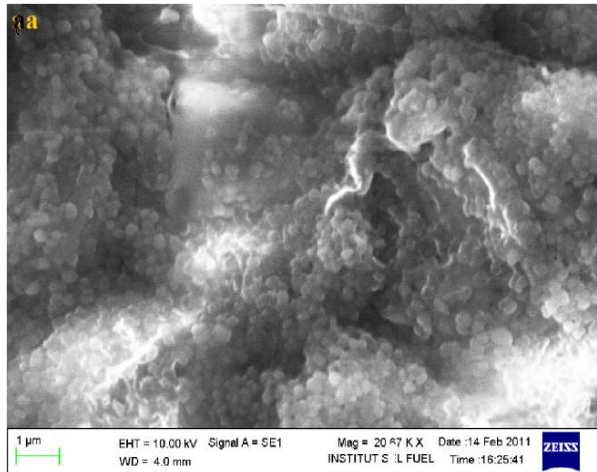
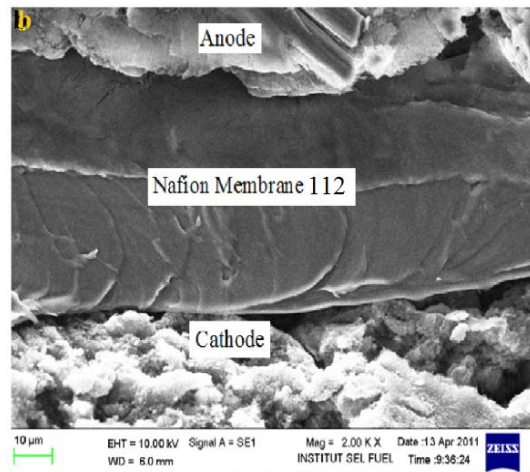


Figure III.3.b Scanning electron microscopic (SEM) for catalyst layer (Pt/PTFE/C) 20 wt% without Nafion<sup>®</sup>



**Figure III.4.a** Scanning electron microscopic of catalyst layer (Pt/PTFE/C-Nafion using 20 %Pt/C magnificated 1 μm



**Figure III.4.b** SEM of Membrane electrode assembly (MEA) and Cross Section of membrane (112) Fabricated in Sel Fuel Institute Ukm

### III.2 XPS Technique

XPS analyses for Proton exchange membrane fuel cells (PEMFCs) in this work consist to analyse two electrodes structures 10 wt% Pt/C and 20 wt% Pt/C.

The first structure 10 wt% Pt/C consist to characterize the surface of electrode with diffusion layer (GDL, Catalyst layer prepared electrode, and the Catalyst layer E-TEK electrode (commercial)).

Second Structure is 20 wt% Pt/C consists to characterize the electrode before test ( $E_{bT}$ ), and cathode after test ( $E_{CaT}$ ) with thickness of 300-400  $\mu\text{m}$  and surface area of  $1\text{cm}^2$  for both.

XPS analysis for Proton exchange membrane fuel cells (PEMFCs) electrodes for both diffusion layer and catalyst layer, generally give the same XPS spectra pattern except the catalyst.

The wide scan XPS spectra for diffusion layer (PTFE/C), and catalyst layer (Pt/C/PTFE) are presented in Fig III.5.a-b with the data given in the Tables III.1 and III.2. Four major photoelectron peaks are presented in Fig III.5.a, and five major photoelectron peaks presented in Fig III.5.b. Four peaks are present in the Diffusion layer correspond to the atom of carbon ( $C_{1s}$ ), fluorine ( $F_{1s}$ ), oxygen ( $O_{1s}$ ), and silicone ( $Si_{2p}$ ), which are identified by their binding energies in the region of 285.0 eV, 689.5 eV, 532.7, and 103.0 eV. In the catalyst layer, five peaks are observed corresponding to the atom of carbon ( $C_{1s}$ ), fluorine ( $F_{1s}$ ), oxygen ( $O_{1s}$ ), silicone ( $Si_{2p}$ ), and platinum ( $Pt_{4f}$ ) which are identified by their binding energies are in the region of 284.3 eV, 689.3, 532.4 eV, 102.9 eV, and 74.1 eV. Broader and more intense peaks are identified as Auger peaks arising from the de-excitation of the corresponding atoms as indicated in the same spectra.

The results of the XPS analysis on the prepared electrodes are in agreement with that of the commercial electrode (E-TEK) with the presence of the same components (C, O, F, Pt, and Si) as shown in the Tab III.3 except that Si doesn't appear in the prepared electrode due to the purity of platinum supported carbon black. Five major photoelectron peaks appear in (E-TEK) electrode correspond to the atoms of carbon ( $C_{1s}$ ), fluorine ( $F_{1s}$ ), oxygen ( $O_{1s}$ ), silicone ( $Si_{2p}$ ), and platinum ( $Pt_{4f}$ ) which are identified by their binding energies in the region of 284.5 eV, 289.4 eV, 232.9 eV, 102.8, and 72.4 eV respectively.

**CHAPTER III DEGRADATION AND MODELING OF ELECTRODE FOR (PEMFCs)**

Table III.1 Semi-quantitative analysis of (Pt/C/PTFE) catalyst layer using XPS technique

Peak	BE (eV)	FWHM Ev	Atomic Conc%	Mass Conc%
<b>C<sub>1s</sub></b>	285.0	1.6	59.5	47.5
<b>O<sub>1s</sub></b>	532.7	3.7	7.9	8.5
<b>F<sub>1s</sub></b>	689.5	3.0	28.5	36.0
<b>Si<sub>2p</sub></b>	103.0	1.3	3.8	7.2
<b>Pt<sub>4f</sub></b>	73.5	0.19	0.05	0.6

Table III.2 Semi-quantitative analysis of (PTFE/C) diffusion layer of using XPS technique

Peak	BE(eV)	FWHMMeV	Atomic Conc %	Mass Conc%
<b>C1s</b>	284.3	2.2	57.98	44.96
<b>O1s</b>	532.4	3.1	6.62	6.85
<b>F1s</b>	689.3	2.8	32.93	40.43
<b>Si1s</b>	102.9	0.2	2.17	3.94

Table III.3 Semi-quantitative analysis of (E-TEK) electrode using XPS technique

Peak	BE(eV)	FWHM EV	Atomic Conc %	Mass Conc%
C1s	284.5	1.1	53.7	41.8.2
O1s	532.9	1.49	2.9	3.0
F1s	689.4	1.9	41.7	51.3
Si1s	102.8	0.6	1.4	2.6
Pt4f	72.4	0.4	0.08	2.6

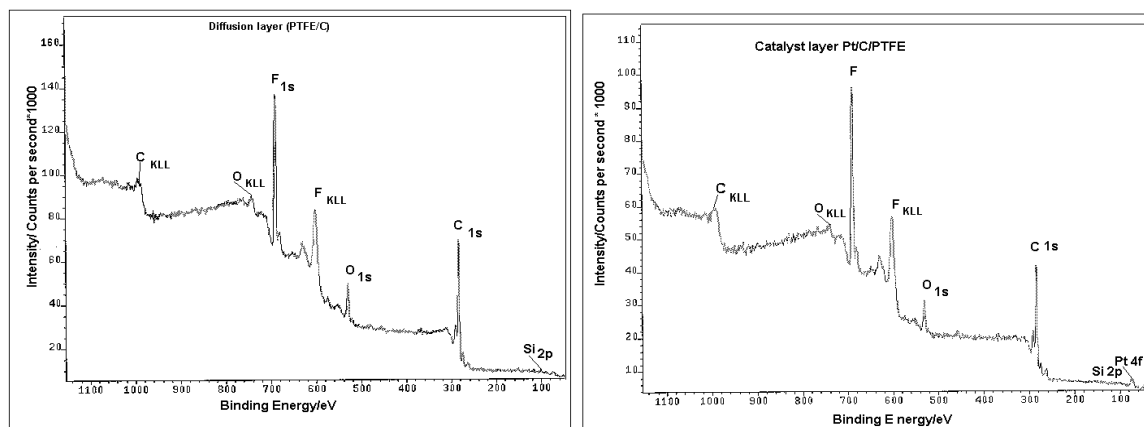


Figure III.5.a XPS survey spectrum of a- (PTFE/C) and b- (Pt/C/PTFE) catalyst layer electrode

XPS can be used for semi-quantitative analysis based on the peak area of individual atoms. The results for the PTFE/C diffusion layer and the Pt/C/PTFE catalyst layer samples are shown in the Tab III.1 and Tab III.2. Narrow scan of each element is shown in Figures III.5.a and III.5.b for both the diffusion layer and the catalyst layer. An intensive peak is observed whenever there is a high amount of element present in the electrode. In our case, carbon and fluorine give intensive peaks in the PTFE/C diffusion layer and in the Pt/C/PTFE catalyst layer.

The elemental or atom compositions represent the elemental compositions at about 10-20 atom layers from the sample surfaces, which are expected on the elemental composition surfaces of the samples. The compositions of carbon for both samples are slightly higher, which may be due to some sample contamination. Narrow scan for Pt <sub>4f</sub> in Fig III.5.a shows no platinum at all.

### 2.1 Carbon (C<sub>1s</sub>)

C<sub>1s</sub> peak is very important peak in any XPS studies because all of the charging effects is corrected to graphite carbon (C<sub>1s</sub>) at 284.5 eV.

The C<sub>1s</sub> core level spectrum of the PTFE/C diffusion layer is presented in Fig III.6.a and its curve fitting parameters for carbons are presented in Tab III.4.a.

Fig III.6.a shows that the C<sub>1s</sub> peak at 285.0 eV is broad with FWHM = 1.3 eV. The best fit for carbon C<sub>1s</sub> peak yields six peaks at binding energies 284.5 eV, 285.7 eV, 287.0 eV, 289.3

eV, 292.1 eV, and 294.9 eV. The close reading of the energies is a result of good conductivity and macroscopic extent to the structural integrity, as observed in graphite [72].

The carbon C<sub>1s</sub> peak at 284.5 eV is assigned to the graphite carbon atom or -C not bonded to either F or O atom. The second peak at 285.7 eV is attributed to the carbon atom C-O. The third peak at 287.0 eV is attributed to carbon atom attached to the oxygen atom C=O. The fourth peak at 289.3 eV is ascribed to carbon atom attached to the fluorine atom -CF. The fifth peak at 292.1 eV is ascribed to the carbon atom attached to -CF<sub>2</sub> atoms. The sixth peak at 294.9 eV is ascribed to the atom carbon attached to -CF<sub>3</sub>.

Figure III.6.b shows that the C<sub>1s</sub> core-level spectrum of the Pt/C/PTFE catalyst layer exhibits similar features to those shown in Fig III.6.a for PTFE/C diffusion layer. Figure III.6.b shows that the C<sub>1s</sub> peak at 284.3 eV is broad with FWHM = 1.4 eV. Figure III.6.b shows the C<sub>1s</sub> spectrum treated by catalyst supported carbon, with the aid of the assignment of the fluorine peaks. The curve fitting C<sub>1s</sub> spectrum yields six component peaks as shown in Fig III.6.b, except for one peak with a small intensity about 4% at binding energy 289.1 eV corresponds to carbon attached to the hydrogen and fluorine atoms (-CHF). It is evident that the -CF<sub>2</sub> and -CH<sub>3</sub> groups obviously stem from the perfluoro functional groups as demonstrated in [73]. In our case, the appearance of -CH and -C- groups should be reasonably ascribed to the cross-linking between the main polymeric chains, and the -CF<sub>2</sub> components which dominate on the surface more than the -CF and -CF<sub>3</sub> containing peaks as presented in Fig III.6.b. The second peak at 285.8 eV is due to the oxygenated state of the metal/oxygen environment (C-O-Pt) which forms the principal difference between the PTFE/C diffusion layer and the Pt/C/PTFE catalyst layer. The change in intensities of peaks, especially at 285.8 eV and 292.4 eV may be due to the interaction between the catalyst and the matrix of the PTFE/C diffusion layer.

## CHAPTER III DEGRADATION AND MODELING OF ELECTRODE FOR (PEMFCs)

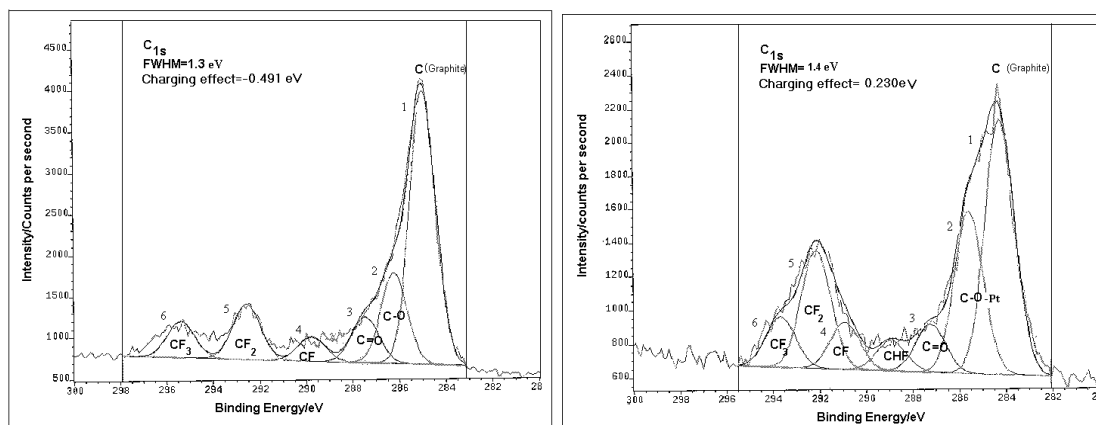


Figure III.6.a Cure Fitting XPS-spectra for carbon ( $C_{1s}$ ) a)-(PTFE/C) and b- (Pt/C/PTFE) catalyst layer electrode

Table III.4.a XPS parameters for carbon ( $C_{1s}$ ) curve fitting for the diffusion layer (PTFE /C)

Component name	Model name	BE(eV) (corrected)	FWHM Ev	Intensity(%)	Quant'n Factor	Assign
$C_{1s}$ peak1	Gaussian	284.5	1.3	50.2	0.25	C
$C_{1s}$ peak 2	Gaussian	285.7	1.3	17.2	0.25	-C-O
$C_{1s}$ peak 3	Gaussian	287.0	1.3	8.5	0.25	-C =O
$C_{1s}$ peak 4	Gaussian	289.3	1.3	4.6	0.25	-CF
$C_{1s}$ peak 5	Gaussian	292..1	1.3	10.5	0.25	-CF <sub>2</sub>
$C_{1s}$ peak 6	Gaussian	294.9	1.3	6.8	0.25	-CF <sub>3</sub>

Table III.4.b XPS parameters for carbon ( $C_{1s}$ ) curve fitting for the Pt/C/PTFE catalyst layer

Component Name	Model Name	BE (eV) (Corrected)	FWHM eV	Intensity	Quant'n Factor	Assign
$C_{1s}$ peak1	Gaussian	284.5	1.4	36	0.25	-C
$C_{1s}$ peak 2	Gaussian	285.8	1.4	22	0.25	-C-O-Pt
$C_{1s}$ peak 3	Gaussian	287.5	1.4	6.6	0.25	-C =O
$C_{1s}$ peak 4	Gaussian	289.1	1.4	4.3	0.25	-CHF
$C_{1s}$ peak 5	Gaussian	290.2	1.4	6.6	0.25	-CF
$C_{1s}$ peak 6	Gaussian	292.4	1.4	16.6	0.25	-CF <sub>2</sub>
$C_{1s}$ peak 7	Gaussian	293.9	1.4	7	0.25	-CF <sub>3</sub>



**2.2 Oxygen (O<sub>1s</sub>)**

The narrow scan XPS-spectra for oxygen is shown in Figures III.7.a and 7.b, which the curve fitting parameters for oxygen are presented in Tables III.5.a and III.5.b. Fig III.7.a shows that for the PTFE/C diffusion layer, the O<sub>1s</sub> peak at 532.7 eV is broad with FWHM=2.1eV. The best fit for oxygen O<sub>1s</sub> peak yields three peaks at 530.0 eV, 532.3eV, and 533.9 eV, which correspond to the different chemical states C-O, O=C, and H-O-H, respectively. This fit internal exists C-O with that obtained in C<sub>1s</sub> as demonstrated (that is mean the oxygen atom bond with carbon atom during the contact carbon oxygen) the in curve fitting of C<sub>1s</sub> spectrum Fig III.7.a.This oxygen concentration is due to the environment [74].

The O<sub>1s</sub> spectrum of the Pt/C/ PTFE catalyst layer as shown in Fig III.7.b, has a similar shape to that of the PTFE/C diffusion layer, in which the O<sub>1s</sub> peak at 532.4 eV is broad with FWHM=2.0 eV. The best fit for oxygen O<sub>1s</sub> peak yields three peaks at 530.7 eV, 532.3eV and 533.9 eV, which may correspond to the shift of the centroid to a slightly higher binding energy. This is due to the incorporation of the catalyst in the electrode layer. The peaks positioned at 530.7 eV, 532.3 eV and 533.9 eV are almost similar to those observed for the PTFE/C diffusion layer. However the peak at 530.7 eV is assigned to the metal oxygen bond formation Pt-O [75,76].. The second peak is ascribed to the oxygen atom attached to the carbon atom C=O and the third peak at 533.9 eV corresponds to the oxygen atom attached to the two-hydrogen atoms H-O-H [77].

Table III.5.a XPS parameters for oxygen (O<sub>1s</sub>) curve fitting for the PTFE/C diffusion layer

Component name	Model Name	BE (eV) (corrected)	FWHM eV	Intensity	Quant'n Factor	Assign
O <sub>1s</sub> peak 1	Gaussian	530.0	2.1	28.3	0.6	C-O
O <sub>1s</sub> peak 2	Gaussian	532.3	2.1	53.0	0.6	C =O
O <sub>1s</sub> peak 3	Gaussian	533.9	2.1	18.1	0.6	H-O-H

Table III.5.b XPS parameters for oxygen ( $O_{1s}$ ) curve fitting for the (Pt/C/PTFE) catalyst layer

Component name	Model name	BE (eV) (corrected)	FWHM eV	Intensity	Quanta's factor	Assign
O1s peak 1	Gaussian	530.7	2.0	25.6	0.6	Pt- O
O1s peak 2	Gaussian	532.3	2.0	52.6	0.6	C = O
O1s peak 3	Gaussian	533.9	2.0	21.8	0.6	H-O-H

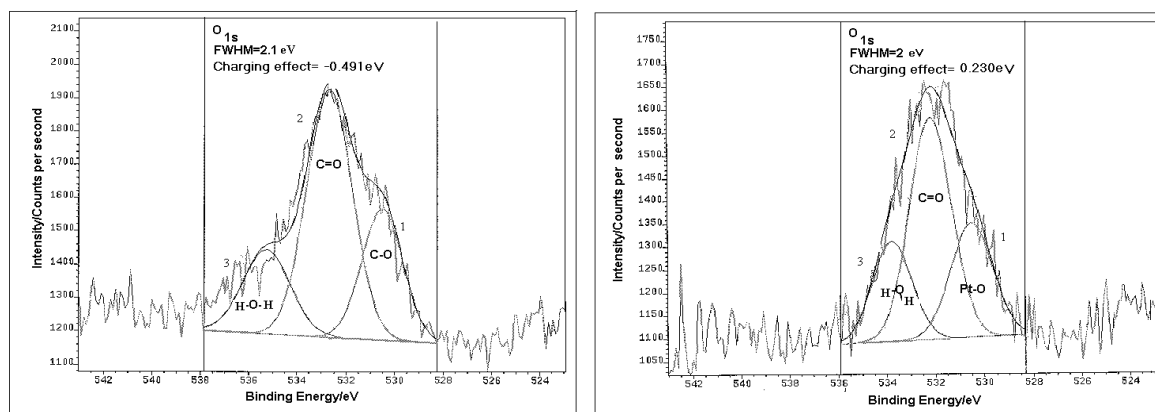


Figure III.7 Curve Fitting XPS-spectra for Oxygen ( $O_{1s}$ ) a-(PTFE/C) and b- (Pt/C/PTFE) catalyst layer electrode

### 2.3 Fluorine ( $F_{1s}$ )

Fluorine is the most important element in the structure of electrode because it is used as a binder for Pt/C and wet proofing of the electrode.

The narrow scan XPS-spectra for fluorine are shown in Figures III.8.a-b. The curve fitting parameters for fluorine are presented in Tables III.6.a-b. Fig III.8.a shows that for the PTFE/C diffusion layer, the  $F_{1s}$  peak at 689.5 eV is broad with FWHM=2.4 eV. The best fit for fluorine  $F_{1s}$  peak yields two peaks at 689.2 eV, and 692.2 eV, which are attributed to the presence of two different environments with a chemical shift of 3 eV. The peak at 689.2 eV corresponds to  $CF_2$  in the diffusion layer as reported in the literature [77] and the peak at 692.2 eV is correspond to  $-CF_3$  type of interaction. On the other hand, the peak at 689.2 eV corresponds to  $CF_2$  in the dry state as shown in Fig III.8. The minimum peak at 692.2 eV correspondents to the  $CF_2$  in wet state (dissolved in water) as shown in Fig III.8.

**CHAPTER III DEGRADATION AND MODELING OF ELECTRODE FOR (PEMFCs)**

Figure III.8 b shows the  $F_{1s}$  spectrum of the Pt/PTFE/C catalyst layer, where  $F_{1s}$  peak at 689.3 eV is broad with FWHM=2.3 eV. The best fit for fluorine  $F_{1s}$  peak yields two peaks at 689.2 eV, and 690.8 eV, which can be attributed to the presence of two different environments. The maximum peak is at 689.2 eV, and the minimum peak is at 690.8 eV with a chemical shift of 1.6 eV. The peak at 689.2 eV corresponds to  $CF_2$  in the catalyst layer [77]. the peak at 690.8 eV corresponds  $CF_3$ .

Table III.6.a XPS parameters for fluorine ( $F_{1s}$ ) curve fitting for the PTFE/C diffusion

Component name	Model name	BE (eV) (corrected)	FWHM EV	Intensity	Quant'n Factor	Assign
$F_{1s}$ peak 1	Gaussian	689.2	2.4	72.0	1.00	-CF2
$F_{1s}$ peak 2	Gaussian	692.2	2.4	27.5	1.00	-CF3

Table III.6.b XPS parameters for fluorine ( $F_{1s}$ ) curve fitting for the Pt/PTFE/C catalyst layer

Component name	Model name	BE (eV) (corrected)	FWHM EV	Intensity	Quant'n Factor	Assign
$F_{1s}$ peak 1	Gaussian	689.2	2.2	78.7	1.00	-CF2
$F_{1s}$ peak 2	Gaussian	690.8	2.3	21.4	1.00	-CF3

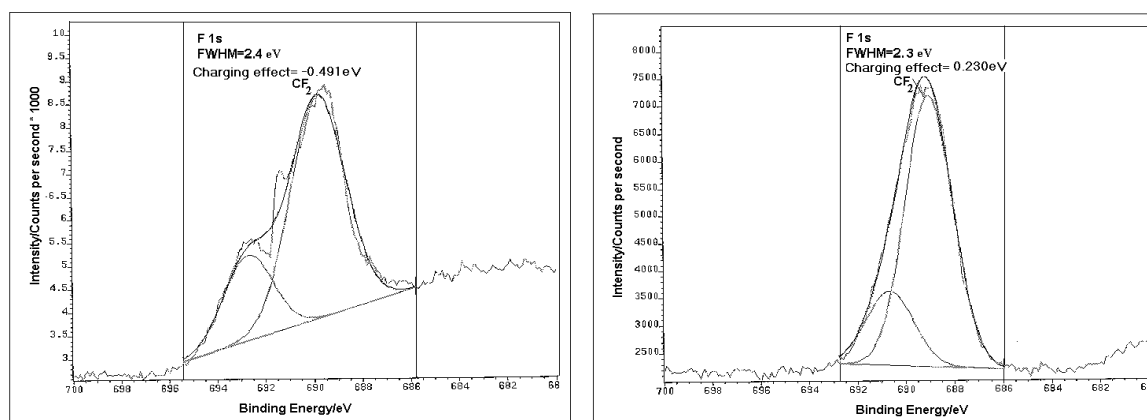


Figure III.8 Curve Fitting XPS-spectra for Fluorine ( $F_{1s}$ ) a-(PTFE/C) and b- (Pt/C/PTFE) catalyst layer electrode

### 2.4 Silicon (Si<sub>2p</sub>)

Silicon is also present in the electrode as silicon dioxide (SiO<sub>2</sub>). Silicon comes from impurity in the carbon and exists in small quantity. In the fitting curve of the spectrum yields SiO<sub>2</sub> as a single peak at 102.3 eV in the diffusion layer. According to the representative chemical shift data for Si<sub>2p</sub>, the binding energy for SiO<sub>2</sub> should be at 102.5 eV [77]. In the catalyst layer the peak is not very clear and the SiO<sub>2</sub> exists in a trace amount as SiO<sub>2</sub> as show in Fig III.9.a.

Table III.7.a XPS parameters for silicon (Si<sub>2p</sub>) curve fitting for the PTFE/C diffusion layer

Component name	Model Name	BE(eV) (corrected)	FWHM EV	Intensity	Quant'n Factor	Assign
Si <sub>2p</sub> peak 1	Gaussian	102.3	3.3	77.4	0.27	Si-O-Si

Table III.7.b XPS parameters for silicon (Si<sub>2p</sub>) curve fitting for the Pt/PTFE/C catalyst layer

Component name	Model Name	BE(eV) (corrected)	FWHM EV	Intensity	Quant'n Factor	Assign
Si <sub>2p</sub> peak 1	Gaussian	102.5	3.3	68.0	0.27	Si-O-Si

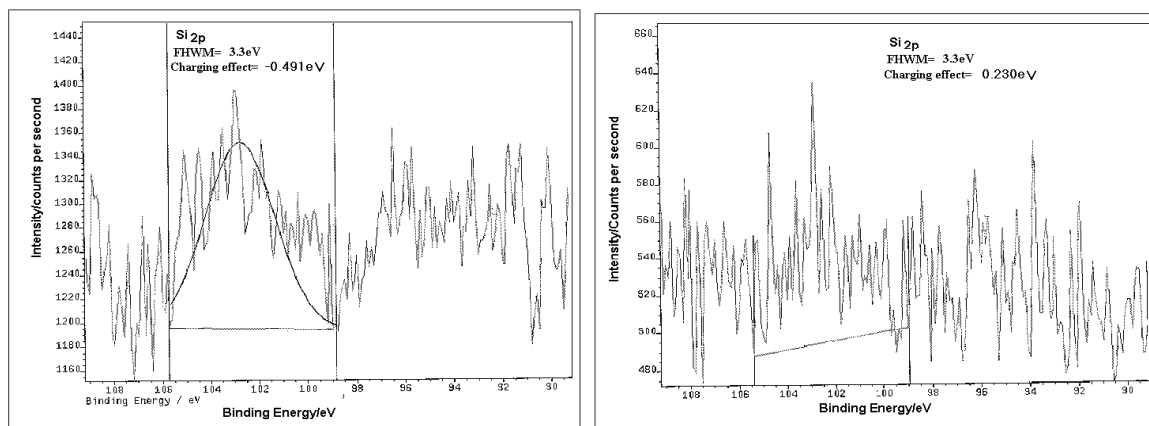


Figure III.9 Curve Fitting XPS-spectra for silicon (Si<sub>2p</sub>) a-(PTFE/C) and b- (Pt/C/PTFE) catalyst layer electrode

### 2.5 Platinum (Pt<sub>4f</sub>)

The Pt<sub>4f</sub> spectrum of the PTFE/C diffusion layer shows no existence of platinum in this layer as shown in Fig III. 10.a. Fig III. 10.b shows that the Pt<sub>4f</sub> spectrum of the Pt/PTFE/C catalyst layer at 74.1 eV is broad with FWHM = 2.5 eV. The best fit for platinum Pt<sub>4f</sub> peak yields two intense

peaks of  $4f_{7/2}$  and  $4f_{5/2}$  at the binding energies of 71.8 eV and 75.0 eV, respectively. The Pt  $4f_{7/2}$  and Pt  $4f_{5/2}$  signals are asymmetrically shaped towards the higher binding energies. The peak at 71.8eV (Pt  $4f_{7/2}$ ) represents  $Pt^0$  while some of the Pt oxidize from  $Pt^0$  to Pt-O at binding energy of 75.0 eV [78].

Table III.8 XPS Parameters for platinum (Pt  $4f$ ) curve fitting for the Pt/PTFE/C catalyst layer

Component name	Model name	BE(eV) (correcte)	FWHM eV	Intensity	Quant'n Factor	Assign
Pt $4f_{7/2}$ peak1	Gaussian	71.8	2.5	56.3	4.4	Pt <sup>0</sup>
Pt $4f_{5/2}$ peak 2	Gaussian	75.0	2.5	43.6	4.4	Pt-O

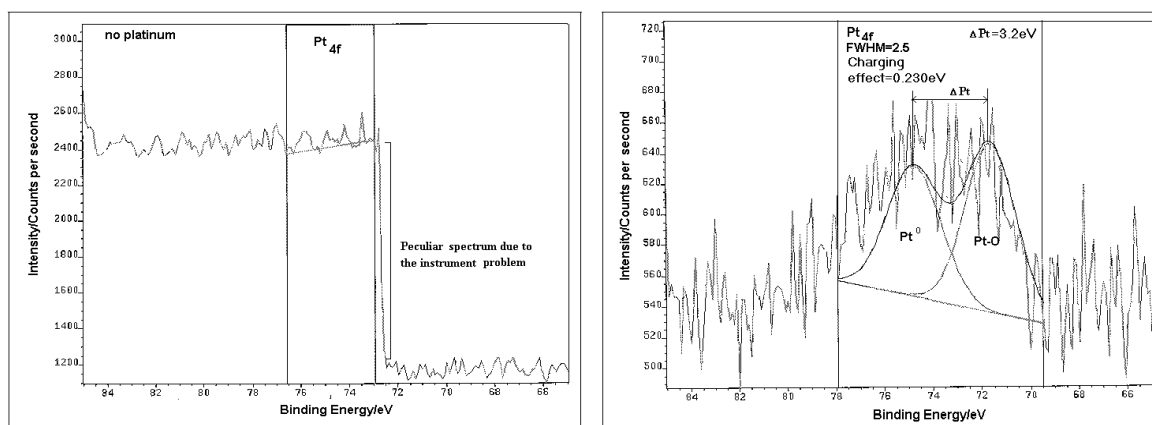


Figure III.10 Curve Fitting XPS-spectra for platinum (Pt  $4f$ ) a-(PTFE/C) and b- (Pt/C/PTFE) catalyst layer electrode

### III.3 Electrode Degradation

#### III.3.1 Operating cathode in a single cell 25 cm<sup>2</sup>

The MEA are fixed in single cell 25cm<sup>2</sup> supply from ElectroChem, equipped with two graphite plates with a ribbed channel for the distribution of reactant gases behind the porous gas-diffusion electrodes, a gasket containing the gas inlet and outlet, and a copper plate used as the current collector from the fuel cell positioned behind each of the graphite plates. The single cell is connected to a GasHub,Ltd. test station, which is equipped with two humidifiers for oxygen and hydrogen that can operate at various humidifier temperatures, and with two flow controllers for hydrogen and air. This test station was connected to the digital voltlab computer to obtain a single cell output voltage versus current density and power density.

**CHAPTER III DEGRADATION AND MODELING OF ELECTRODE FOR (PEMFCs)**

The electrode prepared with  $0.3 \text{ mg}_{\text{Pt}}/\text{cm}^2$  was operated in a single cell  $25 \text{ cm}^2$  with aggressive conditions of the parameters such as: pressures, humidifier temperatures, flow rate of air /hydrogen. The values of parameters were measured during the operation, and the on/off switch of the single cell.

Fig III.11.a shows the variation in the air flow rate applied to the single cell  $25 \text{ cm}^2$  at room temperature ( $\approx 30^\circ \text{C}$ ) and at pressures of  $\text{air}/\text{H}_2 = 2/1$  bar. From the plotted voltage and power density vs. current density, the increasing flow rate of air from 0.4-0.6-0.9-1.2-1.8-2.4 and 3 L/min with a fixed hydrogen flow rate at 0.6 L/min increased the power density and current density. A flow rate of 3 L/min produces the best values for the open circuit voltage (OCV)  $E_o = 0.81 \text{ V}$ , current density  $\{103.96 \text{ mA}/\text{cm}^2\}$  and power density  $\{33.12 \text{ mW}/\text{cm}^2\}$ , compared to the other air flow rate conditions. This explains the free water in the electrode when oxygen reduction occurs in the cathode and the lower water resistance at the electrode surface (electrode-graphite plates).

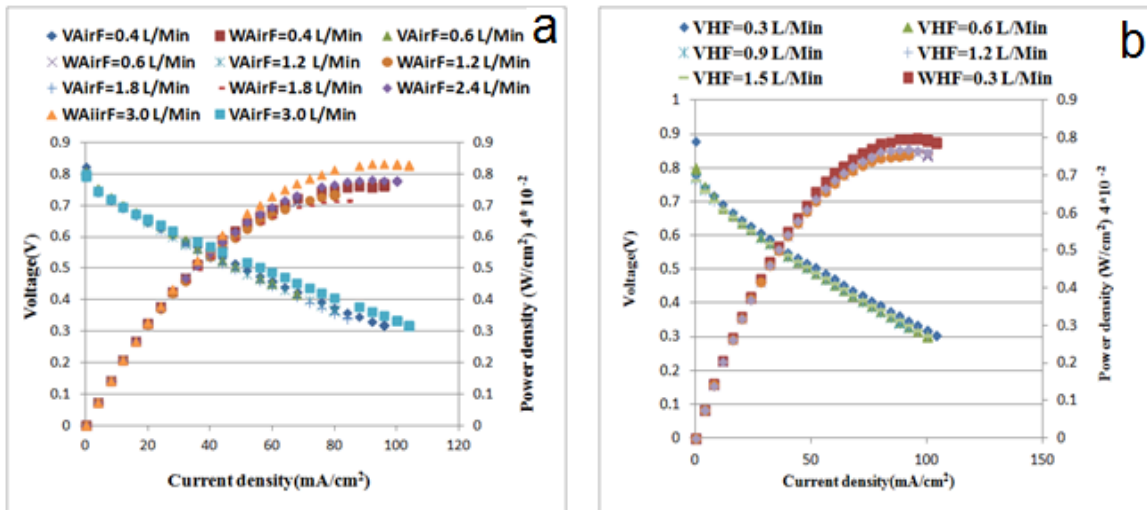


Figure III.11.a Cell voltage and power density vs. current density plots of single cell ( $25 \text{ cm}^2$ ) with various air flow rates. b- Cell voltage and power density vs. current density plots of single cell ( $25 \text{ cm}^2$ ) with various hydrogen flow rates.

Fig III.11.b shows the variation in the hydrogen flow rates applied to the single  $25\text{-cm}^2$  cell at room temperature ( $\approx 30^\circ\text{C}$ ) and a pressure of  $\text{air}/\text{H}_2 = 2/1$  bar, using 20 wt% Pt/C loaded  $0.3 \text{ mg}_{\text{Pt}}/\text{cm}^2$ . The voltage and power density vs. current density plots show the increase of the

**CHAPTER III DEGRADATION AND MODELING OF ELECTRODE FOR (PEMFCs)**

voltage and power density with decreasing hydrogen flow rate from 0.3-0.6-0.9-1.2 and 1.8 L. A hydrogen flow rate of 0.3 L/min produces better values for the open circuit voltage (OCV)  $E_o = 0.83$  V, current density =  $103.96 \text{ mA/cm}^2$  and power density =  $31.56 \text{ mW/cm}^2$  compared to for a hydrogen flow rate at 1.5 L/min corresponding to  $E_o = 0.77$  V, current density =  $91.96 \text{ mA/cm}^2$  and power density  $30.72 \text{ mW/cm}^2$ . The best value for the hydrogen flow rate is 0.3 L/min and for air is 0.6 L/min; these values produce better values for the open circuit voltage, power density and current density as shown in Table 1, the results of which were in accordance with the stoichiometry factor  $\frac{1}{2}$  from the  $\text{H}_2 + \frac{1}{2} \text{O}_2 \rightarrow \text{H}_2\text{O}$  equation. The low flow rate of hydrogen and high air flow rate with the appropriate ratio contribute to attaining high performance. Fig. III.12.a shows the voltage and power density vs. current density plots of a single cell ( $25 \text{ cm}^2$ ), operating with various humidifier temperatures ( $55, 65, 75^\circ\text{C}$ ) for air and for hydrogen plus  $5^\circ\text{C}$  ( $T_{\text{Air}} + 5^\circ\text{C}$ ), using same electrode with an operating flow rate of  $\text{air}/\text{H}_2 = 1.2/0.6 \text{ L/min}$  at room temperature ( $\approx 30^\circ\text{C}$ ) and pressures of  $\text{air}/\text{H}_2 = 2/1 \text{ bar}$ . The effect of the humidifier temperatures produces better performance at low humidifier temperatures ( $55/60 \text{ H}_2/\text{air}$ ), as demonstrated in Fig III.12.a and Tab III.9.

Table III.9 Characteristics of the electrode at various air/H<sub>2</sub> flow rates

<b>Air flow rate (L/min)</b>	<b>0.4</b>	<b>0.6</b>	<b>1.2</b>	<b>1.8</b>	<b>2.4</b>	<b>3</b>
<b><math>E_{o\text{air}}</math> (V)</b>	0.81	0.8	0.8	0.8	0.79	<b><u>0.8</u></b>
<b><math>b_{\text{air}}</math> (V/dec)</b>	0.04	0.03	0.03	0.03	0.03	<b><u>0.03</u></b>
<b><math>P \{\text{mW/cm}^2\}</math></b>	30.56	28.48	29.4	28.68	31.24	<b><u>33.12</u></b>
<b><math>I \{\text{m/cm}^2\}</math></b>	95.96	67.96	79.96	83.96	91.96	<b><u>103.96</u></b>

<b>H<sub>2</sub> flow rate (L/min)</b>	<b>0.3</b>	<b>0.6</b>	<b>0.9</b>	<b>1.2</b>	<b>1.5</b>
<b><math>E_{o\text{H}_2}</math> (V)</b>	<b><u>0.83</u></b>	0.8	0.77	0.77	0.77
<b><math>b_{\text{H}_2}</math> (V/dec)</b>	<b><u>0.05</u></b>	0.01	0.02	0.02	0.03
<b><math>P \{\text{mW/cm}^2\}</math></b>	<b><u>31.56</u></b>	30.36	30.24	30.72	30.72
<b><math>I \{\text{m/cm}^2\}</math></b>	<b><u>103.96</u></b>	55.96	91.96	91.96	91.96

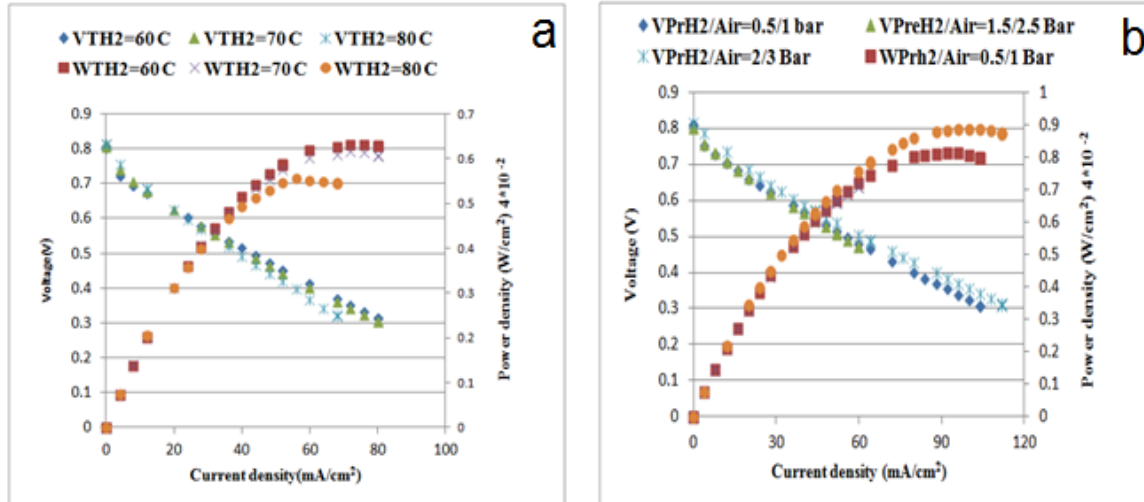


Figure III.12.a Cell voltage and power density vs. current density plots of single cell (25 cm<sup>2</sup>) with various humidifier temperatures. b- Cell voltage and power density vs. current density plots of single cell (25 cm<sup>2</sup>) with various air/H<sub>2</sub> pressures ratio.

Fig III.12.b shows the voltage and power density vs. current density plots of a single cell (25 cm<sup>2</sup>) with various pressures ratio of air/H<sub>2</sub>, and a flow rate of air/H<sub>2</sub>=1.2/0.6 L/min at room temperature (≈30°C), which demonstrated that the increasing pressure ratio of air/hydrogen increased the current density and power density and the performance of the other electrode parameters. Tab III.10 shows the results for an air/H<sub>2</sub> pressure ratio of equal to 3/2 the power density, 35.48 {mW/cm<sup>2</sup>}, and a current density 99.96 mA/cm<sup>2</sup>} compared to the results for the low pressure ratio.

Table III.10 Characteristics of electrodes with various pressure ratios and humidifier temperatures of air/H<sub>2</sub>

Pressures ratio of air /H <sub>2</sub> ( bar)	1/0.5	2/1.5	3/2
<b>E<sub>o</sub> air /H<sub>2</sub> (V)</b>	0.81	0.80	<b>0.83</b>
<b>b<sub>air /H<sub>2</sub></sub> (V/dec)</b>	0.03	0.03	<b>0.04</b>
<b>P {mW/cm<sup>2</sup>}</b>	32.56	28.40	<b>35.48</b>
<b>I {m/cm<sup>2</sup>}</b>	91.96	59.96	<b>99.96</b>



Humidifier temperatures	55/60	65/70	75/80
air/H <sub>2</sub> (°C)			
<b>E<sub>oAir</sub> (V)</b>	<b>0.81</b>	0.81	0.81
<b>b<sub>Air</sub> (V/dec)</b>	<b>0.04</b>	0.04	0.04
<b>P {mW/cm<sup>2</sup>}</b>	<b>25.16</b>	24.38	21.88
<b>I {m/cm<sup>2</sup>}</b>	<b>80.0</b>	80.0	68.0

**III.3.2 SEM 20 wt% Pt/C**

For the second electrode structure with the loading 0.3mg/cm<sup>2</sup> using 20wt% Pt/C, this structure analyzed by SEM to identify the distribution of the catalyst layer and also diffusion layer (GDL) as presented as : Fig III.13.a. Shown the diffusion layer almost the same as before in the first structure , that can observe the distribution of teflon (PTFE) all over the layer, and Fig III.13.b shown the surface of electrode without Nafion<sup>®</sup> solution, Which shown the catalyst distribution with some agglomeration mentioned by yellow circles. Fig III.14.a. shown the surface of electrode with Nafion<sup>®</sup> solution, Which shown the catalyst supported carbon distribution with some agglomeration. Figure III.14.b shown the cross section of membrane assembly (MEA) using Nafion<sup>®</sup> 112.

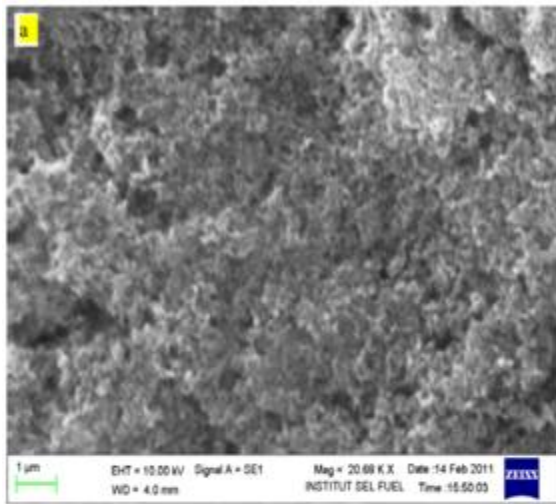


Figure III. 13. a Scanning electron microscopic (SEM) for diffusion layer (GDL) Magnificated 1μm

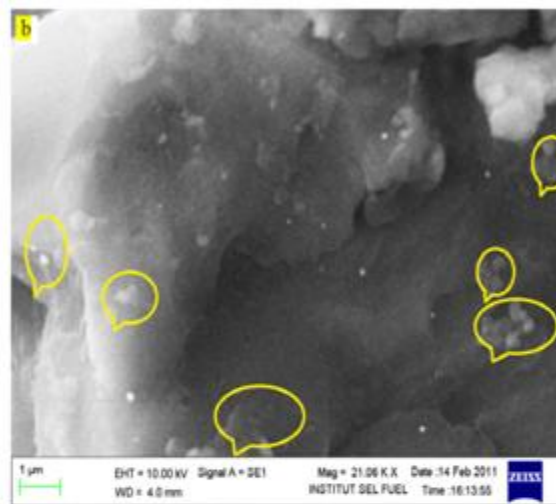


Figure III. 13. b Scanning electron microscopic (SEM) for catalyst layer (Pt/PTFE/C) without Nafion<sup>®</sup> using 20 wt% Pt/C

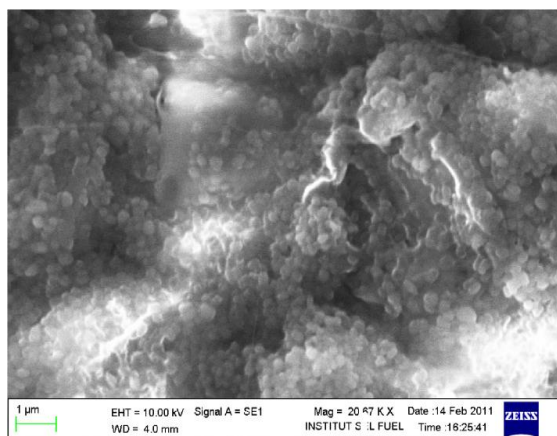


Figure III. 14. a Scanning electron microscopic (SEM) for catalyst layer (Pt/PTFE/C-Nafion<sup>®</sup>) using 20 wt% Pt/C magnified 1µm

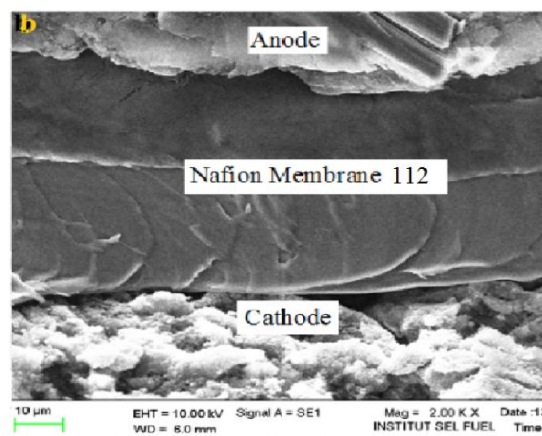


Figure III. 14. b Scanning electron microscopic (SEM) for MEA and cross section using membrane 112 fabricated in sel fuel Ukm

### III. 3. 3 XPS Analysis for Cathode before test ( $E_{bT}$ ) and after test ( $E_{CaT}$ )

XPS analysis is one of the physical techniques to identify the composition and chemical state for elements presented in the electrode surface. Two samples of electrodes passed to XPS analysis. Electrode (Cathode) before test ( $E_{bT}$ ), and cathode after test ( $E_{CaT}$ ) with catalyst layer thickness 30-40 µm in the average and surface area of 1cm<sup>2</sup> for both electrodes. This analysis contains two steps one is electrode before testing  $E_{bT}$  another is cathode  $E_{CaT}$  after 100 hours of operation. These two electrodes ( $E_{bT}$ ,  $E_{CaT}$ ) were loaded of 0.3 mg<sub>Pt</sub>/cm<sup>2</sup> using 20 wt% Pt/C. The wide scan XPS spectra for the electrode 20 wt% Pt/C before operation (testing) and after testing ( $E_{bT}$ ,  $E_{CaT}$ ) are presented in the Fig 15.a.b. five peaks corresponding to the atom of carbon ( $C_{1s}$ ), fluorine ( $F_{1s}$ ), oxygen ( $O_{1s}$ ), platinum ( $Pt_{4f}$ ) and sulfur ( $S_{2p}$ ). These two Fig 15.a.b. give us a preliminary idea on the microstructure aging for electrode operating in the system. The changes in both electrodes are clearly by changing in electrode compositions as carbon peak, fluorine, oxygen, platinum and sulfur.

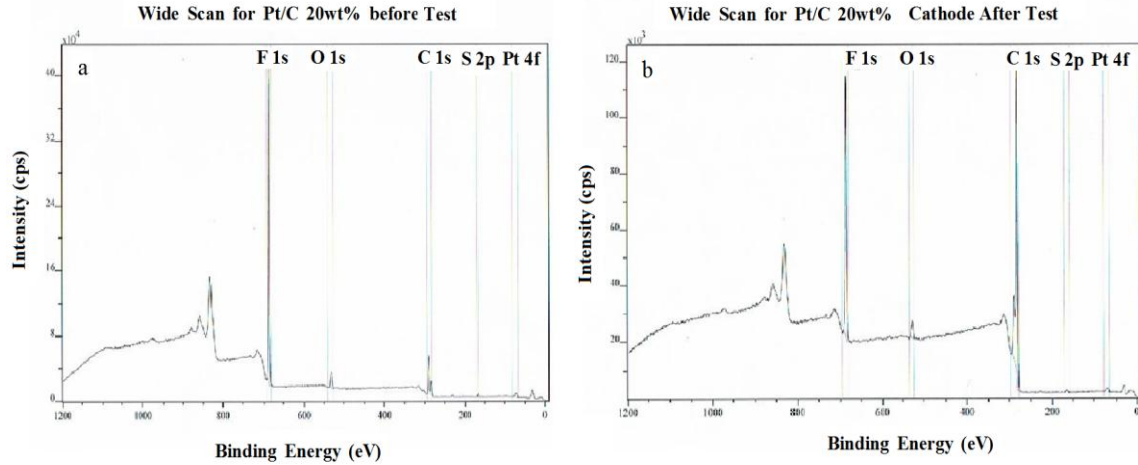


Figure III.15.a.b XPS survey spectrum of catalyst layer before testing ( $E_{bT}$ ) and after testing ( $E_{CaT}$ ).

The semi-quantitative

analysis based on the peak area of individual atoms. The results for the catalyst layer of electrode 20 wt % Pt/C before testing and after testing ( $E_{bT}$ ,  $E_{CaT}$ ) catalyst layer samples are shown in the Tab III.11. Narrow scan of each element is shown in Fig III. 16.a..b, which shows a clear increasing in carbon C-C (Graphite) state and decrease in  $CF_2$  [79], with slight increasing in C=O, and decreasing in  $CF_3$  in  $E_{CaT}$  compared to  $E_{bT}$ . In PEMFC the cathode potential is always bigger than anode hydrogen oxidation from 200 mV to 400 mV for oxygen potential [2], for this reason the electrochemical reactions in electrode operating in single cell 25  $cm^2$  effect on the microstructure for cathode and anode, but more in cathode. The new chemical states appear as detachments between carbon and fluorine, and carbon oxygen bonds as oxidation states give the high amount presented in peaks changes. F 1s from 27.41  $E_{bT}$  decrease to 26.74  $E_{CaT}$  with the difference of 0.67% mass concentration. This is due to the break bond from  $-(CF_2)_n$  to  $C-O-(CF_2)_n$ , The C 1s from 68.72  $E_{bT}$  increase to 69.76  $E_{CaT}$  due to carbon corrosion during the operation, with the difference of -1.04%, in the O1s from 2.34  $E_{bT}$  to 2.08  $E_{CaT}$  with the difference of 0.26% maybe replacement Pt by Carbon C to stabilize the catalyst to PtO (this change is due to reduction of carbon from oxygen to metal), the Pt 4f from 2.55 for  $E_{bT}$  decrease to 0.82 for  $E_{CaT}$  with the difference of 1.73% as shown in Fig III. 17 a,b and Tab III.11. This percentage is due to the detachment from the support and dissolution toward into electrolyte Nafion® as reported by [80]. The peak at 167.861 eV corresponds to O=S=O and the second

peak at 169.227 correspond at  $-\text{SO}_3$  (O -S-O)  $\text{O} \begin{array}{c} \text{O} \\ | \\ \text{S} \\ | \\ \text{O} \end{array}$  with the S  $2p$  from 0.71 for  $E_{bT}$  to 0.61 for  $E_{CaT}$  increase to 0.1% in mass concentration respectively. Furthermore carbon in presence of water according to the reactions:  $\text{C} + \text{H}_2\text{O} \rightarrow \text{CO}_2 + 4\text{H}^+ + 4\text{e}^- \equiv E > 0.207 \text{ V}$  and  $\text{C} + \text{H}_2\text{O} \rightarrow \text{H}_2 + \text{CO}$ . The electrochemical corrosion of the carbon surface leads to changes in the surface chemistry of the carbon [81]. Two intensive peaks is observed for the electrode before testing ( $E_{bT}$ ) and after testing  $E_{CaT}$  but in different way for electrode after testing ( $E_{CaT}$ ). Which present high amount of elements fluorine  $-\text{CF}_2$  and carbon in the electrode ( $E_{bT}$ ). The C1s spectrum in cathode electrode 20 wt% Pt/C after operating more than 100 hours.

$\text{C}_{1s}$  peak is very important peak in any XPS studies because all of the charging effects is corrected to graphite carbon ( $\text{C}_{1s}$ ) at 284.5 eV as reference for all binding energies. The  $\text{C}_{1s}$  core level spectrum of the catalyst layer for Electrode before testing ( $E_{bT}$ ) and ( $E_{CaT}$ ) are presented in Fig III.16.a.b.

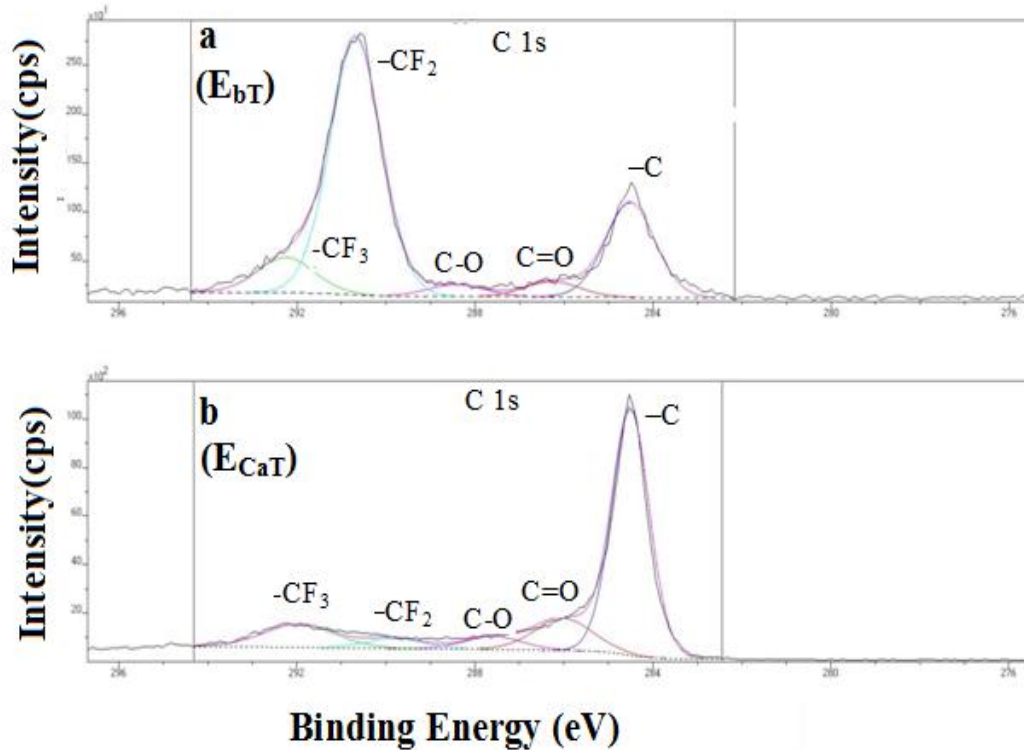


Figure III.16.a.b Core Fitting XPS-spectra for carbon ( $\text{C}_{1s}$ ) of catalyst layer before testing ( $E_{bT}$ ) and ( $E_{CaT}$ )

**CHAPTER III DEGRADATION AND MODELING OF ELECTRODE FOR (PEMFCs)**

The carbon C<sub>1s</sub> peak at 284.5 eV is assigned to the graphite carbon atom or -C not bonded to F, O, S or Pt atom. The second peak at 286.285 eV is attributed to the carbon atom C-O. The third peak at 288.422 eV is attributed to carbon atom attached to the oxygen atom C=O. The fourth peak at 290.694 eV, is attributed to carbon atom attached to the fluorine atom —CF<sub>2</sub>, and the fifth peak at 292.268 eV is ascribed to the carbon atom attached to Fluorine atoms -CF<sub>3</sub>.

Tabl III.11 Cathode microscopic evolution (aging) for (E<sub>bT</sub>) and (E<sub>CaT</sub>). for electrode 20 wt% Pt/C loaded 0.3 mgPt/cm<sup>2</sup>

Peaks	BE(ev) (E <sub>bT</sub> )	BE(ev) (E <sub>CaT</sub> )	FWHM eV(E <sub>bT</sub> )	FWHM eV(E <sub>CaT</sub> )	Atomic Conc% (E <sub>bT</sub> )	Atomic Conc% (E <sub>CaT</sub> )	Mass Conc% (E <sub>bT</sub> )	Mass Conc% (E <sub>CaT</sub> )	ΔMC%	ΔMA%
<b>F<sub>1s</sub></b>	687.0	689.135	2.901	2.375	62.45	19.10	27.41	26.74	0.67	43.35
<b>O<sub>1s</sub></b>	531.7	531.535	5.289	1.391	6.20	1.76	2.34	2.08	0.26	4.44
<b>C<sub>1s</sub></b>	290.0	284.535	2.901	0.835	30.50	78.82	68.72	69.76	-1.04	-48.32
<b>S<sub>2p</sub></b>	168.0	167.735	3.136	0.268	0.63	0.26	0.71	0.61	0.1	0.37
<b>Pt<sub>4f</sub></b>	75.0	71.485	6.233	1.437	0.22	0.06	2.55	0.82	1.73	0.16

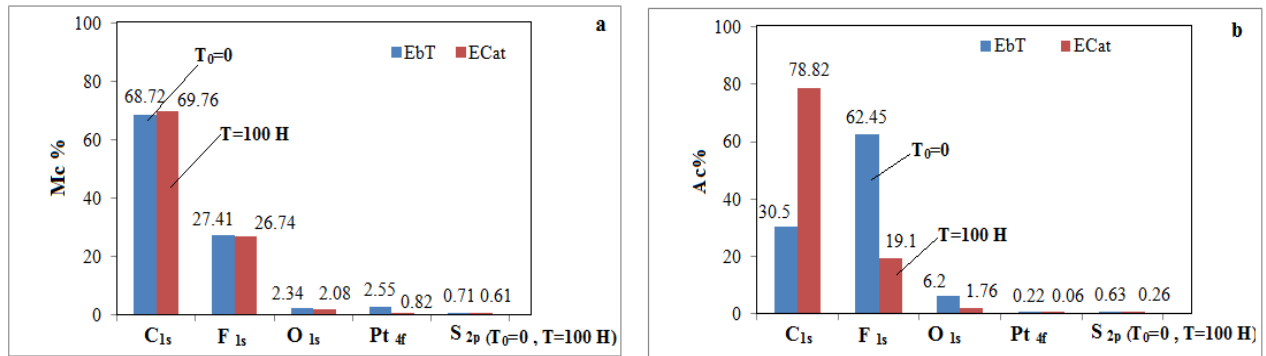


Figure III.17.a Cathode mass concentrations for (E<sub>bT</sub>) and b- Cathode mass concentration degradation (E<sub>CaT</sub>) for electrode 20 wt% Pt/C loaded 0.3 mgPt/cm<sup>2</sup>

The C<sub>1s</sub> core level spectrum of the cathode (catalyst layer) after testing (E<sub>CaT</sub>) for Electrode 20 wt% Pt/C loaded 0.3 mgPt/cm<sup>2</sup> is presented in Fig III.16.b The carbon C<sub>1s</sub> peak at 284.5 eV is assigned to the graphite carbon atom or -C not bonded to either F or O, S, or Pt atom also the seem as in (E<sub>bT</sub>). The second peak at 286.030 eV is attributed to the carbon atom C-O. The third

peak at 287.604 eV is attributed to carbon atom attached to the oxygen atom C=O, the operating conditions as pressure, temperature humidifiers, on/off, flow rate can make modification in the microstructure as carbon corrosion and others element in the electrode microstructure, The fourth peak at 289.819 eV, is ascribed to carbon atom attached to the fluorine atoms –CF<sub>2</sub>, and the fifth peak at 291.966 eV is ascribed to the carbon atom attached to –CF<sub>3</sub> atoms. The concentrations of all Carbone state decrease exception the Carbone graphite increase this due to the detachment of carbon support from the catalyst Pt/C.

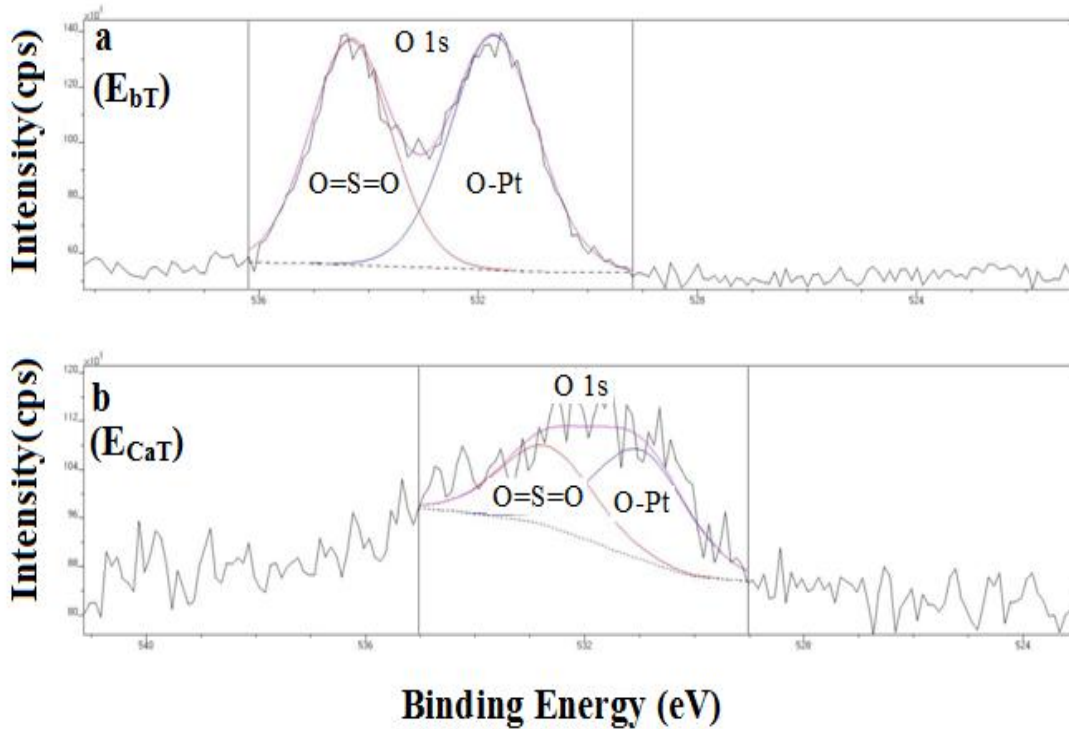


Figure III.18.a-b Cure fitting XPS-spectra for oxygen (O<sub>1s</sub>) of catalyst layer before testing (E<sub>bT</sub>) and (E<sub>CaT</sub>)

The O<sub>1s</sub> spectrum of cathode after testing for Electrode (E<sub>CaT</sub>) shown in Fig III.18.b, has almost a similar shape to (E<sub>bT</sub>) electrode (catalyst layer) before testing only the changing in the concentrations. The best fit for oxygen O<sub>1s</sub> peak yields two peaks at 530.985 eV and 532.682 eV, which may correspond to the shift of the centroid to a slightly higher binding energy. The interaction between carbon and oxygen or catalyst supported carbon to oxygen atom. The peaks positioned at 530.985 eV and 532.682 eV are almost similar to those observed for the electrode before testing (E<sub>bT</sub>). However the peak at 530.985 eV is assigned to the metal oxygen bond

formation O-Pt The second peak at 532.682 eV is ascribed to the oxygen atom attached to the sulfur atom O=S=O. the concentration of O 1s vary from 2.34  $E_{bT}$  to 2.08  $E_{CaT}$  with the difference of 0.26%. This changer due to reduction of carbon from oxygen to metal. Fluorine is the most important element in the structure of electrode because it is used as a binder for Pt/C and wet proofing of the electrode. The F1s peak at 687.0 eV is broad with FWHM=2.901eV. Figure III.19.a shown the best fit for fluorine F<sub>1s</sub> peak at 687.777 eV, which are attributed -CF<sub>2</sub> in catalyst layer for electrode before testing ( $E_{bT}$ ). Fig III.19.b shows the best fit for fluorine F<sub>1s</sub> peak yields two peaks at 688.249 eV, and 689.287eV, which can be attributed to the presence of two different states. The maximum peak is at 689.287 eV, and the minimum peak is at 688.249 eV with a chemical shift of 1.031 eV. The peak at 689.287 eV corresponds to C-O-CF<sub>2</sub> in the catalyst layer and the peak at 688.249 eV corresponds to -CF<sub>2</sub>. The decreasing in mass concentration of F 1s from 27.41  $E_{bT}$  to 26.74  $E_{CaT}$  with the difference of 0.67%, This due to break bound from - (CF<sub>2</sub>)<sub>n</sub>- to C-O--(CF<sub>2</sub>)<sub>n</sub>.

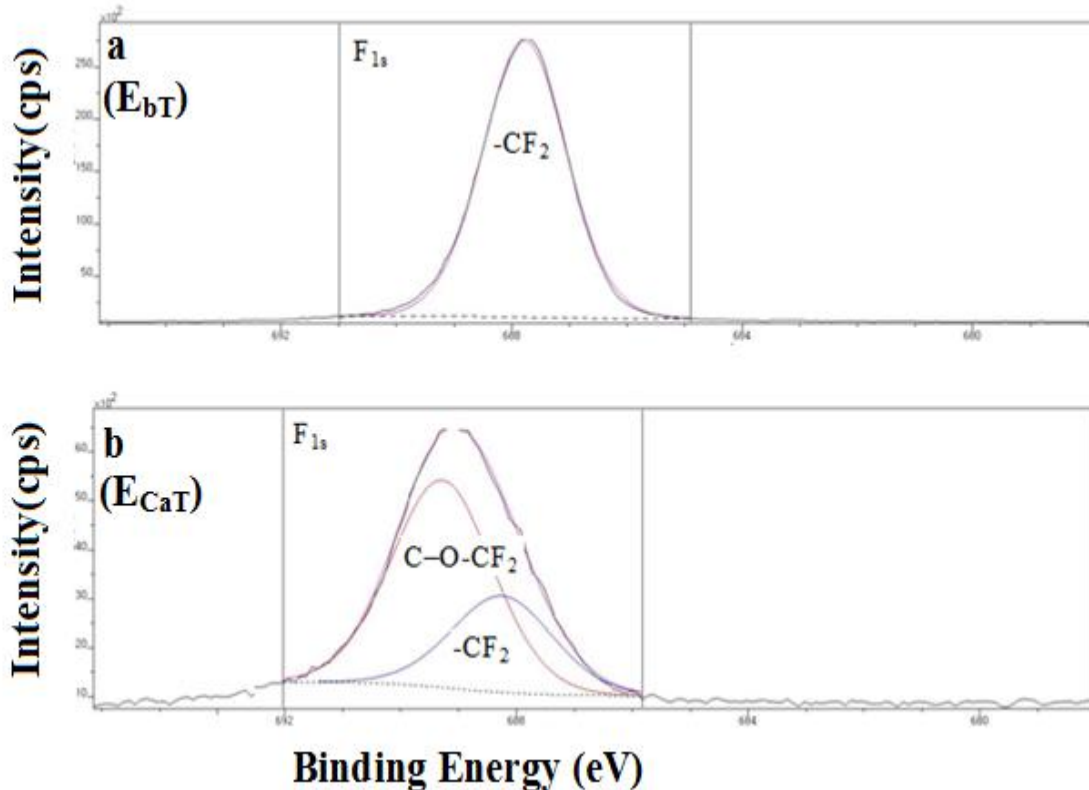
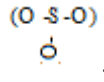


Figure III-19.a.b Cure fitting XPS-spectra for oxygen (F<sub>1s</sub>) before ( $E_{bT}$ ) and after testing for Electrode ( $E_{CaT}$ )

Figure III.20.a shows the best fit for sulfur ( $S_{2p}$ ) come from Nafion® solution. Two intense peaks at the binding energies of 168.148 eV and 169.299 eV respectively. The peak at 168.148 eV

correspond at  $O=S=O$  and the second peak at 169.299 correspond at  $-SO_3$  ( $O-S-O$ ) 

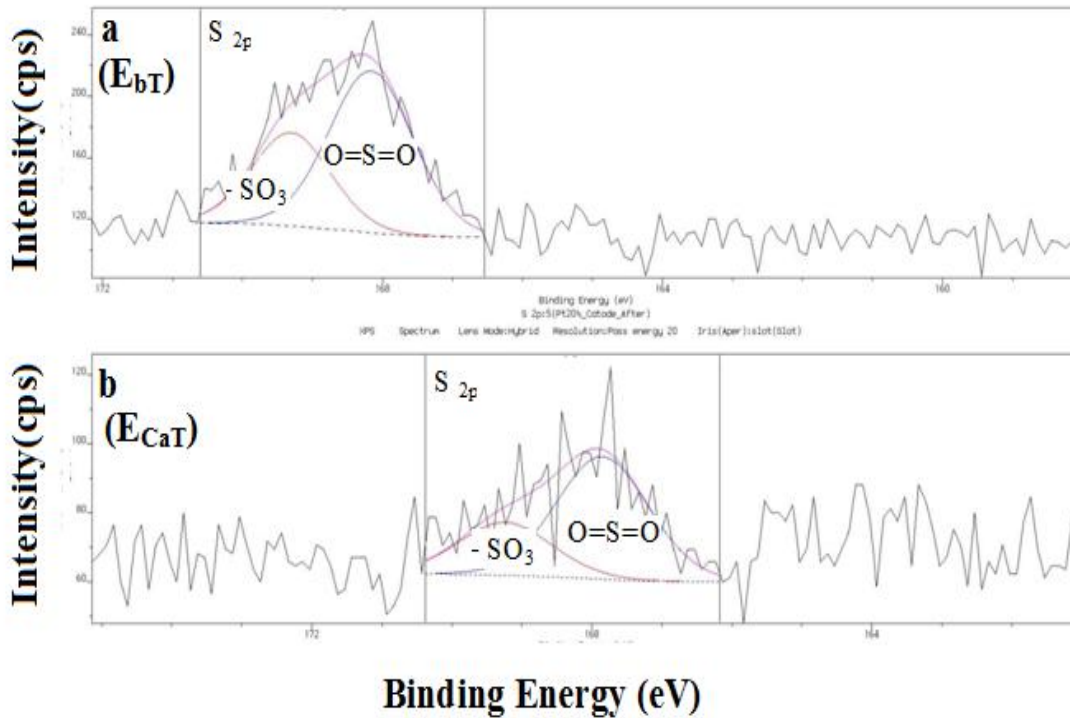


Figure III.20.a-b Cure fitting XPS-spectra for oxygen ( $S_{2p}$ ) of catalyst layer before testing ( $E_{bT}$ ) and after test ( $E_{CaT}$ )

Fig III.20.b shows  $S_{2p}$  spectrum and almost the same shape as  $E_{bT}$ . In the Fig III.20.b shows two intense peaks of  $S_{2p}$  at the binding energies of 167.861 eV and 169.227.eV respectively. The peak at 167.861 eV correspond at  $O=S=O$  and the second peak at 169.227 correspond at  $-SO_3$  ( $O-S-O$ ). the mass concentration of  $S_{2p}$  decrease from 0.71 in  $E_{bT}$  to 0.61 for  $E_{CaT}$  with the difference of 0.1%. Fig III.21.a-b shows The  $Pt_{4f}$  spectrum of the catalyst layer for electrode before testing ( $E_{bT}$ ) and cathode after testing ( $E_{CaT}$ ). Fig 21.a. Shows that the  $Pt_{4f}$  spectrum of the catalyst layer for electrode before testing at 75.0eV is broad with FWHM = 6.233 eV and Fig III.21.b Shows that the  $Pt_{4f}$  spectrum of the cathode after testing ( $E_{CaT}$ ) (catalyst layer) at 71.485



broad with FWHM = 1.437 eV. Fig III. 21.a. shows the best fit for platinum Pt<sub>4f</sub> peak for electrode before test ( $E_{bT}$ ). Four intense peaks of 4f<sub>7/2</sub> and 4f<sub>5/2</sub> at the binding energies of 71.530 eV , 72.526 and 74.803, 75.661 eV respectively. The Pt 4f<sub>7/2</sub> and Pt 4f<sub>5/2</sub> signals are asymmetrically shaped towards the higher binding energies (71.530 eV , 72.526) . The peak at 71.530 ev (Pt 4f<sub>7/2</sub>) represents Pt<sup>0</sup> while some of the Pt oxidize from Pt<sup>0</sup> to (PtO) at binding energy of 72.526 eV [81].The second signal peaks at, 75.661 eV shaped also towards the higher binding energies (74.803, 75.661 eV). The peak at 74.803eV Pt<sup>0</sup> and 75.661 eV PtO correspond to oxidation state.

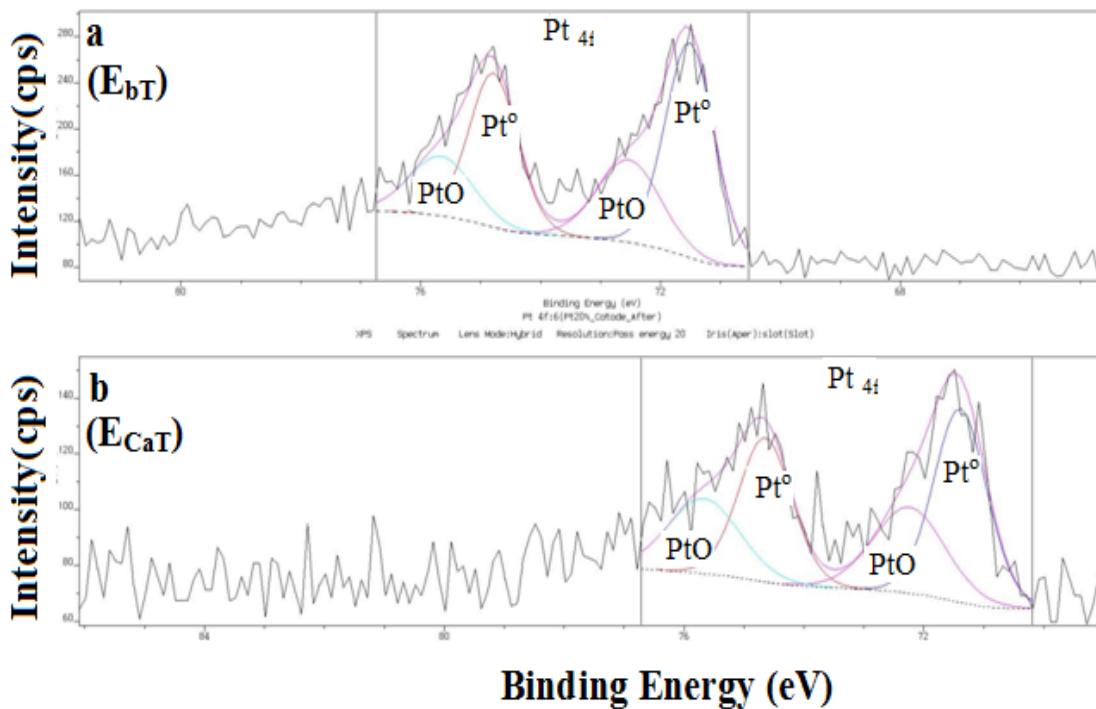


Figure III.21.a-b Curve fitting XPS-spectra for platinum (Pt<sub>4f</sub>) of catalyst layer before and after testing ( $E_{bT}$ ) and ( $E_{CaT}$ )

Fig III.21.b. shows similarity fitting for platinum Pt<sub>4f</sub> peak as electrode before testing. Four intense peaks of 4f<sub>7/2</sub> and 4f<sub>5/2</sub> at the binding energies of 71.414 eV, 72.253 eV and 74.667, 75. 75.682 eV respectively. The Pt 4f<sub>7/2</sub> and Pt 4f<sub>5/2</sub> signals are asymmetrically shaped towards the higher binding energies (71.414eV, 72.253 eV) . The peak at 71.414 eV (Pt 4f<sub>7/2</sub>) represents Pt<sup>0</sup> while some of the Pt oxidize from Pt<sup>0</sup> to PtO at binding energy of 72.253 eV

[80,82]. The second signal peaks at, 75.661 eV shaped also towards the higher binding energies (74.667 eV, 75.682eV). The peak at 74.667 eV corresponds to Pt<sup>0</sup> and 75.682eV correspond to Pt-OI oxidation state. the difference between electrode before testing and cathode after test is in the mass concentration f

rom 2.55 for  $E_{bT}$  to 0.82 for  $E_{CaT}$  with the difference of 1.73%, this percentage due to the detachment from the support and dissolution into electrolyte Nafion<sup>®</sup> as reported by [79]. this electrode degradation due to the microstructure of electrode changer in the catalyst and components including fluorine , carbon, oxygen and sulfur as presented in Table 11. The main degradation modes include Pt Catalyst particles growth and Pt migration both of these degradation mechanisms are believed to be closely associated with the dissolution of Pt a Pt oxidation/dissolution process occurs due to voltage cycling and high potentials on the cathode that results in movement or migration of the Pt in a dissolved state. Platinum particles losses accelerated when the cathode operating as start-up and shut-down [80, 83].

### **III. 3. 4 XRD Analyses**

XRD analysis was performed using Bruker AXS Brand machine Model D8. The anode using K $\alpha$ 1 as source of energy with wave length 1.54060 KV. The scan type 2Th/T start from 5- 80 end, with the step size 0.025 o with Timing for one step is 0.1 s. The XRD machine operating with Generator 40 Kv, 40mA, UKM Applied Physic Dept Malaysia. The Deconvolution peaks interpretation using a Free software Fitik<sup>®</sup> is used to deconvolute the diffraction peaks. the functions are used for the deconvolution of Pearson VII-type functions. Bragg's law Equation allows the determination of the lattice parameter and the position of the vertex of the diffraction peak.

Figure 22 Presented the XRD for Pt/C 20 wt % Raw material Powder Peak no:01 .the crystallite size shown best cristillite size between 35-40<sup>o</sup> (2 $\Theta$ ) ,the crystallinity phase consider optimal for this structure Pt/C , the cristallinite size in the Area is About 81,3 A<sup>o</sup>, second point for this XRD scan, the cristallinite size in the Area 45-48<sup>o</sup> (2 $\Theta$  is About 101.1 A<sup>o</sup>, so the cristality phase decrease in Pt/C 20 wt % with increasing the cristallinite size from 81,3 A<sup>o</sup> to 90 A<sup>o</sup> for the first scan 2 $\Theta$  = 35-40<sup>o</sup>. the second scan point the cristallite size from 101.1 A<sup>o</sup> at 2 $\Theta$  = 45-48<sup>o</sup> in Pt/C 20 wt % Raw material Powder to 150 A<sup>o</sup> in  $E_{Cat}$ . The decreasing in the cristallite size decrease the phase cristalline. This is for catalyst for the support carbon the

changes is clear. the cristallinity size decrease from 183.7 Å at  $2\theta$  22-27° the cristallite size variee from 324 Å in Pt/C 20 wt % to 637 Å, which increase the amorphous phace phase in decrease in the cristalline phase. this decreasing monte by XPS and TEM Techniques.

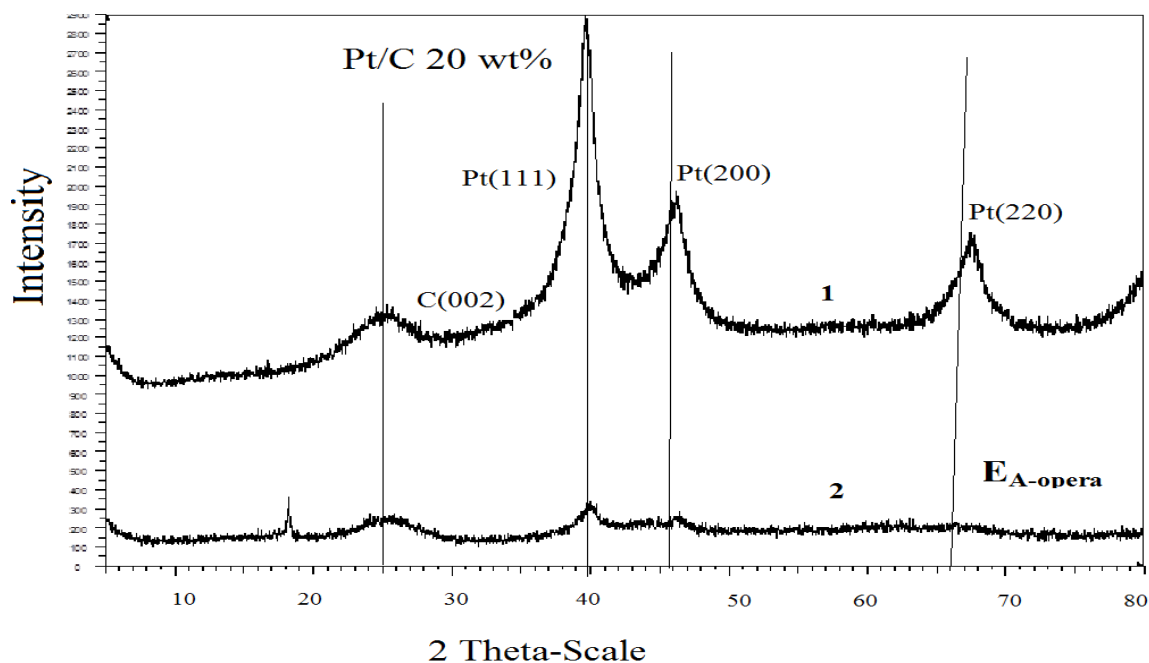


Figure III.22 XRD for 1. Catalyst 20 wt% Pt/C before operation and, 2. Catalyst (Cathode) after operation  $E_{Cat}$  loaded  $0.3\text{mg}_{Pt}/\text{cm}^2$

### III. 3. 5 Transmission electron microscopy (TEM)

TEM is a microscopy technique whereby a beam of electrons is transmitted through an ultra-thin specimen, interacting with the specimen as it passes through to give a picture for the specimen need to analyze. The catalyst particle sizes evolution was characterized by TEM and energy dispersive X-ray (EDX) analysis using a Philips CM 120 microscope/EDX analyzer equipped with a LaB6 filament. To prepare the sample, a small drop of the solution was put on an Au grid and the solvent was evaporated. The cycled catalysts are recovered by ultrasonification of the Electrode in ethanol. TEM observations allow determining the mean size of platinum particles and also evaluating the corrosion and degradation of the catalyst and carbon support. However, great care has to be taken with the counting of the particles. In our case, only isolated-like particles with sizes lower than 6 nm were taken into

account; in each case, 12 Values of particles sizes and 12 after and before test respectively were measured for the statistics. For the determination of particle size, it was reasonably assumed in first approximation that platinum particles were sphere shape. The average particle sizes were calculated using the following equation:  $\bar{d} = \sum n_i d_i/n$ . The electrode before testing ( $E_{bT}$ ) and the electrode after testing ( $E_{CaT}$ ) are presented in Fig 23. a and b. The Pt nanoparticles, which are visible as darker grey/black dots on a brighter gray carbon background, are all round in shape with a narrow size distribution. Furthermore, the Pt distribution on the support is very homogeneous before test – 20wt Pt/C/Teflon solution as row material to calculate the initial sizes Fig III.23.a The distinctive shape of the carbon support in the Fig III.23.b are totally different because the detachment of the catalyst from carbon support after testing more than 100h with different operating conditions, and in the state a consider as fresh no much oxidation and agglomeration support. Furthermore the Pt particles in Fig III.23.a can appear as concentrated and attached to the carbon support, which give a big surface area for catalyst. On the other hand the Pt after testing in Fig III.23.b no much Pt particles a few point of catalyst explain catalyst detachment (dissolution) from the carbon support and goes somewhere toward to the membrane electrolyte and dissolved as spices at high voltage (0.75 V) and harsh conditions imposed for operating electrode [37,84].

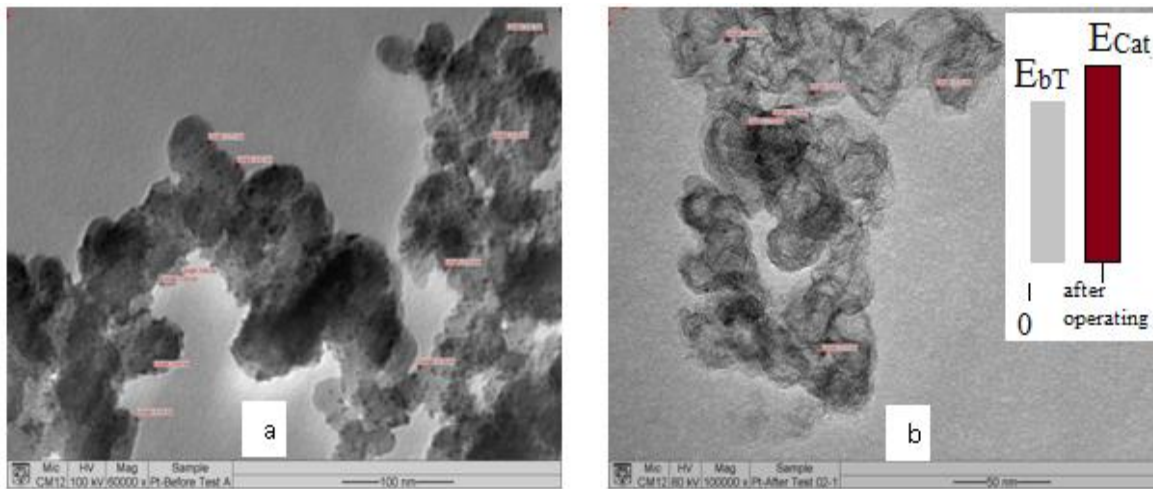


Figure III.23 TEM of electrode 20 wt% Pt/C –a before testing and –b after testing in single cell  
25 cm<sup>2</sup>

The Pt/C catalyst has a mean particle size close to 4.0 nm then the effect of aggressive operating conditions was studied.. Clearly, it appears that the mean particle size has increased compared to the Pt before test from (4.14±0.9) to (5.57) nm for the fresh catalyst support carbon and after 100 h operating. The evolution of particles sizes due the environment evolution as sonacated preparation, operating condition, start On/Off the operating for many times. The aggressive conditions as hot gas by increasing the humidifiers temperature, water accompanied the Air gas to the cell all these parameters change in the particles size of catalyst Pt and support carbon too.

### **III.4 PEM fuel cell modeling**

Model for PEM fuel cell used to analyze the impact of individual fuel cell's operating parameters on cell's performance. Using the present model, it is also possible to determine the activation loss parameters of the PEM fuel cell. The model is well adapted for PEM cell and it incorporates the essential physical and electrochemical processes that happen in cell along its operation

#### **III.4.1 Electrode preparation and single cell operation in fuel cell test apparatus.**

As previous work [19, 85].electrode preparation consist, a substrate made from carbon cloth "A" with thickness 350  $\mu\text{m}$ , platinum-supported carbon 10 wt% Pt/C, activated carbon black, and Teflon (PTFE) 60 wt% have been used. Two different platinum loadings have been used in preparation of the electrodes. One electrode was with platinum loading 0.18  $\text{mg Pt cm}^{-2}$ ; while the second was with platinum loading 0.38  $\text{mg Pt cm}^{-2}$ . The composition of catalyst layer was 70 wt% Pt/C and 30 wt% Teflon (PTFE). Detailed electrode preparation can be found in reference.

During operation of PEM fuel cells, the following processes take place within the electrode: (i) the reactant gases diffuse through the porous backing layer; (ii) at the gas-electrolyte interface, the gases dissolved and then diffuse to the electrolyte-electrode interface; (iii) electrocatalytic reaction inside the catalyst layer precedes the gas adsorption at the electrode surface; (iv) ionic transport occurs in the electrolyte, but electronic transport takes place in the electrode.

Oxygen and hydrogen were passed through humidifiers before being fed into the cell cells. Hydrogen fed into the anode at a flow rate of 140  $\text{ml min}^{-1}$  and 1 atm. Oxygen entered the fuel cell through the cathode at a flow rate of 380  $\text{ml min}^{-1}$  and 2 atm. The electrons generated from the anode were connected to a digital multimeter, with an external variable resistance to

measure the current and voltage produced by the cell. Electric conductivity was measured by using resistivity meter (Loresta-GP MCP-T600). The specific resistance of the gas diffusion layer composed of 70 wt% Pt/C and 30 wt% PTFE was measured to be 0.21  $\Omega$  cm. The parameters of the fuel cells used in the simulation are listed in the Table III.12.

Table III.12 Experimental and calculated parameters used in the simulation

Parameters	Value	Parameters	Value
Temperature, $T$	298 K	Diffusion layer electronic conductivity, $\sigma_d$	$5 \Omega^{-1} \text{cm}^{-1}$
Pressure, $P$	1 atm	Diffusion coefficient of $H_2$ into $H_2O$ , $D_{H_2,H_2O}$	$1.6 \times 10^{-4} \text{m}^2 \text{s}^{-1}$
Electrode Area	$25 \text{cm}^2$	Diffusion coefficient of $O_2$ into $H_2O$ , $D_{O_2,H_2O}$	$3.11 \times 10^{-5} \text{m}^2 \text{s}^{-1}$
Membrane thickness, $l_m$	117 $\mu\text{m}$	Diffusion coefficient of $H_2O$ into membrane, $D_{H_2O,m}$	$3 \times 10^{-10} \text{m}^2 \text{s}^{-1}$
Diffusion layer thickness, $l_d$	350 $\mu\text{m}$	Equivalent weight, $EW$	$1100 \text{g mol}^{-1}$
$P_{O_2}$	2 atm	Dry membrane density, $\rho_{dry}$	$2020 \text{Kg m}^{-3}$
$P_{H_2}$	1 atm		

### III. 4. 2. Basic fuel cell operation

PEM fuel cell consists of membrane, through which hydrogen ions diffuse from anode to cathode. Schematic of a PEM fuel cell is shown in Fig III. 24.

The hydrogen diffuses through the electrode until it reaches the catalytic layer of the anode where it reacts to form protons and electrons, as shown below in the reaction:



The protons are transferred through membrane to the catalytic layer of the cathode. Electrons pass through external electric circuit to cathode. On cathode side of a fuel cell, protons, electrons and oxygen react according to the following reaction:



Then, the overall chemical reaction of the PEM fuel cell is

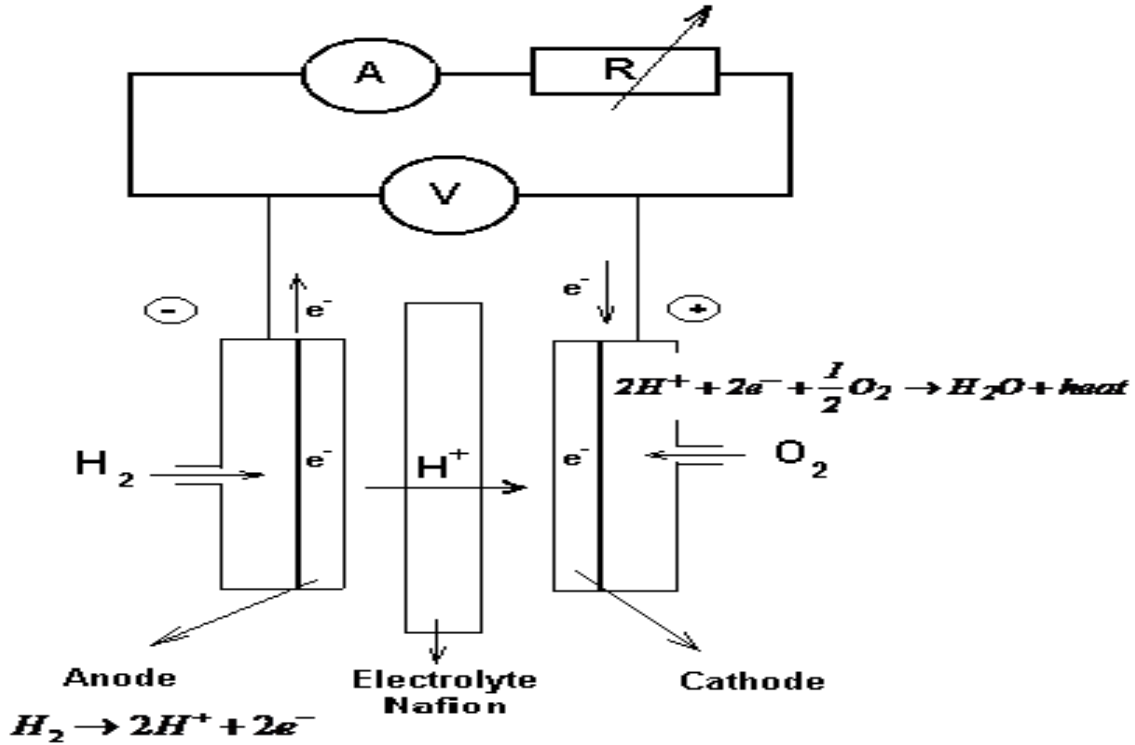


Figure III.24 Schematic of functioning principle of PEM fuel cell.

### III.4.3 Model formulation

#### 4.3.1 Electrochemical model

The output voltage of a single cell can be defined as the result of the following [86, 87]:

$$V_{cell} = E - V_{activation} - V_{ohmic} - V_{concentration} \quad \text{III.4}$$

In the equation above, E is the thermodynamic potential of the cell and it represents its reversible voltage;  $V_{activation}$  is the voltage drop due to the activation of the anode and cathode, a measure of the voltage drop associated with the electrodes;  $V_{ohmic}$  is the ohmic voltage drop, a measure of the ohmic voltage drop resulting from the resistances of the conduction of protons through the solid electrolyte and the electrons through its path; and  $V_{concentration}$  represents the voltage drop

resulting from the reduction in concentration of the reactants gases or, alternatively, from the transport of mass of oxygen and hydrogen; and fuel cell's output power density is given by:

$$P_{cell} = V_{cell}i \quad \text{III.5}$$

Each one of the terms of Eq. III.4 is discussed and modeled separately in the subsections that follow.

#### **4.3.1.1. Cell reversible voltage**

Fuel cell's output voltage is determined by cell's reversible voltage that arises from potential difference produced by chemical reaction and several voltage losses that occur inside a cell. Fuel cell's reversible voltage is a function of temperature and partial pressures of reactants and product as is shown in the following equation:

$$E = \frac{\Delta G}{2F} + \frac{\Delta S}{2F} (T - T_{ref}) + \frac{RT}{2F} \left[ \ln(P_{H_2}) + \frac{1}{2} \ln(P_{O_2}) \right] \quad \text{III.6}$$

Where  $\Delta G$  is the change in the free Gibbs energy;  $F$  is the constant of Faraday;  $\Delta S$  is the change of the entropy;  $R$  is the universal constant of the gases; while  $P_{H_2}$  and  $P_{O_2}$  are the partial pressures of hydrogen and oxygen, respectively. Variable  $T$  denotes the cell operation temperature and  $T_{ref}$  the reference temperature. Using the standard pressure and temperature (SPT) values for  $\Delta G$ ,  $\Delta S$  and  $T_{ref}$ , Eq. III.6 can be simplified to [86]:

$$E = 1.229 - 0.85 \times 10^{-3} (T - 298.15) + 4.31 \times 10^{-5} T \left[ \ln(P_{H_2}) + \frac{1}{2} \ln(P_{O_2}) \right] \quad \text{III.7}$$

#### **4.3.1.2. Activation voltage drop**

Activation polarization is related to the energy barrier that must be overcome to initiate a chemical reaction between reactants. At low current draw, the electron transfer rate is slow and a portion of the electrode voltage is lost in order to compensate for the lack of electro-catalytic activity. Expression for activation losses is given by:



$$V_{activation} = \frac{RT}{2\psi F} \ln\left(\frac{i}{i_0}\right) \quad \text{III.8}$$

$\psi$  is electron transfer coefficient, and is unit less. This value describes the proportion of the electrical energy applied that is harnessed in changing the rate of an electrochemical reaction. It is this value that differs from one material to another.  $i$  represents cell's current density, whereas  $i_0$  is exchange current density.  $i_0$  is the value on the Tafel plot when the current begins to move away from zero, because of higher anode exchange current density, cathode activation losses are significantly higher so anode activation losses are negligible. Value of cathode exchange current density also depends on operating parameters what is shown by:

$$i_{0c} = 2Fk_c \exp\left(\frac{2.46\beta F}{RT}\right) \quad \text{III.9}$$

$\beta$  and  $k_c$  are symmetry factor and factor related to reaction speed, respectively.

#### 4.3.1.3. Ohmic voltage drop

Ohmic voltage drop or (Ohmic polarization) occurs to resistive losses in the cell. These resistive losses occur within the electrolyte (ionic), in the electrodes (electronic and ionic), and in the terminal connections in the cell (electronic). Since the stack plates and electrolyte obey Ohm's law, the amount of voltage lost in order to force conduction varies mostly linear throughout this region. This is the working region of the fuel cell.

$$V_{ohmic} = i(r_{ion} + r_{el}) \quad \text{III.10}$$

The following expression for the ionic resistance is used [86]:

$$r_{ion} = l_m \frac{181.6 \left[ 1 + 0.03i + 0.062 \left( \frac{T}{303} \right)^2 i^{2.5} \right]}{(\lambda - 0.634 - 3i) \exp \left[ 4.18 \left( \frac{T - 303}{T} \right) \right]} \quad \text{III.11}$$

where  $l_m$  is the thickness of the membrane. The parameter  $\lambda$  is influenced by the membrane preparation [88] and it can be related to relative humidity of the membrane  $\phi$  by the following expression [89]:

$$\lambda = 0.043 + 17.8\phi - 39.8\phi^2 + 36.0\phi^3 \quad \text{III.12}$$

The electronic resistance can be written as:

$$r_{el} = \frac{2l_d}{\sigma_d} \quad \text{III.13}$$

where  $l_d$  is diffusion layer thickness and  $\sigma_d$  is diffusion layer electronic conductivity.

#### **4.3.1.4. Concentration or mass transport voltage drop**

Mass transport or concentration polarization results when the electrode reactions are hindered by mass transfer effects. In this region, the reactants become consumed at greater rates than they can be supplied while the product accumulates at a greater rate than it can be removed. Ultimately these effects inhibit further reaction altogether and the cell voltage drops to zero. Expression for fuel cell's concentration losses is given by:

$$V_{concentration} = -\frac{RT}{2F} \ln \left( 1 - \frac{i}{i_L} \right) \quad \text{III.14}$$

$i_L$  represents limiting current density. This parameter describes maximum current density that can flow through electrode. Concentration polarization results from restrictions to the transport of the fuel gases to the reaction sites. This usually occurs at high current because the forming of product water and excess humidification blocks the reaction sites. This polarization is also affected by the physical restriction of the transfer of oxygen to the reaction sites on the cathode side of the fuel cell. Concentration polarization can be reduced by using thinner electrodes which shortens the path of the gas to the sites [90, 91]. Jordan et al. [91] have observed a dramatic change in slope of the voltage versus current density plot using air oxidant. Such a change, indicative of a diffusion-limited reaction, was not so apparent when pure oxygen is used as the oxidant. The same behavior was also observed by other researchers [92]. This is consistent with the experimental data showed in Fig III. 25. Hence, in parameter estimation we have neglected the effect of concentration polarization drop.

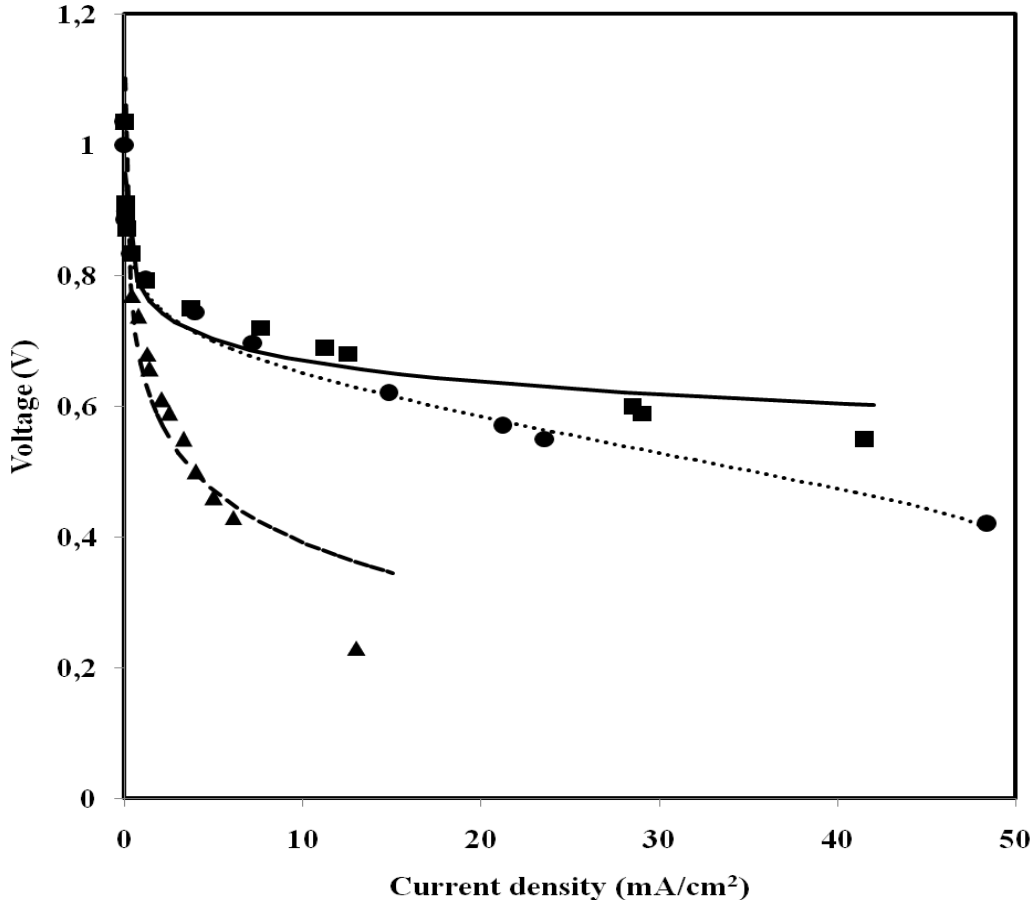


Figure III.25 Fuel cell's voltage as a function of cell's current density at  $T = 298\text{K}$ , data:  $\blacktriangle$  Pt loading =  $0.18 \text{ mg cm}^{-2}$ ,  $\blacksquare$  Pt loading =  $0.38 \text{ mg cm}^{-2}$  and  $\bullet$  E-TECK electrode with Pt loading =  $0.4 \text{ mg cm}^{-2}$  [9]; model: (dashed line) Pt loading =  $0.18 \text{ mg cm}^{-2}$ , (solid line) Pt loading =  $0.38 \text{ mg cm}^{-2}$  and (dotted line) E-TECK electrode with Pt loading =  $0.4 \text{ mg cm}^{-2}$

#### 4.4.1. Determination of the activation loss parameters

The experimental data of the cell voltage versus current density (Fig III. 25) for the two fabricated electrodes and the commercial electrode E-TECK with Pt loadings  $0.18$ ,  $0.38$  and  $0.4 \text{ mg cm}^{-2}$ , respectively, are fitted to the present model using a non linear least squares method. Characteristics of fabricated and commercial electrodes are listed in Table III.12. The activation loss parameters,  $\psi$  and  $i_0$ , are determined and listed in Table III.13. Both parameters depend on Pt loading. The increase of Pt loading will cause an increase of  $\psi$  and  $i_0$ . This can be attributed to the increase of the active sites for hydrogen adsorption.

Table III.13 Variation of the parameters  $\psi$  and  $i_0$  with platinum loading at T = 298K

Parameters	Fabricated electrode 0.18 mg Pt cm <sup>-2</sup>	Fabricated electrode 0.38 mg Pt cm <sup>-2</sup>	E-TECK electrode 0.4 mg Pt cm <sup>-2</sup>
$\psi$	0.13	0.28	0.3
$i_0$ (A cm <sup>-2</sup> )	2.94 x 10 <sup>-9</sup>	4.95 x 10 <sup>-8</sup>	2.86 x 10 <sup>-8</sup>

An inconsistency between the polarization curves for the prepared electrode with Pt loading 0.38 mg cm<sup>-2</sup> and the commercial on E-TECK with Pt loading 0.4 mg cm<sup>-2</sup> is observed. The cell voltage in E-TECK dropped slightly faster than the former electrode. Also, the value of  $i_0$  is decreased from 4.95 x 10<sup>-8</sup> A cm<sup>-2</sup> (prepared electrode with Pt loading 0.38 mg cm<sup>-2</sup>) to 2.86 x 10<sup>-8</sup> A cm<sup>-2</sup> (E-TECK electrode with Pt loading 0.4 mg cm<sup>-2</sup>). This may be attributed to the fabrication process in the preparation of electrode with Pt loading 0.38 mg cm<sup>-2</sup>, which creates a better particle distribution of electrocatalyst. The localization of platinum in the catalyst layer can be improved via the spraying technique [85]. The values of  $i_0$  estimated are lower than that reported by Amphlett et al. [93], which are 107.6 x 10<sup>-8</sup> A cm<sup>-2</sup> at 298K. From these results, it can be concluded that not only Pt loading will affect the value of  $i_0$ .

Typically the value of  $\psi$  is in a very narrow range; it ranges from about 0.1 to 0.5. The exchange current density constant varies over a wide range, and thus has a dramatic effect on the performance of fuel cells at low current densities. Hence, it is vital to design fuel cells with high exchange current densities.

#### **4.4.2. Effect of the temperature on the performance of the PEM fuel cell**

Fuel cell's voltage as a function of cell's current density is shown in Fig III.25. In Fig III. 26 cell's power density is shown as a function of current density for two different temperatures. We can see from these figures that fuel cell's efficiency is low and that significant part of theoretical output voltage is lost because of different losses inside a cell. We can also notice that increase of fuel cell's operating temperature will cause increase of cell's output voltage and power. If we increase temperature from 298K to 353K, fuel cell voltage would increase for 28% (Fig III. 26). The reason for this is that higher temperatures improve mass transfer within the fuel cells and results in a net decrease in cell resistance as a result it improves the reaction rate.

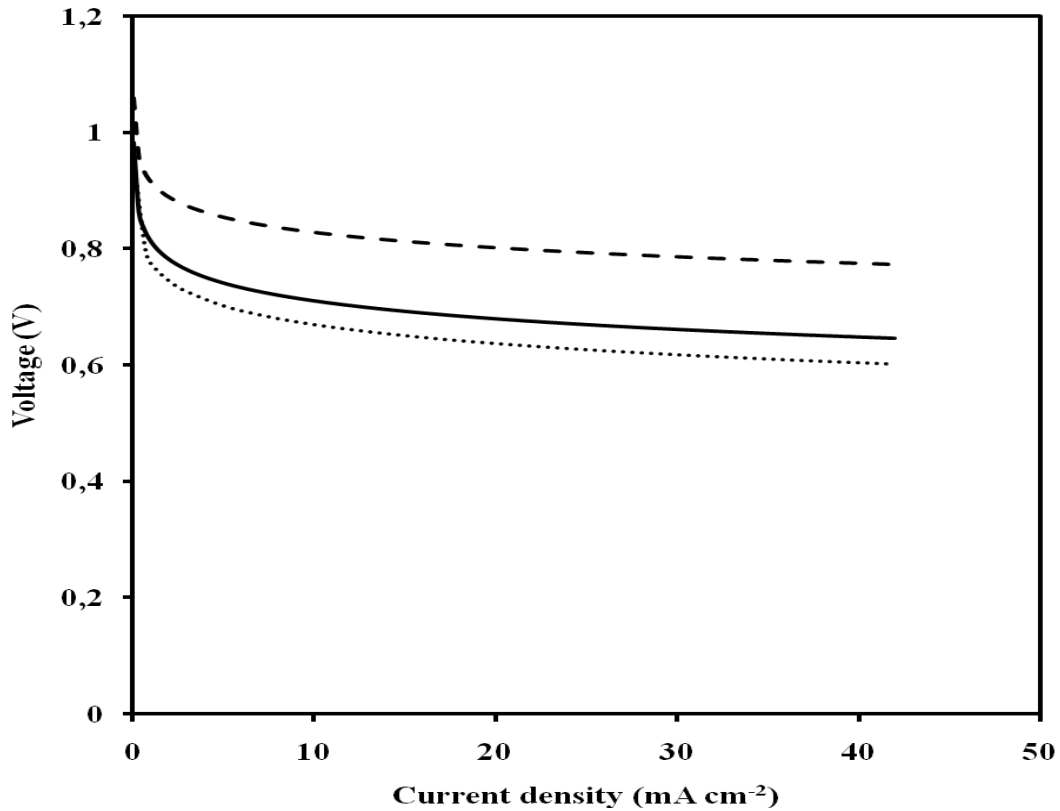


Figure III. 26 Fuel cell's voltage as a function of cell's current density for different temperatures at Pt loading =  $0.38 \text{ mg cm}^{-2}$ ; model: (dotted line) 298K, (solid line) 313K and (dashed line) 353K

#### 4.4.3. Effect of the partial pressures

Change in output power related with increase in partial pressures is shown in Fig III. 27. We can see that power increase because of reactant pressure increase is 1.1% and is smaller than change caused by temperature variations.

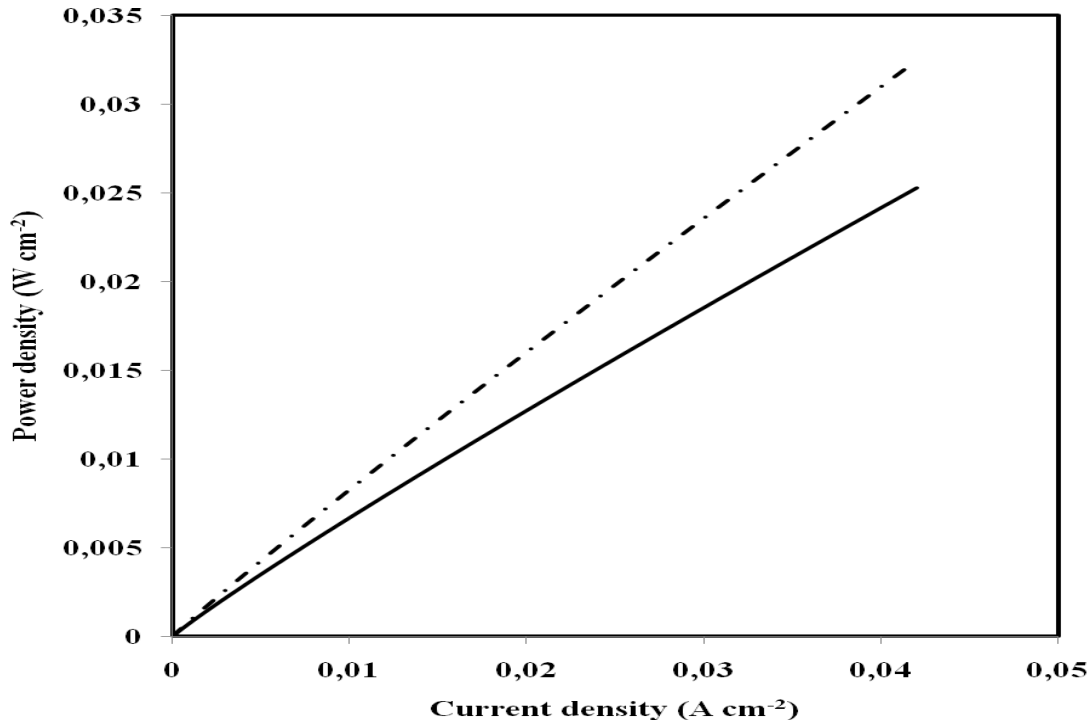


Figure III. 27 Fuel cell's power density as a function of cell's current density for different temperatures at Pt loading =  $0.38 \text{ mg cm}^{-2}$ ; model: (solid line) 298K and (dashed line) 353K

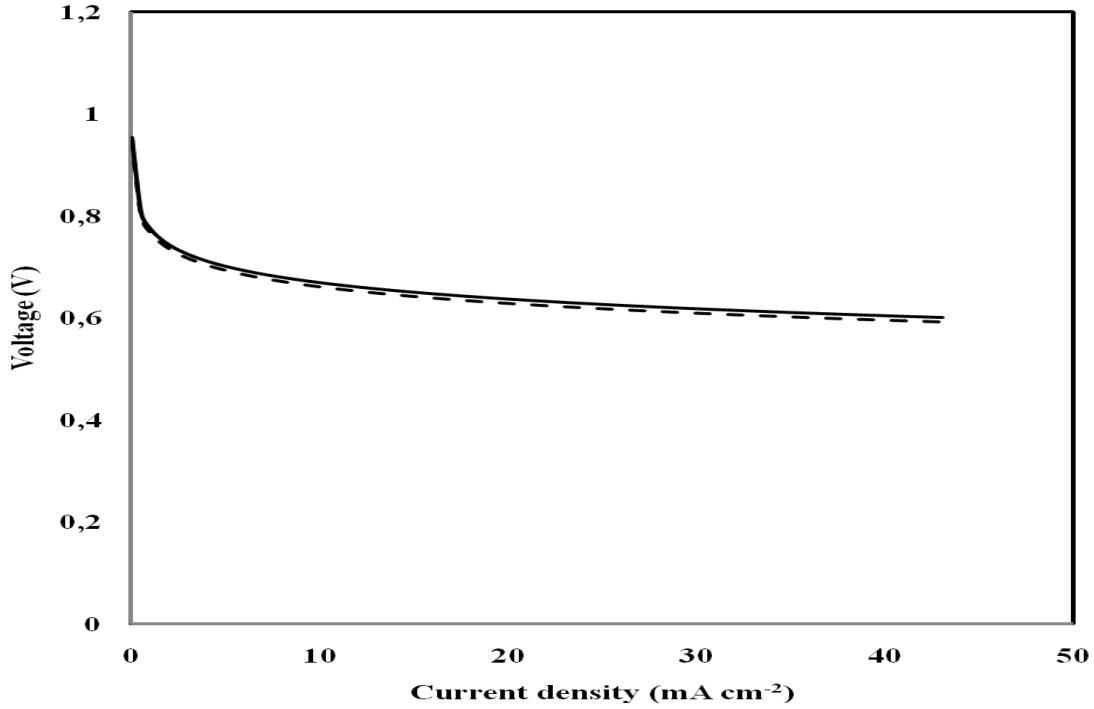


Figure III. 28 Fuel cell's voltage as a function of cell's current density for different fuel cell's reactants partial pressure at  $T = 298\text{K}$  and  $\text{Pt loading} = 0.38 \text{ mg cm}^{-2}$ ; model: (dashed line)  $P_{\text{H}_2} = 0.995 \times 10^5 \text{ Pa}$  and  $P_{\text{O}_2} = 0.606 \times 10^5 \text{ Pa}$ , (solid line)  $P_{\text{H}_2} = 1.01 \times 10^5 \text{ Pa}$  and  $P_{\text{O}_2} = 1.01 \times 10^5 \text{ Pa}$

From these simulations shown in Fig III, 27 and Fig III.28 that must pay attention on cell temperature, which is very important in proton exchange membrane fuel cells, while the reactant pressures are less significant on output voltage and power as demonstrated in previously.





# **CONCLUSION**

## CONCLUSION

### CONCLUSION

The first structure for electrode 10wt% Pt/C loaded  $0.38 \text{ mg/cm}^2$ , the surface for diffusion Layer (GDL) contain carbon black and Teflon binder (PTFE/C) no catalyst was observed, but for the of catalyst layer (Pt/C/PTFE) the catalyst as slight particles with good distribution on the surface of electrode, also the chemical states for both diffusion and catalyst layer showed almost showed the same chemical state except the catalyst (Pt) incorporated in the matrix PTFE /C. The gas diffusion layer (GDL) has big effect on the electrode performance, which use as a support of catalyst.

The physical parameters effect as pressure, humidifiers temperatures and flow rate well appear in this work, which can conclude that the effect of increasing the pressure, leads to an increase in the current and power, the current increase from 2.299 to 2.499 A and power from 0.814 to 0.887 Watt for Air/H<sub>2</sub> 0.5/1 bar and 2/3 bar respectively. On the other hand the increasing of Air pressure eliminates the water in the cathode channel side and increase the electrode performance. Flow rate of Hydrogen and Air, shown the stoichiometry coefficient for Air and Hydrogen is 2/1 and the best value is given by flowrate 0.3 L/min for H<sub>2</sub> and 0.6 l/min for Air, which correspond to the current and power equal to 2.599 A and 0.789 Watt respectively. The hydrogen and air flow rates gives the best value of flow rate of 0.3 L/min for H<sub>2</sub> and 0.6 L/min for air, where the current density and power density is  $103.96 \text{ \{mA/cm}^2\}$  and  $31.56 \text{ \{mW/cm}^2\}$ , respectively. Low humidifier temperatures give advantage to the operating fuel cell.

The electrode degradation due to the microstructure of electrode changes in the catalyst and components including carbon, fluorine, oxygen and sulfur. The cathode microstructure evidently damage after testing ( $E_{CaT}$ ) compared to the cathode before testing ( $E_{bT}$ ). the chemical states for ( $E_{CaT}$ ) change compared to the initial state of cathode ( $E_{bT}$ ). The C 1s from 68.72  $E_{bT}$  increase to 69.76  $E_{CaT}$  with the difference of -1.04 % due the carbon corrosion during the operation and transform to graphite state (C-C) , F 1s from 27.41  $E_{bT}$  decrease to 26.74  $E_{CaT}$  with the difference of 0.67% mass concentration. This due to break bound from  $-(CF_2)_n-$  to  $C-O-(CF_2)_n$  , in the O1s from 2.34  $E_{bT}$  to 2.08  $E_{CaT}$  with the difference of 0.26% maybe replacement Pt by Carbon C to stabilize the catalyst to PtO (this changer due to reduction of carbon from

## CONCLUSION

oxygen to metal), the Pt 4f from 2.55 for  $E_{bT}$  decrease to 0.82 for  $E_{CaT}$  with the difference of 1.73% this percentage due to the detachment from the support and dissolution toward into electrolyte Nafion®. The peak at 167.861 eV correspond at O=S=O and the second peak at

169.227 correspond at  $-SO_3$  (O-S-O)  $\text{O} \text{---} \text{S} \text{---} \text{O}$  with the S  $2p$  from 0.71 for  $E_{bT}$  to 0.61 for  $E_{CaT}$  increase to 0.1% in mass concentration.

The corrosion of carbon support happened in both electrodes, and the carbon corrosion was much more severe after test. The XRD and TEM Shown the decrease of the particle size of Pt and detachment from the support. Catalyst followed along with the dissolution/redeposit ion mechanism the particle sizes of cathode Pt catalysts after test markedly increased. The size of cathode catalyst within, utilization, and agglomeration of cathode catalyst are main factors of the performance decay of PEMFC.

TEM photograph for Pt/C catalyst has a mean particle size close to 4.0 nm in raw material (Pt/C) before test and, then the effect of aggressive operating conditions change the catalyst particle size from  $(4.14 \pm 0.9)$  to  $(5.57)$  nm maybe due to the agglomerate process also the detachment of catalyst from the support.

PEM fuel cell model analyze the influence of fuel cell operating parameters (temperature, partial pressures) on fuel cell's performance. The model showed that temperature has significant influence on output voltage and power. However, the influence of partial pressures is less significant. Both the electron transfer coefficient and exchange current density are platinum loading dependent. The exchange current density constant varies significantly with platinum loading, and thus has a dramatic effect on the performance of fuel cell at low current densities. This parameter is vital to design the PEM fuel cell.

# **REFERENCES**

## REFERENCES

### References:

- [1] Larminie J & Dicks A., Fuel cell systems Explained SAE International. John Wiley & sons 2003.
- [2] Viswanathan B., Aulice Scibioh M., Fuel Cells Principe and application. University Press (India), 2007. Page. 2.
- [3] David G. Lovering., Fuel Cells Grove Anniversary Symposium '89. Elsevier, Applied Science Publishers Ltd England, 1990, pp. 9.
- [4] Ryan O Hayre., Suk-Won Cha., Whitney Colella., Fritz B.Prinz., Fuel Cell Fundamentals. John Wiley&Sons , Inc., Hoboken, New Jersey. 2006, pp:235-250.
- [5] Ziao Zhang., Preparation and Characterization of proton exchange membrane for direct methanole fuel cells. Doctorate Thesis. Department of chemical engineering, Universitat Rovira I Virgili (URV). 2005, pp: 21-23.
- [6] James Larminie., Andrew Dicks., Fuel Cell Systems Explained, Second Edition 2nd Edition, wiley, England. ISBN-10: 0768012597, 2003, pp: 142-152.
- [7] Goodenough J. B., Hamnett A., B. J. Kennedy., R. Manoharan., and Weeks S.A., Methanol oxidation on unsupported and carbon supported Pt + Ru anodes. J. Electroanal. Chem., 240 (1988) pp: 133-145.
- [8] Supramaniam Srinivasan., Fuel Cell from Fundamentals to Applications. Springer Science business Media, LCC united State of America. 2006.
- [9] Matthew M.Mench., Fuel cell engines. John Wiley & Sons, Inc, New Jersey. 2008, pp:381
- [10] Ahmad A.Pesaran., Gi-Heon Kim., Jeffrey D.Gonder., PEM Fuel Cell Freeze and Rapid Startup Investigation. National Renewable Energy Laboratory. US. NREL Milestone Report. 2005.
- [11] Mass S., Finsierwalder F., Frank G., Hartmann B., Merten G., Crbon supportmoxidation in PEM fuel cell cathodes., L.Power source. 176 (2008), pp: 444–451.
- [12] Coutanceau C., Croissant M.J., Napporn T., Lamy C. Electrocatalytic reduction of dioxygen at platinum particles dispersed in a polyaniline film. Electrochimica Acta 46 (2000), pp: 579–588
- [13] Grolleau C., Coutanceau C., Pierre F., Leger J.-M., Effect of potential cycling on structure and activity of Pt nanoparticles dispersed on different carbonsupports reduction of oxygen Electrochim. Acta 53 (2008), pp: 7157-7165

## REFERENCES

- [14] Cédric Grolleau., Etude D'électrocatalyseurs Pour PEMFC En Couche mince, thèse de doctorat, l'université de poitiers France, (2009).
- [15] Ogden J.M., Steinbugler M.M., Kreutz T.G., Development of anode catalysts for direct methanol fuel cell. *J. Power Sources*, 79 (1999), pp: 143.
- [16] Koidesch K & Simader G., *Fuel Cells And Their Applications*, New York, VCH publisher, Inc. 1996. pp: 38-41.
- [17] Zohir Sekkal., introduction a la thermodynamique chimique., 3 eme edition., ben Aknoun Alger, 1984.
- [18] Row D.R., *Princip and application of electrochemistry*, fourth Edition CIT East Madras 600036, India (1994).
- [19] Chebbi Rachid., fabrication of low platinum loading electrode for proton exchange membrane fuel cells System (PEMFCs). Master thesis, University kebangsaan Malaysia (Ukm), Bangi Malaysia 2001.
- [20] Miachon S. & Aldebert P., Internal hydration  $H_2/O_2$  100 cm<sup>2</sup> polymer fuel cell pile a combustible. *J. Power Sources* **56** (1995), pp: 31-36.
- [21] Ying Song., Yu Wei., Hui Xu., Minkmas Williams., Yuxiu Liu., Leonard J.Bonville., Russell Kunz. H., James M.Fenton., Improvement in high temperature proton exchange membrane fuel cells cathode performance with ammonium carbonate. *J. Power Sources*, 141 (2005), pp: 250–257.
- [22] Aulice Scibioh M., *Fuel cells principle and application*. University Press (India), 2007, Page.2.
- [23] Chang Sun Kong., Do-Young Kim., Han-Kyu Lee., Yong-Gun Shul., and Tae-Hee., Influence of pore-size distribution of diffusion layer on mass-transport problems of proton exchange membrane fuel . *J. Power Sources* 108 ( 2002), pp: 185-191.
- [24] Bin Fang., Jin Luo., Peter N. Njoki., Rameshwori Loukrakpam., Derrick Mott., Bridgid Wanjala., Xiang Hu.,Chuan-Jian Zhong., Nanostructured PtVFe catalysts: Electrocatalytic performance in proton exchange membrane fuel cell. *J. Electrochemistry Communications*, 11 (2009), pp: 1139–1141.
- [25] Jin Luo., Nancy Kariuki., Li Han., Lingyan Wang., Chuan-Jian Zhong., He T.,Preparation characterization of carbon-supported PtVFe electrocatalysts. *Electrochimica Acta*, 51 (2006), pp: 4821–4827.

## REFERENCES

- [26] Shuo Chen., Hubert A. Gasteiger., Katsuichiro Hayakawa., Tomoyuki Tada., and Yang Shao-Horna., Platinum-Alloy Cathode Catalyst Degradation in Proton Exchange Membrane Fuel Cells: Nanometer-Scale Compositional and Morphological Changes. *J. Electrochemical Society*, 157 (1)(2010), pp: A82- A97.
- [27] Lin J.F., Wertz J., Ahmad R., Thommes M., Kannan A. M., Effect of carbon paper substrate of the gas diffusion layer on the performance of proton exchange membrane fuel cell. *J. Electrochimica Acta*, 55 (2010), pp: 2746–2751.
- [28] Zhen-BoWang., Peng-Jian Zuo., Xin-PengWang., Jie Lou., Bo-Qian Yang., Ge-Ping Yin., Studies of performance decay of Pt/C catalysts with working time of proton exchange membrane fuel cell. *J Power Sources* 18(2008), pp: 245–25
- [29] Wan Ramli Wan Daud., Abu Bakar Mohamad., Kadhum Abdul Amir., Chebbi Rachid., Iyuke Sunny E. Performance optimization of PEM fuel cell during MEA fabrication. *Energy Conversion and Management*, 45 (2004), pp: 3239–3249.
- [30] Caillard A., Charles C., Ramdutt D., Boswell R and Brault P., Effect of Nafion and platinum content in a catalyst layer processed in a radio frequency helicon plasma system. *J. Phys. D Appl. Phys*, 42 (2009), pp: 045207.
- [31] Yuyan Shao., Geping Yin., Yunzhi Gao., and Pengfei Shi., Durability Study of Pt/CNTs Catalyst under Simulated PEM Fuel Cell Conditions. *J. Electrochemical Society*, 152 (12) (2005), pp: A1093-A1097.
- [32] Mayrhofer Karl.J.J., Josef C. Meier., Sean J. Ashton ., Gustav K.H. Wiberg ., Florian Kraus .,Marianne Hanzlik., Matthias Arenz., Fuel cell catalyst degradation on the nanoscale. *J. Electrochemistry Communications*, 10 (2008). pp: 1144–1147.
- [33] Yuyan Shao., Geping Yin., Yunzhi Gao., Understanding and approaches for the durability issues of Pt-based catalysts for PEM fuel cell. *J Power Sources*, 171 (2007). pp: 558–566.
- [34] Stevens D.A., Hicks M.T., Haugen G.M., and Dahn J. R., Ex Situ and In Situ Stability studies of PEMFC Catalysts Effect of Carbon Type and Humidification on Degradation of the Carbon .*J Electrochemical Society*, 152 (12) (2005), pp: A2309-A2315
- [35] Ferreira-Aparicioa P., Gallardo-López B., Chaparroa A.M., Daza L., Physico -chemical study of the degradation of membrane-electrode assemblies in a Proton exchange membrane fuel cell stack. *J Power Sources* 196 (9) (2011) pp: 4242-4250.

## REFERENCES

- [36] Siroma Z., Fujiwara N., Ioroi T., Yamazaki S., Yasuda K., Miyazaki Y., Dissolution of Nafion® membrane and recast Nafion® film in mixtures of methanol and water. *J. Power Sources* 126 (2004), pp: 41-45.
- [37] Ferreira P.J., La O.G.J., Shao-Horn Y., Morgan D., Makharia R., Kocha S., and Gasteiger H., Instability of Pt/C Electrocatalyst in proton exchange Membrane Fuel Cells. *J. Electrochemical Society*, 152 (12) (2005), pp: A2256-A2271
- [38] Chengde Huang., Kim Seng Tan., Jianyi Lin., Kuang Lee Tan., XRD and XPS analysis of the degradation of the polymer electrolyte in H<sub>2</sub>-O<sub>2</sub> fuel cell. *Chemical Physics Letters* 371 (2003), pp: 80–85.
- [39] Valérie Parry., Gregory berthome., Jean-charles Joud., Olivier Lemaire., Alejandro A.Franco., XPS investigations of the proton exchange membrane fuel cell active layers aging: Characterization of the mitigating role of an anodic CO contamination on cathode degradation. *J. Power Sources*, 196 (2011), pp: 2530–2538.
- [40] Ticianelli E A., Derouin C.R., Redondo A., Srinivassan S., Method to advance technology of proton exchange membrane fuel cell., *J.Electrochem.soc.*, 135(9) (1998), pp: 2209-2214.
- [41] David Cohen. Earth's natural wealth: <https://www.newscientist.com> an audit 23 May, 2007.
- [42] Besenhard J.O., and Fritz H.P., The Electrochemistry of Black Carbons. *Angewandte Chemie International Edition in English*, 22(12) (1983), pp : 950-975.
- [43] Harris P.J.F., New Perspectives on the Structure of Graphitic Carbons. *Critical Reviews in Solid State and Materials Sciences*, 30 (4) (2005), pp:. 235-253.
- [44] Nikolay Dementev ., Sebastian Osswald., Yury Gogotsi., and Eric Borguet., Purification of carbon nanotubes by dynamic oxidation in air. *J. Materials Chemistry*, 19 (42) (2009), pp:. 7904-7908.
- [45] Chiang I.W., Brinson B.E., Smalley R.E., Margrave J.L., and Hauge R. H., Purification and Characterization of Single Wall Carbon Nanotubes. *J. Physical Chemistry B*, 105 (6) (2001), pp: 1157-1161.
- [46] Itkis M.E., Perea D. E., Niyogi S., Rickard S.M., Hamon M.A., Hu H., Zhao B., and haddon R.C., Purity Evaluation of As-Prepared Single-Walled Carbon Nanotube Soot by Use of Solution-Phase Near-IR Spectroscopy. *Nano Letters*, 3(3) (2003), pp: 309-314.
- [47] Dicks A.L., The role of carbon in fuel cells. *J. Power Sources*, 156 (2) (2006), pp: 128-141.



## REFERENCES

- [48] Logothetidis S., Optical and electronic properties of amorphous carbon materials. *Diamond and Related Materials*, 12 (2) (2003), pp: 141-150.  
*N.M.R. Peres a,b, F. Guinea a,c, A.H. Castro Neto*
- [49] Peres N.M.R., Guinea F., and Castro Neto A.H., Electronic properties of two-dimensional carbon. *Annals of Physics*, 321(7) (2006), pp: 1559-1567.
- [50] Xanthakis J.P., Effects of short-range order on the electronic structure and optical properties of amorphous carbon. *Diamond and Related Materials*, 9(7) (2000), pp: 1369-1373.
- [51] Molina-Sabio M., Gonzalez M. T., Rodriguez-Reinoso F., Sepulveda Escribano A., Effect of steam and carbon dioxide activation in the micropore size distribution of activated carbon. *Carbon* 34, (1996), pp: 505–509
- [52] Cazorola-Amoros D., Salinas-Martinez C., Alcaniz-Monge J., Gardner M., North A., Dore J., Characterization of activated carbon fibers by small angle X-Ray scattering. *Carbon* 36, (1998), pp: 309–312
- [53] Oya S.Yoshida., Alcañiz Monge J., Linares Solano A., Formation of mesopores in phenolic resin-derived carbon fiber by catalytic activation. *Carbon*, 33(1995), pp: 1085-1090.
- [54] Zabaniotou A., Madau P., Oudenne P. D., Jung C.G., Delplancke M.P., Fontana A., Active carbon production from used tire in two-stage procedure: industrial pyrolysis and bench scale activation with H<sub>2</sub>O–CO<sub>2</sub> mixture. *J. Analytical and Applied Pyrolysis*, 72 (2004), pp: 289–297.
- [55] Tay J.H., Chen X.G., Jeyaseelan S., Graham N., Optimising the preparation of activated carbon from digested sewage sludge and coconut husk. *Chemosphere*, 44 (2001), pp: 45–51
- [56] Babel K., Jurewicz K., KOH activated carbon fabrics as supercapacitor material. *J. Physics and Chemistry of Solids*, 65 (2004), pp: 275-280
- [57] Mora E., Blanco C., Pajares J.A., Santamaría R., and Menéndez R., Chemical activation of carbon mesophase pitches. *J. Colloid and Interface Science*, 298 (1) (2006), pp: 341-347
- [58] Fierro V., Torne-Fernandez V., Celzard A., Methodical study of the chemical activation of Kraft lignin with KOH and NaOH. *Microporous and Mesoporous Material*, 101 (3) (2007), pp: 419–431.

## REFERENCES

- [59] Freeman J. J., Gimblett F. G. R., Roberts R. A., Sing K. S. W., Studies of activated charcoal cloth. III, Mesopore development induced by phosphate impregnants. *Carbon*, 26 (1988), pp: 7–11.
- [60] Marcelo Carmo., Antonio R.dos Santos., Joao G.R. Poco , Marcelo Linardi., Physical and electrochemical evaluation of commercial carbon black as electrocatalysts supports for DMFC applications. *J. Power Sources*, 173 (2007), pp: 860–866
- [61] Cownden R., Nahon M., and Rosen M. A., Modeling and analysis of a solid polymer fuel cell system for transportation applications, *Int. J. Hydrogen Energy*, 26 (2001), pp: 615–623.
- [62] Andrew R., and Xianguo L., Mathematical modeling of proton exchange membrane fuel cells, *J. Power Sources*, 102 (2001), pp: 82–96.
- [63] Bevers D., and Wöhr M., Simulation of a polymer electrolyte fuel cell electrode, *J. Applied Electrochemistry*, 27 (1997), pp: 1254–1264.
- [64] Maggio G., Recupero V., and Pino L., Modeling polymer electrolyte fuel cells an innovative approach, *J. Power Sources*, 101 (2001), pp: 275–286.
- [65] Amphlett J.C., Mann R.F., Peppley B.A., Roberge P.R., and Rodrigues A., A model predicting transient responses of proton exchange membrane fuel cells, *J. Power Sources*, 61 (1996), pp: 183–188.
- [66] Hamelin J., Agbossou K., Laperrière A., Laurencelle F., and Bose T.K. Dynamic behavior of a PEM fuel cell stack for stationary applications, *Int. J. Hydrogen Energy*, 26 (2001), pp: 625–629.
- [67] Van Bussel H.P.L.H., Koene F.G.H., and Mallant R.K.A.M. Dynamic model of solid polymer fuel cell water management, *J. Power Sources*, 71 (1998), pp: 218–222.
- [68] Ralph T.R., Hards G.A. & Keating J.E., Low cost electrodes for proton exchange membrane fuel cells. *J. Electrochem. Soc*, **144** (11) (1997), pp: 3845-3856.
- [69] Mukerjee, S., Srinivasan, S. & Appleby A.J., Effect of sputtered film of platinum of low platinum loading electrodes on electrode kinetics of oxygen reduction in proton exchange membrane fuel cells. *J. Electrochimica. Acta*, **38** (12)(1993), pp: 1661-1669.
- [70] Sasi G Kumar., Raja M., & Parthasarathy S., High performance electrodes with very low platinum loading for polymer electrolyte fuel cells. *J. Electrochimica Acta*, **40** (3) (1994), pp: 285-290.

## REFERENCES

- [71] Hards G.A., Ralph T.R., & Cooper S.I., High Performance Low Cost Membrane Electrode Assemblies For Solid Polymer Fuel Cell. Johnson Matthey Technology Center, (1992). pp: 5.
- [72] Ye Siyu., Vijn A.K. & Dao L.H., A new fuel cell electrocatalyst based on carbonized polyacrylonitrile foam. *J. Electrochem. Soc*, **144** (1) (1997), pp: 90-95.
- [73] Janqi W., Daming F., Huanzhong W., Manfred Rembold., & Fritz T., An XPS investigation of polymer surface dynamics. I. A. study of surfaces modified by CH<sub>4</sub> and CF<sub>4</sub>/CH<sub>4</sub> plasmas. *J. Applied Polymer Science*, **50** (1993), pp: 585-599.
- [74] Ghose M., Characterization of PTFE-bonded porous carbon electrodes tested in a 100 w phosphoric acid fuel cell (PAFC) stack using XPS and ICP-AES. techniques. *J. Applied electrochem*, **28** (1998), pp: 955-962.
- [75] Arico A.S., Creti P., Antonucci P.L., Cho J., Kim H., & Antonucci V., Optimization of operating parameters of direct methanol fuel cell and physio-chemical investigation of catalyst-electrolyte interface. *J. Electrochimica Acta* **43** (1998), pp: 3719-3729.
- [76] Trotter P.J., Mason M., & Gerenser L.J. Bonding in silver complexes of carboxylic acid substituted Thionamides examined by infrared, Laser-Raman, and X-ray photoelectron spectroscopy. *J. Physical Chem*, **81** (13) (1977), pp: 1325-1334.
- [77] Moulder J.F., Stickle W., Sobol P., & Bomben K., *Handbook of X-ray Photoelectron Spectroscopy*. Perkin-Elmer Corporation. 1992.
- [78] Antonucci P.L., Alderucci V., Giordano N., Cocke D.L., & Kim H., On the role of surface functional group in Pt carbon interaction. *J. Applied electrochem*, **24** (1993), pp: 58-65
- [79] Chiu K.F., Wang K.W., Hydrophobic coatings on carbon electrodes for proton exchange membrane fuel cells., *Surface & Coatings technology*., 202 (2007), pp: 1231-1235.
- [80] Zhen-Bo-Wang., Peng-Jian Zuo., Yuan-Yuan Chu., Yu-Yan Shao., Ge-Ping Yin., Durability studies on performance degradation of Pt/C catalysts of proton exchange membrane fuel cell. *Int. J. Hydrogen Energy*, 34 (2009), pp: 4387-4394.
- [81] Siroma Z., Fujiwara N., Ioroi T., Yamazaki S., Yasuda K., Miyazaki Y., Dissolution of Nafion® membrane and recast Nafion® film in mixtures of methanol and water. *J. Power Sources*, 126 (2004), pp: 41-45

## REFERENCES

- [82] Zhaolin liu., Leong Ming Gan., Liang Hong., Werxiang Chen., Jim Yang Lee., Carbon supported Pt nanoparticules as catalyst for proton exchange membrane fuel cells., *J. Power source.*, 139 (2009), pp: 73-78.
- [83] Hui Li., Shanna Knights., Zheng Shi., John W.Van Zee., Jiujun Zhang., Proton exchange membrane fuel cells contamination and Mitigation strategies. Taylor and Francis and CRC Press. 2010.
- [84] Adriano C.Fernandos., Valdecir A.Paganin., Edson A.Ticianelli., Degradation study of Pt-based alloy catalyst for oxygen reduction reaction in proton exchange membrane fuel cells., *J. Electroanalytical Chemistry.*, 648 (2010), pp: 156-162.
- [85] Chebbi R., Beicha A., Wan Ramli Wan Daud and Zaamouche R., Surface analysis for catalyst layer (PT/PTFE/C) and diffusion layer (PTFE/C) for proton exchange membrane fuel cells systems (PEMFCs). *Applied Surface Science*, 255 (2009). pp: 6367–6371.
- [86] Mann R.F., Amphlett J.C., Hooper M.A.I., Jensen H.M., Peppley B.A., and Roberge P.R., Development and application of a generalised steady-state electrochemical model for a PEM fuel cell. *J. Power Sources*, 86 (2000), pp: 173-180.
- [87] Amphlett J.C., Mann R.F., Peppley B.A., Roberge P.R., and Rodrigues A., A model predicting transient responses of proton exchange membrane fuel cells. *J. Power Sources*, 61 (1996), pp: 183-188.
- [88] Nguyen M. G., and White R.E., A water and heat management model for proton-exchange-membrane fuel cells. *J. Electrochem. Soc.*, 140 (1993), pp: 2178-2186.
- [89] Springer T.E., Zawodzinski T.A., and Gottesfeld S., Polymer electrolyte fuel cell model. *J. Electrochemical Society*, 138 (8) (1991), pp: 2334-234.
- [90] Hirschenhofer J.H. Fuel Cell Status, *IEEE AES Systems Magazine*, (1994), pp: 10-15.
- [91] Jordan L.R., Shukla A.K., Behrsing T., Avery N.R., Muddle B.C., and Forsyth M., Diffusion layer parameters influencing optimal fuel cell performance. *J. Power Sources*, 86 (2000), pp: 250–254.
- [92] Song J. M., Cha S.Y. and Lee W.M., Optimal composition of polymer electrolyte fuel cell electrodes determined by the AC impedance method. *J. Power Sources*, 94 (2001), pp: 78-84.
- [93] Amphlett J.C., Baurnet R.M., and Mann R.F., Performance modeling of the Ballard Mark IV solid polymer electrolyte fuel cell. *J. Electrochemical Society*, 142 (1995), pp: 1-15.

## **PUBLICATIONS LIST**

### **Publications list**

1- Rachid Chebbi, Abdellah Beicha, W.R.W. Daud, Radia Zaamouche **Surface analysis for catalyst layer (Pt/PTFE/C) and diffusion layer (PTFE/C) for Proton Exchange Membrane Fuel Cells Systems (PEMFCS)**. Applied Surface Science. Volume 255 (2009), pages 6367-6371.

2-Chebbi Rachid,W.Ramli,W,Daud. Abu Bakar Mohamad, Abd. Amir H. Kadhum **Review of parameters affecting performance of (Pt/C) electrode for proton exchange membrane fuel cells (PEMFCS)**. Advanced Materials Research, 235 (2011), pp 43-49.

doi:10.4028/www.scientific.net/AMR.233-235.43

3- Chebbi Rachid , Wan Ramli Wan Daud, Beicha Abdellah , Mohd Ambar Yarmo. **Physical parameters affecting on the electrode performance for proton exchange membrane fuel cells (PEMFCS)**. Advanced Materials Research. Vol. 1105 (2015) pp 320-324.

doi:10.4028/www.scientific.net/AMR.1105.320